THE UNIVERSITY OF MICHIGAN
COLLEGE OF ENGINEERING
Department of Nuclear Engineering

Technical Report

ON THE THEORY OF SUPERHYPERFINE INTERACTION IN IRON GROUP ION COMPLEXES

Inan Chen
Chihiro Kikuchi

ORA Project 04381

under contract with:

NATIONAL AERONAUTICS AND SPACE ADMINISTRATION
GRANT NO. NSG-115-61
WASHINGTON, D.C.

administered through:

OFFICE OF RESEARCH ADMINISTRATION ANN ARBOR

April 1964

ensm

UMR 1174

ABSTRACT

The super-hyperfine (SHF) interaction -- interaction between the delocalized d electrons and the ligand nuclear spins in transition metal ion complexes -- has been treated by molecular orbital (MO) theory. The wave functions of the delocalized d electrons are approximated by linear combinations of atomic orbitals (LCAO) of transition metal ion and ligand ions, nearest and next nearest.

In Chapter I, the existing theory of transition metal ion complexes and studies on SHF interactions are reviewed.

In Chapter II, the formulation of molecular orbital theory and various simplified approaches to the exact theory are discussed.

The Hamiltonian for the interaction between electrons and nuclear spins are derived, in Chapter III, from the non-relativistic limit of the Dirac relativistic wave equation. This Hamiltonian is used, in the following chapter, to obtain the expressions of the SHF interaction tensor A^n in terms of the MO parameters (mixing coefficients) and crystal structure factors (interionic distances and bond angles). The details of the derivation are given, in Chapter IV, for the next nearest ligands in cubic $A_{II}B_{VI}$ compounds containing S state iron group ions. However, the formulation is quite general and can be easily applied to complexes of other structure.

The rest of Chapter IV is devoted to the analysis of SHF structures observed in electron paramagnetic resonance (EPR) and

electron-nuclear double resonance (ENDOR) spectra. Experimental observables are related to the components of SHF interaction tensor. An attempt is made to deduce the amount of d electron delocalization from these relations. Unfortunately, existing experimental results are not precise enough to give more than an "order of magnitude" values.

In Chapter V, the SHF structures observed in the EPR spectrum of vanadium doped tin oxide (which has rutile structure), $SnO_2:V^{4+}$, are discussed. From MO theory, two mechanisms for the next nearest ligand SHF interaction are derived. By taking the ratio of the observed SHF structures associated with two sets of non-equivalent ligands, it is possible to determine the relative importance of the two mechanisms in this complex.

The attempt to deduce, from SHF structure data, the amount of d electron delocalization, which is very difficult to obtain from first principle calculation, necessitates further information, both experimental and theoretical. The development of ENDOR technique and electronic computing facility casts delightful future on this approach.

TABLE OF CONTENTS

LIST OF TABLES

LIST OF FIGURES

CHAPTER I

INTRODUCTION

The physics and chemistry of the transition metal ion complexes have been of considerable academic interest since the end of the last century. Along with the development of quantum theory, effort has been made to explain the electronic structure of these complexes with the new theory. The problem turns out to be one of the most difficult tasks common in many branches of physics - the many-body problem. The solution can only be obtained by successive approximations, and even with the high speed computational facilities available today, a first principle calculation is still difficult and the result unreliable. Consequently, the development of a semi-empirical theory to exaplain observed phenomena is both necessary and appropriate.

On the other hand, since the development of solid state maser, laser and other solid state electronic magnetic devices, interest has been stimulated in the physics of crystals containing transition metal ions. A better understanding of the electronic structure of such crystals would be useful in developing better devices.

A. Theory of Transition Metal Ion Complex

Transition metal ions are characterized by the partially filled shells of d-electrons. When a transition metal ion forms

a complex with a number of surrounding anions or molecules or substitutes the host cation in a crystal as an impurity, the d-electrons are no longer localized at the metal ion but move in orbits which extend to the whole complex.* The most direct evidence of this d-electron delocalization is the observed superhyperfine structure (SHFS),** stemming from the interaction of the electron spin with the magnetic moments of the ligand nuclei. Furthermore, the ligand nuclear moments act as a number of electron detectors embedded in the crystal and hence supply information about the motion of the electrons. Thus the study of SHF interaction is one of the most powerful tools for the understanding of the electronic structure of such complexes.

Crystal field theory[1] has been very successful in predicting the splitting of d-electron levels[2] in a complex and also fairly successful in interpreting experimental results[3] quantitatively. In this theory, the ligand ions are considered to be fixed point charges producing an electrostatic field having the symmetry of the complex. The d-electrons are affected by this non-spherical field but are assumed not to overlap the ligand ions and hence give no SHF interaction. Furthermore, in covalent complexes, the large discrepancies between experimental results and theoretical calculations served to emphasize the need of modifying the model.

The second approximation is usually called "ligand field theory"[4]. In this model, the electronic structure of the ligand

*Hereafter, we shall use the term "complex" in a wide sense, i.e., it includes the cluster consisting of an impurity ion and its ligands in a crystal.

**Also called "Transferred Hyperfine Structure" by Marshall and Stuart.[12]

ions and the delocalization of the d-electrons are taken into account. Experimental evidences, other than the SHF interaction, which point to the need of modifying the crystal field theory are the reductions of parameters in crystal field theory such as g factors, Coulomb and exchange integral parameters.[5]

B. Survey of Studies on SHF Interaction

The first observation of SHF interaction was made by Griffiths, et al.[6] in iridium complexes, $IrCl_6^{--}$ and $IrBr_6^{--}$. In the electron paramagnetic resonance (EPR) spectra of these complexes they observed an anomalous hyperfine structure which can only be explained as arising from the interaction of d electrons with the surrounding halogen nuclei. Later, Tinkham[7] observed similar phenomena in the EPR spectra of ZnF_2 (rutile structure, see Chapter V) containing iron group ion impurities. Assuming that d-electron orbitals are augmented by small amounts of ligand orbitals of the proper symmetry, he estimated that the magnetic electrons have a probability of about 6% each of being in fluorine n = 2 and n = 3 orbits.

SHF interaction was also observed in nuclear magnetic resonance (NMR) experiments. Shulman and Jaccarino[8] observed the frequency shift of the NMR line of the fluorine in MnF_2. This shift was explained as due to the mixing of the fluorine orbitals with the manganese orbitals.

Later this problem of fluorine hyperfine interaction was re-examined by many investigators. Mukherji and Das[9] calculated

the interaction by orthogonalizing d wave function to the ligand wave functions. The calculated value of the hyperfine interaction is about half the experimental value. Keffer, et al.[10] considered both the orthogonalization of the d wave functions and the charge transfer from ligand to the cation. The results are in reasonable agreement with the NMR measurement of Shulman and Jaccarino. Clogston, et al.[11] related Keffer's approach to the idea of covalent bonding, and introduced molecular orbital treatment of the problem. They noticed that for other than perfect octahedral symmetry, there will not exist a coordinate system in which the SHF interaction tensors for all of the ligand nuclei are simultaneously diagonal, and observed the effect of the off-diagonal components in EPR spectrum of ZnF_2:Mn.

From the neutron diffraction form factor measurements, Marshall and Stuart[12] assert that in complexes the d wave functions are expanded over the free ion values and the SHF interaction in MnF_2 can be explained by the Heitler-London model using this expanded d wave function. However, Alperin[13] reported that the neutron diffraction form factor measurement indicates a decrease in the Ni^{++} d wave function in nickel oxide. Also, Marshall and Stuart obtained their result by neglecting the π bonding. However, NMR measurement on $KNiF_3$ and $KMnF_3$ by Shulman and Knox[14] and Hartree-Fock calculation by Sugano and Shulman[15] have shown that the π admixture is quite large.

All the above mentioned observations are the SHF interaction with nearest ligands. The SHF interaction with next nearest ligands has been observed in cubic crystals of group II-VI compounds containing

S state ions of transition metals. The interaction constants are almost isotropic and have the following values:

In CdS:Mn and CdTe:Mn[16], $A_{Cd} = 2.6 \times 10^{-4}$ cm^{-1};

In CdSe:Mn[17], $A_{Cd} = 2.7 \times 10^{-4}$ cm^{-1};

In ZnS:Mn[17], $A_{Zn} = 0.75 \times 10^{-4}$ cm^{-1}.

It was pointed out by Schneider, et al.[17] that the ratio of A_{Cd} to A_{Zn} is roughly the same as the ratio of the nuclear magnetic moment of cadmium to that of zinc. This means that the magnetic electron has almost the same probability of being in the next nearest ligand site in spite of the increase in the lattice constants of the above cited crystals from sulfide to telluride. This also indicates that the covalency increases in these crystals from sulfide to telluride. They also pointed out that no SHF interaction of nearest ligand has been observed although the nearest ligands S^{33}(0.74%), Se^{77}(7.5%), and Te^{125}(7.03%) have small but finite abundances.

Most recently, From, Kikuchi and Dorain[18], and Kasai[18a] observed two sets of SHF structure in $SnO_2:V^{4+}$ (which has rutile structure) associated with tin nuclei at non-equivalent sites. The interaction is anisotropic and has much larger value compared to those of Group II-VI compounds.

SHF structures in TiO_2 containing transition metal impurities are also observed by Yamaka[19] and Chang[20].

Observation of SHF interaction by electron-nuclear double resonance (ENDOR) has just been started. Ludwig and Lorenz[21] reported on the observation of cadmium hyperfine structure in CdTe containing Cr^+ ion. The interaction is anisotropic.

No ligand field theoretical (molecular orbital) treatment of next nearest ligand SHF interaction has been published.

The purpose of this thesis is to present a theoretical investigation of SHF interaction due to next nearest ligands in two types of complexes.

CHAPTER II

MOLECULAR ORBITAL THEORY OF d-ELECTRONS

As mentioned in Chapter I, Section A, ever since the experimental observation of d-electron delocalization in transition metal ion complex, it has been generally accepted that the point charge model "crystalline field theory" should be replaced by the "ligand field theory."

In ligand field theory, the wave functions of the delocalized d-electrons are approximated by the (anti-bonding) molecular orbitals ψ_a constructed from the linear combinations of atomic orbitals (LCAO) of the impurity and the ligands,

$$\psi_a = c_o d + \sum_\mu c_\mu \phi_\mu \qquad (2\text{-}1)$$

where d represents an atomic d orbital of the impurity, ϕ_μ's represent atomic orbitals of ligands, and C_o, C_μ's are numerical coefficients usually known as "mixing coefficients".

The valence electrons of the complex are described by (bonding) molecular orbitals. These are also LCAO's of impurity and ligands where the ligand orbitals are the major constituents.

The wave function of the many-electron system is represented by the antisymmetrized products (Slater determinant) of all occupied molecular orbitals,

$$\Psi = (n!)^{-1/2} \sum_P (-1)^p P\left[\psi_{i_1}(x_1)\,\psi_{i_2}(x_2)\cdots\psi_{i_n}(x_n)\right] \qquad (2\text{-}2)$$

where n is the number of electrons in the system; x_1, x_2, ... are the space and spin coordinates of electron 1, 2, ...; and P represents the permutation operator.

By applying the variational principle, i.e., minimizing the energy of the system, constraining the MO's to the orthonormality, we obtain the Hartree-Fock equation for the molecular orbital, ψ_i:

$$H_{eff}(x_1)\,\psi_i(x_1) = E_i\,\psi_i(x_1) \tag{2-3}$$

with the effective Hamiltonian (for electron 1)

$$H_{eff}(x_1) = \frac{p_1^2}{2m} - e^2\sum_g \frac{Z_g}{r_{1g}} + e^2\int dx_2\,\frac{\rho(x_2,x_2)-\rho(x_2,x_1)P_{12}}{r_{12}} \tag{2-4}$$

where

$$\rho(x_1,x_2) = \sum_{i=1}^{n}\psi_i(x_1)\,\psi_i^*(x_2) \tag{2-5}$$

is the Fock-Dirac density matrix, and P_{12} is the "interchange operator" with respect to the coordinates x_1 and x_2.[22]

Physically, this is an independent-particle model, according to which each electron in a many-electron system moves under the influence of the external field (nuclear charges) and an average field of all other electrons.

Details of the Hartree-Fock process for LCAO-MO have been worked out by Roothaan.[23] This method leads to a secular equation with the self-consistent field (SCF) scheme for the determination of MO energies and the mixing coefficients. We shall discuss this scheme by a simpler but equivalent way in the following.

A. LCAO-MO Secular Equation

Let us represent the MO ψ_i by LCAO as

$$\psi_i = \sum_{\nu=0}^{N} C_{i\nu} \varphi_\nu \tag{2-6}$$

where $C_{i\nu}$ is the mixing coefficient of ν-th AO in i-th MO, and φ_ν's are normalized but not necessarily orthogonal atomic orbitals.

If we substitute this expression of ψ_i in Equation (2-3), multiply by φ_μ^* from left on both sides of the equation, and integrate over all space, we get

$$\sum_\nu (H_{\mu\nu} - E_i S_{\mu\nu}) C_{i\nu} = 0 \tag{2-7}$$

where

$$H_{\mu\nu} = \int \varphi_\mu^* H_{eff} \varphi_\nu \, d\tau \tag{2-8}$$

and

$$S_{\mu\nu} = \int \varphi_\mu^* \varphi_\nu \, d\tau \tag{2-9}$$

Equation (2-7) is the secular equation for the determination of MO energy E_i and the mixing coefficients $C_{i\nu}$'s.

This is an "improper" eigenvalue problem. It is "improper" because the AO's φ_ν are not orthogonal in general, i.e., $S_{\mu\nu} \neq \delta_{\mu\nu}$, and the unknown eigenvalue E_i appears not only on the diagonal of the secular determinant as in the usual eigenvalue problem, but also in the off-diagonal positions. This kind of eigenvalue problem can be solved by a combination of two successive diagonalizations as shown in Appendix B.

Further complication in the solution of Equation (2-7) arises from the fact that the matrix element $H_{\mu\nu}$ itself contains the unknown coefficients $C_{i\nu}$'s through the term ρ in the operator H_{eff}. Therefore, the solution of this problem must be done by an iterative procedure, starting with a set of first estimation on $C_{i\nu}$'s, repeating until self consistent results are obtained. This is illustrated by the following cycle:

$$\{C_{i\nu}\} \longrightarrow \rho \longrightarrow H_{eff} \longrightarrow \{\psi_i\}$$

In principle, the secular equation (2-7) must be solved for all electrons in the complex. However, the inner shell electrons of the constituent ions are quite localized and have little to do with the bonding. Therefore, the secular determinant breaks into blocks, one for each inner shell of each ion, and one for the valence electrons of all the ions. Since we are interested in the valence electrons only, we consider only the block corresponding to the AO's of these electrons.

Further reduction of the secular equation can be attained by taking into consideration the symmetry of the complex. Since the Hamiltonian of the system is invariant under the symmetry operations of the point group of the complex, the wave functions of the system can be classified according to their properties under symmetry operations giving one of the irreducible representations of the point group. The basis functions of the MO, φ_ν can also be classified in this way. If we use such "symmetry orbitals" as basis functions, then since the matrix element of the Hamiltonian between two basis functions belonging

to different irreducible representations vanishes and since two such functions are orthogonal, the secular determinant breaks up into blocks one for each irreducible representation. In this way the secular determinant can be reduced in its order.

However, even with these reductions, SCF-LCAO-MO calculation requires a tremendous amount of work for symmetry lower than spherical, and the results become less reliable as the number of ions increases. No such calculation has been done for a system more complicated than NH_3.[24]

B. Simplified LCAO-MO Method

The closest approach to the SCF-LCAO-MO calculation which has been done for transition metal complex is the calculation of crystalline field splitting by Sugano and Shulman.[15] Using the results of Hartree-Fock calculations for atoms[25], neglecting overlap and covalency effect in the Hamiltonian, they calculated the matrix elements of the Hamiltonian and overlap integrals. This is equivalent to the first step in the SCF calculation. They did not carry out the iterative procedure, but obtained good agreement with experimental results for the crystalline field splitting of $KNiF_3$.

Another simplified approach is the "semiempirical" MO calculation of Wolfsberg and Helmholz.[26] In this method, the diagonal elements of the matrix H are approximated by some empirical energy values, and off-diagonal elements are calculated from an empirical formula

$$H_{\mu\nu} = f\, S_{\mu\nu}\, \frac{H_{\mu\mu} + H_{\nu\nu}}{2} \qquad (2\text{-}10)$$

or

$$H_{\mu\nu} = -f\, S_{\mu\nu} \sqrt{H_{\mu\mu} \cdot H_{\nu\nu}} \qquad (2\text{-}11)$$

where f is a constant usually assigned a value of about 2. The second formula is proposed by Ballhausen and Gray.[27]

The overlap integrals $S_{\mu\nu}$ can be computed by using either Slater radial functions or, if available, Hartree-Fock functions. The method of evaluation is given in Appendix A.

Valence state ionization energies (VSIE) are used for the empirical values of the diagonal elements of H by Wolfsberg and Helmholz[26], and in an earlier paper by Ballhausen and Gray.[27] The method of evaluating VSIE is given by Moffitt[28] for the first short period elements. The applicability of this method to other (heavier) ions has not been justified.

Another approximation to the matrix elements $H_{\mu\mu}$'s is the atomic one electron orbital energy obtained from Hartree-Fock calculations of atoms (e.g., Watson and Freeman[25]). This energy differs from the exact $H_{\mu\mu}$ by the interaction with the electrons centered at other ions. Sugano and Shulman's calculation shows that this difference is not always negligible.

Jørgensen[29] has pointed out that this semiempirical method may lead to a wrong ordering of MO levels with respect to experimental results.

In a recent paper Gray and Ballhausen[30] proposed a general rule for qualitative determination of the MO energies. They are:

(1) The order of AO energies is taken to be σ(ligand), π^b(ligand), nd(metal), (n+1)s (metal), π^*(ligand), (n+1)p (metal).

(2) The amount of mixing of AO in MO is roughly proportional to overlap integral and inversely proportional to their AO energy difference.

(3) Other things being approximately equal, σ bonding MO is more stable than π bonding MO, and σ antibonding MO correspondingly less stable than π antibonding MO.

(4) The relative MO ordering is considered final only if it is fully consistent with the available experimental results, exact differences in the MO levels can only be obtained from experiment.

Two simplified MO calculations for tetrahedral complexes including next nearest ligands are given in Appendix C. In one of them, spectroscopic data[31] are used for the matrix elements $H_{\mu\mu}$, and in the other, Hartree-Fock orbital energies are used.

CHAPTER III

HAMILTONIAN FOR THE MAGNETIC INTERACTION BETWEEN ELECTRONS AND NUCLEI

The Hamiltonian for the interaction of an electron with a nuclear magnetic moment at the origin has been derived by Fermi and others[32] as:

$$\mathcal{H} = 2\beta_e g_n \beta_N \left\{ r^{-3} \underline{I}\cdot(\underline{L}-\underline{S}) + 3r^{-5}(\underline{I}\cdot\underline{r})(\underline{S}\cdot\underline{r}) + \frac{8\pi}{3}\delta(\underline{r})\underline{I}\cdot\underline{S} \right\} \qquad (3\text{-}1)$$

where β_e and β_N are Bohr and nuclear magnetons respectively, and g_n is the nuclear g factor.* $\underline{I}$, $\underline{L}$, and $\underline{S}$ are, respectively, nuclear spin, electronic orbital, and electronic spin angular momentum operators in units of $\hbar$. This Hamiltonian can be derived from Dirac's relativistic wave equation for one electron as the non-relativistic limit. A simplified alternate derivation is given by Blinder[33] recently.

In our problem, the electrons interact with a system of nuclei. The Hamiltonian for the interaction of <u>one</u> electron with a system of nuclei can be derived by generalization of the derivation of Equation (3-1). This is given in the following.

Dirac's wave equation for an electron (with charge -e) in electromagnetic field (characterized by vector potential $\underline{A}$ and scalar potential ϕ) can be written as

$$\left\{ -c\,\underline{\alpha}\cdot\left(\underline{p} + \frac{e}{c}\underline{A}\right) - \beta mc^2 - e\phi \right\} \underline{\Psi} = E_R \underline{\Psi} \qquad (3\text{-}2)$$

*Nuclear g factor is defined such that nuclear magnetic moment $\underline{\mu}_n = g_n \beta_N \underline{I}_n$

with

$$\underline{\alpha} = \begin{pmatrix} 0 & \underline{\sigma} \\ \underline{\sigma} & 0 \end{pmatrix}, \qquad \beta = \begin{pmatrix} 1 & 0 \\ 0 & -1 \end{pmatrix}$$

where $\underline{\sigma}$ is the Pauli spin matrices

$$\sigma_x = \begin{pmatrix} 0 & 1 \\ 1 & 0 \end{pmatrix}, \qquad \sigma_y = \begin{pmatrix} 0 & -i \\ i & 0 \end{pmatrix}, \quad \sigma_z = \begin{pmatrix} 1 & 0 \\ 0 & -1 \end{pmatrix}$$

The sources of the electromagnetic field are a system of point nuclei of infinite masses with charges $Z_n e$ and magnetic dipole moments $g_n \beta_N I_n$, $n = 1, 2, 3, \ldots$. Accordingly the scaler and vector potentials are, respectively,

$$\phi = \sum_n \frac{Z_n e}{r_n} \tag{3-3}$$

$$\underline{A} = \sum_n g_n \beta_N \underline{I}_n \times \underline{r}_n / r_n^3 \tag{3-4}$$

where $\underline{r}_n$ is the radial vector from nucleus n to the electron.

The wave function Ψ is a four-component spinor, and we represent it as

$$\Psi = \begin{pmatrix} \Psi_1 \\ \Psi_2 \end{pmatrix} \tag{3-5}$$

where Ψ_1 and Ψ_2 are two-component spinors.

Since we shall be only interested in the non-relativistic limit of the equation, the relativistic energy E_R differ very little from the rest mass energy mc^2. It is convenient to introduce

$$E = E_R - mc^2 \tag{3-6}$$

Note that $E \ll mc^2$.

Thus, Equation (3-2) reduces to the following set of two spinor equations:

$$(E + e\phi + 2mc^2)\,\Psi_1 + c\,\underline{\sigma}\cdot\left(\underline{p} + \frac{e}{c}\underline{A}\right)\Psi_2 = 0 \qquad (3\text{-}7)$$

$$(E + e\phi)\,\Psi_2 + c\,\underline{\sigma}\cdot\left(\underline{p} + \frac{e}{c}\underline{A}\right)\Psi_1 = 0 \qquad (3\text{-}8)$$

From these equations, we see that Ψ_1 (positron component) is smaller than Ψ_2 (electron component) by a factor of order v/c. We can eliminate Ψ_1 between the two equations, yielding:

$$\left\{E + e\phi - \frac{1}{2m}\left[\underline{\sigma}\cdot\left(\underline{p} + \frac{e}{c}\underline{A}\right)\right] K(\underline{r}) \left[\sigma\cdot\left(\underline{p} + \frac{e}{c}\underline{A}\right)\right]\right\}\Psi_2 = 0 \qquad (3\text{-}9)$$

where we defined

$$K(\underline{r}) = K(r_1, r_2, \cdots r_n, \cdots) = \left[1 + \frac{E + e\phi}{2mc^2}\right]^{-1} \qquad (3\text{-}10)$$

Equation (3-9) can be rewritten in the form

$$\mathcal{H}_{eff}\,\Psi_2 = E\,\Psi_2 \qquad (3\text{-}11)$$

where the effective Hamiltonian $\mathcal{H}_{eff}$ can be separated into three parts:

$$\mathcal{H}_{eff} = \mathcal{H}^{(0)} + \mathcal{H}^{(1)} + \mathcal{H}^{(2)} \qquad (3\text{-}12)$$

with

$$\mathcal{H}^{(0)} = -e\phi + \frac{1}{2m}\left(\underline{\sigma}\cdot\underline{p}\right) K(\underline{r}) \left(\underline{\sigma}\cdot\underline{p}\right) \qquad (3.13)$$

$$\mathcal{H}^{(1)} = \frac{e}{2mc}\left\{\left(\underline{\sigma}\cdot\underline{p}\right) K(\underline{r}) \left(\underline{\sigma}\cdot\underline{A}\right) + \left(\underline{\sigma}\cdot\underline{A}\right) K(\underline{r}) \left(\underline{\sigma}\cdot\underline{p}\right)\right\} \qquad (3.14)$$

$$\mathcal{H}^{(2)} = \frac{e^2}{2mc^2}\left\{(\underline{\sigma}\cdot\underline{H})\,K(\underline{r})\,(\underline{\sigma}\cdot\underline{A})\right\} \qquad (3\text{-}15)$$

The first term $\mathcal{H}^{(0)}$ corresponds to the kinetic and potential energies with relativistic corrections plus the spin-orbit interaction. The third term is the self-energy of the nuclear magnet and is of second order in nuclear magnetic moment. The second term $\mathcal{H}^{(1)}$ contains terms linear in nuclear moment and gives the interaction Hamiltonian between electron and nuclei. We shall consider further reduction of this term only.

Recalling the relations

$$\underline{p}\,K(\underline{r}) = K(\underline{r})\,\underline{p} - i\hbar\,\underline{\nabla}\,K(\underline{r}) \qquad (3\text{-}16)$$

and $$(\underline{\sigma}\cdot\underline{a})(\underline{\sigma}\cdot\underline{b}) = \underline{a}\cdot\underline{b} + i\underline{\sigma}\cdot(\underline{a}\times\underline{b}) \qquad (3\text{-}17)$$

where $\underline{a}$ and $\underline{b}$ are two arbitrary vectors commuting with $\underline{\sigma}$ but not each other, Equation (3-14) can be rewritten as

$$\mathcal{H}^{(1)} = h_1 + h_2 \qquad (3\text{-}18)$$

where

$$h_1 = \frac{e}{2mc}K(\underline{r})\left\{\underline{p}\cdot\underline{A} + \underline{A}\cdot\underline{p} + i\underline{\sigma}\cdot(\underline{p}\times\underline{A} + \underline{A}\times\underline{p})\right\} \qquad (3\text{-}19)$$

$$h_2 = -\frac{ie\hbar}{2mc}\left\{\underline{\nabla}K(\underline{r})\cdot\underline{A} + i\underline{\sigma}\cdot\underline{\nabla}K(\underline{r})\times\underline{A}\right\} \qquad (3\text{-}20)$$

Using the expression (3-4) for $\underline{A}$ and the Lorentz condition div $\underline{A}$ = 0, we have

$$\underline{p}\cdot\underline{A} + \underline{A}\cdot\underline{p} = 2\,\underline{A}\cdot\underline{p} = 2\sum_n g_n \beta_N r_n^{-3}\,\underline{I}_n \times \underline{r}_n \cdot \underline{p}$$

$$= 2\sum_n \hbar\, g_n \beta_N r_n^{-3}\,\underline{\ell}_n \cdot \underline{I}_n \qquad (3\text{-}21)$$

where $\hbar\underline{\ell}_n = \underline{r}_n \times \underline{p}$ is the orbital angular momentum of electron with respect to nucleus n. Similarly,

$$\underline{p}\times\underline{A} + \underline{A}\times\underline{p} = -i\hbar\,\nabla\times\underline{A}$$

but

$$[\nabla\times A]_x$$

$$= \left[\nabla \times \sum_n g_n \beta_N r_n^{-3}\,\underline{I}_n \times \underline{r}_n\right]_x$$

$$= \sum_n g_n\beta_N\left\{\frac{\partial}{\partial y}\left[r_n^{-3}(I_{nx}y_n - I_{ny}x_n)\right] - \frac{\partial}{\partial z}\left[r_n^{-3}(I_{nz}x_n - I_{nx}z_n)\right]\right\}$$

$$= \sum_n g_n\beta_N\left\{2r_n^{-3}I_{nx} + 3r_n^{-5}\left[-I_{nx}(y_n^2+z_n^2) + I_{ny}x_n y_n + I_{nz}x_n z_n\right]\right\}$$

$$= \sum_n g_n\beta_N\left\{r_n^{-5}I_{nx}(3x_n^2 - r_n^2) + 3r_n^{-5}(I_{ny}x_n y_n + I_{nz}x_n z_n)\right\}$$

$$= \sum_n g_n\beta_N\left\{-r_n^{-3}I_{nx} + 3r_n^{-5}x_n(I_{nx}x_n + I_{ny}y_n + I_{nz}z_n)\right\}$$

$$= \sum_n g_n\beta_N\left[-r_n^{-3}\underline{I}_n + 3r_n^{-5}\underline{r}_n(\underline{r}_n\cdot\underline{I}_n)\right]_x$$

Thus

$$\underline{p}\times\underline{A} + \underline{A}\times\underline{p} = -i\hbar\sum_n g_n\beta_N\left[-r_n^{-3}\underline{I}_n + 3r_n^{-5}\underline{r}_n(\underline{r}_n\cdot\underline{I}_n)\right] \qquad (3\text{-}22)$$

Introducing the electron spin angular momentum $\underline{S}$ (in units of $\hbar$) by

$$\underline{\sigma} = 2\underline{S} \qquad (3\text{-}23)$$

Then from Equations (3-19, 3-21, 3-22, and 3-23), we have

$$h_1 = 2\beta_e K(\underline{r}) \sum_n g_n \beta_N \left[r_n^{-3} (\underline{l}_n - \underline{S}) \cdot \underline{I}_n + 3 r_n^{-5} (\underline{r}_n \cdot \underline{S})(\underline{r}_n \cdot \underline{I}_n) \right] \quad (3\text{-}24)$$

Before reducing the second part h_2, let us investigate the properties of $K(\underline{r})$ as a function of r_n, $n = 1, 2, \ldots$. From Equations (3-3, and 3-10) we have

$$K(\underline{r}) = \left[1 + (2mc^2)^{-1} \left(E + \sum_n \frac{Z_n e^2}{r_n} \right) \right]^{-1}$$

$$\approx 1 \Big/ \left(1 + \sum_n \frac{Z_n e^2}{2mc^2 r_n} \right)$$

$$\approx 1 \quad (3\text{-}25)$$

in the region where $r_n \gg Z_n e^2/2mc^2 \approx 1.4089 Z_n \times 10^{-13}$ cm. Furthermore,

$$K(\underline{r}) \longrightarrow (\text{const.}) \times r_n \quad \text{as} \quad r_n \longrightarrow 0$$

hence, the expectation values of h_1 will have zero contribution from the points $r_n = 0$, $n = 1, 2, \ldots$ i.e. only non-s orbitals contribute to the expectation values of h_1, and for such orbitals the condition for the validity of Equation (3-25) is always satisfied. Thus we have,

$$h_1 = 2\beta_e \sum_n g_n \beta_N \left[r_n^{-3} (\underline{l}_n - \underline{S}) \cdot \underline{I}_n + 3 r_n^{-5} (\underline{r}_n \cdot \underline{S})(\underline{r}_n \cdot \underline{I}_n) \right]_{r_n > 0} \quad (3\text{-}26)$$

Now let us consider the second part h_2. Since

$$\nabla K(\underline{r}) = \nabla \left[1 + \frac{E + \sum_n \frac{Z_n e^2}{r_n}}{2mc^2} \right]^{-1} = \sum_n \frac{\underline{r}_n}{r_n} \frac{\partial K}{\partial r_n} \quad (3\text{-}27)$$

we have

$$h_2 = -i\beta_e \sum_{n,n'} \left(\frac{\partial \kappa}{\partial r_n}\right) r_n^{-1} \left[\underline{r}_n \cdot \underline{A}_{n'} + i\, \underline{\sigma} \cdot \underline{r}_n \times \underline{A}_{n'} \right] \qquad (3\text{-}28)$$

But since

$$\frac{\partial \kappa}{\partial r_n} = \kappa^2(\,) \, r_n^{-2} \left(\frac{z_n e^2}{2mc^2}\right) \approx 0 \qquad \text{for } r_n \neq 0$$

and

$$\int_0^\infty \frac{\partial \kappa}{\partial r_n} \, dr_n = \kappa(r_n = \infty) - \kappa(r_n = 0) = 1$$

therefore $\frac{\partial \kappa}{\partial r_n}$ is essentially a delta function:

$$\frac{\partial \kappa}{\partial r_n} = \delta(r_n) \qquad (3\text{-}29)$$

Thus Equation (3-28) reduces to

$$h_2 = -i\beta_e \sum_n g_n \beta_N r_n^{-4} \delta(r_n) \left[\underline{r}_n \cdot \underline{I}_n \times \underline{r}_n + i\, 2\underline{S} \cdot \underline{r}_n \times \underline{I}_n \times \underline{r}_n \right]$$

$$= 2\beta_e \sum_n g_n \beta_N \delta(r_n) \left[r_n^{-2} \underline{S} \cdot \underline{I}_n - r_n^{-4} (\underline{r}_n \cdot \underline{S})(\underline{r}_n \cdot \underline{I}_n) \right] \qquad (3\text{-}30)$$

Noting that $\delta(r_n) = 4\pi r_n^2 \delta(\underline{r}_n)$,

and the average over all angles

$$\left[\underline{S} \cdot \underline{I}_n - r_n^{-2} (\underline{r}_n \cdot \underline{S})(\underline{r}_n \cdot \underline{I}_n) \right]_{av} = \frac{2}{3} \underline{S} \cdot \underline{I}_n$$

we have

$$h_2 = 2\beta_e \sum_n g_n \beta_N \frac{8\pi}{3} \delta(\underline{r}_n) \underline{S} \cdot \underline{I}_n \qquad (3\text{-}31)$$

Summing Equations (3-26) and (3-31) we have for the hyperfine interaction Hamiltonian in the field of a system of nuclei,

$$\mathcal{H} = 2\beta_e \sum_n g_n \beta_N \left\{ \left[r_n^{-3} (\underline{l}_n - \underline{S}) \cdot \underline{I}_n + 3 r_n^{-5} (\underline{r}_n \cdot \underline{S})(\underline{r}_n \cdot \underline{I}_n) \right]_{r_n > 0} + \frac{8\pi}{3} \delta(\underline{r}_n) \underline{S} \cdot \underline{I}_n \right\} \qquad (3\text{-}32)$$

Our next task is to obtain a Hamiltonian for many-electron-many-nucleus interaction. Since an exact relativistic wave equation for many-electron system cannot be written in closed form, the many-electron Hamiltonian cannot be derived in the same way as was done in Equation (3-1) or (3-32). However, it is reasonable to assume that to first order in fine structure constant, the many-electron Hamiltonian can be represented by a sum of one-electron operators, Equation (3-32), one for each electron. Thus we obtain the Hamiltonian which will be used for later discussion:

$$\mathcal{H} = \sum_k \sum_n 2\beta_e g_n \beta_N \{[r_{kn}^{-3}(\underline{\ell}_{kn} - \underline{S}_k)\cdot \underline{I}_n + 3 r_{kn}^{-5}(\underline{r}_{kn}\cdot \underline{S}_k)(\underline{r}_{kn}\cdot \underline{I}_n)]_{r_{kn}>0} + \frac{8\pi}{3}\delta(\underline{r}_{kn})\,\underline{S}_k\,\underline{I}_n \tag{3-33}$$

where $\underline{r}_{kn}$ is the radial vector from nucleus n to electron k, $\underline{\ell}_{kn}$ is the orbital angular momentum of electron k with respect to center n (position of nucleus n).

CHAPTER IV

SUPERHYPERFINE INTERACTION IN CdTe:Mn^{++}

The superhyperfine structure due to next nearest ligands has been observed by Lambe and Kikuchi[16], Dorain[16a], and Schneider, et al.[17] in cubic crystals of Group II-VI compounds containing S state transition metal ion impurities (Chapter I,B). In this chapter we shall derive the expressions of the superhyperfine (SHF) interaction tensor A^n (for the next nearest ligand n) from molecular orbital theory, and then discuss the SHF structures observed in electron paramagnetic resonance (EPR) and electron-nuclear double resonance (ENDOR) spectra. We shall take cadmium telluride containing manganese ion, CdTe:Mn^{++}, as an example. However, the discussion applies also to other iron group S state ions in any cubic crystals of II-VI group compounds.

A. Structure and Symmetry Orbitals of the Complex

The transition metal ion impurity in cubic crystal of Group II-VI compound (zincblende structure) is surrounded by four anions tetrahedrally arranged at alternate corners of a cube, the edge length of which is one half of the lattice constant, a. This means that impurity-anion distance is $\sqrt{3}\,a/4$. The next nearest neighbors are twelve cations situated at the centers of the edges of a cube with edge length equal to the lattice constant. Thus impurity-cation distance is $a/\sqrt{2}$. (See Figure 4-1).

Each nearest ligand is bonded to three next nearest ligands and the central impurity ion tetrahedrally. We shall number the nearest

ligands from 1 to 4, as shown in Figure 4-1, and denote the three cations which are bonded to anion i by ia, ib, and ic, i = 1,2,3,4.

The coordinates at the ligands are chosen in the following way with respect to the coordinates (X_o, Y_o, Z_o) of the central ion.

$$\begin{pmatrix} X_1 \\ Y_1 \\ Z_1 \end{pmatrix} = \begin{pmatrix} 1/\sqrt{6} & -\sqrt{2/3} & 1/\sqrt{6} \\ 1/\sqrt{2} & 0 & -1/\sqrt{2} \\ -1/\sqrt{3} & -1/\sqrt{3} & -1/\sqrt{3} \end{pmatrix} \begin{pmatrix} X_o \\ Y_o \\ Z_o \end{pmatrix} \qquad (4\text{-}1)$$

$$\begin{pmatrix} X_{1a} \\ Y_{1a} \\ Z_{1a} \end{pmatrix} = \begin{pmatrix} 1 & 0 & 0 \\ 0 & 1/\sqrt{2} & -1/\sqrt{2} \\ 0 & -1/\sqrt{2} & -1/\sqrt{2} \end{pmatrix} \begin{pmatrix} X_o \\ Y_o \\ Z_o \end{pmatrix} \qquad (4\text{-}2)$$

$$\begin{pmatrix} X_{1b} \\ Y_{1b} \\ Z_{1b} \end{pmatrix} = \begin{pmatrix} 0 & 1 & 0 \\ -1/\sqrt{2} & 0 & 1/\sqrt{2} \\ -1/\sqrt{2} & 0 & -1/\sqrt{2} \end{pmatrix} \begin{pmatrix} X_o \\ Y_o \\ Z_o \end{pmatrix} \qquad (4\text{-}3)$$

$$\begin{pmatrix} X_{1c} \\ Y_{1c} \\ Z_{1c} \end{pmatrix} = \begin{pmatrix} 0 & 0 & 1 \\ 1/\sqrt{2} & -1/\sqrt{2} & 0 \\ -1/\sqrt{2} & -1/\sqrt{2} & 0 \end{pmatrix} \begin{pmatrix} X_o \\ Y_o \\ Z_o \end{pmatrix} \qquad (4\text{-}4)$$

The coordinates of ligands i, ia, ib, and ic (i = 2,3,4) are obtained from the above set (i=1) by twofold rotations around X_o, Y_o, and Z_o axes respectively. For the ligands, left-handed systems are chosen for the convenience of evaluating overlap integrals (see Appendix A).

We shall consider the molecular orbitals formed from linear combinations of (i) impurity (manganese) 4s, 3d orbitals, (ii) nearest

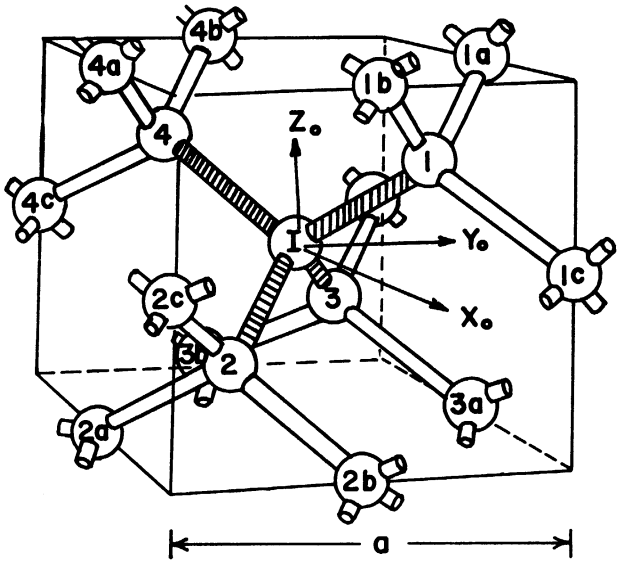

Figure 4-1. Nearest and Next Nearest Ligands in Zincblende Structure.

I : Impurity Ion.
1, 2, 3, 4: Nearest Ligands
ia, ib, ic (i = 1,2,3,4): Next Nearest Ligands.

ligands (tellurium) $\sigma(5s, 5p_z)$ and $\pi(p_x, p_y)$ orbitals, and (iii) next nearest ligands (cadmium) $\sigma(5s, 5p_z)$ orbitals.

The symmetry of the four nearest ligands is that of the point group T_d. Making use of the character table, we can construct the linear combinations of nearest ligand σ and π orbitals, which transform according to the irreducible representations of the T_d group. The results are given in Table 4-1.

The twelve next nearest ligands have octahedral symmetry. In Table 4-2, we present the linear combinations of next nearest ligand σ orbitals, which transform according to the irreducible representations of octahedral group O_h.

Finally, the classification of the manganese orbitals according to the irreducible representations of T_d and O_h groups are given in Table 4-3.

The wave functions of the five unpaired electrons are the manganese 3d orbitals augmented by ligand orbitals of the same symmetry. Thus they can be written as:

$$D_1 = \alpha_e d_1 + \beta_e \varphi_{1\pi} + \gamma_{es} \chi_{1s} + \gamma_{e\sigma} \chi_{1\sigma} \tag{4-5}$$

$$D_2 = \alpha_e d_2 + \beta_e \varphi_{2\pi} + \gamma_{es} \chi_{2s} + \gamma_{e\sigma} \chi_{2\sigma} \tag{4-6}$$

$$D_3 = \alpha_t d_3 + \beta_{ts} \varphi_{3s} + \beta_{t\sigma} \varphi_{3\sigma} + \beta_{t\pi} \varphi_{3\pi} + \gamma_{ts} \chi_{3s} + \gamma_{t\sigma} \chi_{3\sigma} \tag{4-7}$$

$$D_4 = \alpha_t d_4 + \beta_{ts} \varphi_{4s} + \beta_{t\sigma} \varphi_{4\sigma} + \beta_{t\pi} \varphi_{4\pi} + \gamma_{ts} \chi_{4s} + \gamma_{t\sigma} \chi_{4\sigma} \tag{4-8}$$

$$D_5 = \alpha_t d_5 + \beta_{ts} \phi_{5s} + \beta_{tz} \phi_{5z} + \beta_{t\pi} \phi_{5\pi} + \gamma_{ts} \chi_{5s} + \gamma_{tz} \chi_{5z} \qquad (4\text{-}9)$$

These molecular orbitals are the antibonding MO's and hence the coefficients β, γ's are small quantities.

B. Superhyperfine Interaction Tensor

The Hamiltonian for the interaction between the ligand nuclear spins and the unpaired electrons has been derived in Chapter III, Equation (3-33). It is in the form of a sum of one-electron operators,

$$\mathcal{H}_{SHF} = \sum_{k=1}^{5} H(k) \qquad (4\text{-}10)$$

where

$$H(k) = \sum_n 2\beta_k g_n \beta_n \left[\frac{(\underline{l}_{kn} - \underline{s}_k) \cdot \underline{I}_n}{r_{kn}^3} + \frac{3(\underline{r}_{kn} \cdot \underline{s}_k)(\underline{r}_{kn} \cdot \underline{I}_n)}{r_{kn}^5} + \frac{8\pi}{3} \delta(\underline{r}_{kn}) \underline{s}_k \cdot \underline{I}_n \right] \qquad (4\text{-}11)$$

The wave function of the ground state $3d^5\ {}^6S$, can be represented, to first approximation, by a Slater determinant of the five antibonding MO's,

$$\Psi = \left\{ D_1(r_1)\, D_2(r_2)\, D_3(r_3)\, D_4(r_4)\, D_5(r_5) \right\} \qquad (4\text{-}12)$$

The first order perturbation to this state due to the Hamiltonian $\mathcal{H}_{SHF}$ can be evaluated as

$$\langle \Psi | \mathcal{H}_{SHF} | \Psi \rangle = \sum_i \langle D_i(k) | H(k) | D_i(k) \rangle \qquad (4\text{-}13)$$

This perturbation is usually expressed as a spin Hamiltonian in the form

TABLE 4-1

SYMMETRY ORBITALS OF NEAREST LIGANDS

Irreducible Representation	Symmetry Orbital
A_1	$\frac{1}{2}(s_1 + s_2 + s_3 + s_4)$
	$\frac{1}{2}(z_1 + z_2 + z_3 + z_4)$
$E(\theta)$	$\varphi_{1\pi} = \frac{1}{4}[x_1 + x_2 + x_3 + x_4 - \sqrt{3}(y_1 + y_2 + y_3 + y_4)]$
$E(\epsilon)$	$\varphi_{2\pi} = \frac{1}{4}[y_1 + y_2 + y_3 + y_4 + \sqrt{3}(x_1 + x_2 + x_3 + x_4)]$
T_1	$\frac{1}{4}[y_1 + y_2 - y_3 - y_4 - \sqrt{3}(x_1 + x_2 - x_3 - x_4)]$
	$\frac{1}{2}(y_1 - y_2 + y_3 - y_4)$
	$\frac{1}{4}[y_1 - y_2 - y_3 + y_4 + \sqrt{3}(x_1 - x_2 - x_3 + x_4)]$
$T_2(x)$	$\varphi_{3s} = \frac{1}{2}(s_1 + s_2 - s_3 - s_4)$
	$\varphi_{3z} = \frac{1}{2}(z_1 + z_2 - z_3 - z_4)$
	$\varphi_{3\pi} = \frac{1}{4}[x_1 + x_2 - x_3 - x_4 + \sqrt{3}(y_1 + y_2 - y_3 - y_4)]$
$T_2(y)$	$\varphi_{4s} = \frac{1}{2}(s_1 - s_2 + s_3 - s_4)$
	$\varphi_{4z} = \frac{1}{2}(z_1 - z_2 + z_3 - z_4)$
	$\varphi_{4\pi} = \frac{1}{2}(x_1 - x_2 + x_3 - x_4)$

TABLE 4-1 CONT'D

Irreducible Representation	Symmetry Orbital
$T_2(z)$	$\varphi_{5s} = \frac{1}{2}(s_1 - s_2 - s_3 + s_4)$
	$\varphi_{5z} = \frac{1}{2}(z_1 - z_2 - z_3 + z_4)$
	$\varphi_{5\pi} = \frac{1}{4}[x_1 - x_2 - x_3 + x_4 - \sqrt{3}(y_1 - y_2 - y_3 + y_4)]$

TABLE 4-2

SYMMETRY ORBITALS OF NEXT NEAREST LIGANDS

Irreducible Representation	Symmetry Orbitals
A_{1g}	$\frac{1}{\sqrt{12}} \sum_{i=1}^{4} (s_{ia} + s_{ib} + s_{ic})$
	$\frac{1}{\sqrt{12}} \sum_{i=1}^{4} (z_{ia} + z_{ib} + z_{ic})$
$E_g(\theta)$	$\chi_{1s} = \frac{1}{\sqrt{24}} \sum_{i=1}^{4} (s_{ia} + s_{ib} - 2s_{ic})$
	$\chi_{1z} = \frac{1}{\sqrt{24}} \sum_{i=1}^{4} (z_{ia} + z_{ib} - 2z_{ic})$
$E_g(\epsilon)$	$\chi_{2s} = \frac{1}{\sqrt{8}} \sum_{i=1}^{4} (s_{ia} - s_{ib})$
	$\chi_{2z} = \frac{1}{\sqrt{8}} \sum_{i=1}^{4} (z_{ia} - z_{ib})$
$T_{2g}(\xi)$	$\chi_{3s} = \frac{1}{2} (s_{1a} + s_{2a} - s_{3a} - s_{4a})$
	$\chi_{3z} = \frac{1}{2} (z_{1a} + z_{2a} - z_{3a} - z_{4a})$
$T_{2g}(\eta)$	$\chi_{4s} = \frac{1}{2} (s_{1b} - s_{2b} + s_{3b} - s_{4b})$
	$\chi_{4z} = \frac{1}{2} (z_{1b} - z_{2b} + z_{3b} - z_{4b})$
$T_{2g}(\zeta)$	$\chi_{5s} = \frac{1}{2} (s_{1c} - s_{2c} - s_{3c} + s_{4c})$
	$\chi_{5z} = \frac{1}{2} (z_{1c} - z_{2c} - z_{3c} + z_{4c})$

TABLE 4-2 CONT'D

Irreducible Representation	Symmetry Orbitals
T_{1u}	$\frac{1}{\sqrt{8}}(s_{1b} - s_{1c} + s_{2b} - s_{2c} - s_{3b} + s_{3c} - s_{4b} + s_{4c})$
	$\frac{1}{\sqrt{8}}(s_{1a} - s_{1c} - s_{2a} + s_{2c} + s_{3a} - s_{3c} - s_{4a} + s_{4c})$
	$\frac{1}{\sqrt{8}}(s_{1a} - s_{1b} - s_{2a} + s_{2b} - s_{3a} + s_{3b} + s_{4a} - s_{4b})$
	and three similar combinations of P_z orbitals.
T_{2u}	$\frac{1}{\sqrt{8}}(s_{1b} + s_{1c} + s_{2b} + s_{2c} - s_{3b} - s_{3c} - s_{4b} - s_{4c})$
	$\frac{1}{\sqrt{8}}(s_{1a} + s_{1c} - s_{2a} - s_{2c} + s_{3a} + s_{3c} - s_{4a} - s_{4c})$
	$\frac{1}{\sqrt{8}}(s_{1a} + s_{1b} - s_{2a} - s_{2b} - s_{3a} - s_{3b} + s_{4a} + s_{4b})$
	and three similar combinations of P_z orbitals.

TABLE 4-3

IRREDUCIBLE REPRESENTATIONS OF IMPURITY ORBITALS

Orbital	Irred. Rep. in T_d	Irred. Rep. in O_h
4s	A_1	A_{1g}
$d_1 = 3d_{z^2}$	$E(\theta)$	$E_g(\theta)$
$d_2 = 3d_{x^2-y^2}$	$E(\epsilon)$	$E_g(\epsilon)$
$d_3 = 3d_{yz}$	$T_2(x)$	$T_{2g}(\xi)$
$d_4 = 3d_{zx}$	$T_2(y)$	$T_{2g}(\eta)$
$d_5 = 3d_{xy}$	$T_2(z)$	$T_{2g}(\zeta)$

$$\sum_i \langle D_i | H | D_i \rangle = \sum_n \underline{S} \cdot \underline{\underline{A}}^n \cdot \underline{I}_n \qquad (4\text{-}14)$$

where $\underline{S}$ is the total electron spin operator.

The program of this section is to obtain the expression of the SHF interaction tensor $\underline{\underline{A}}^n$ in terms of MO and geometric parameters.

The Hamiltonian (4-11) consists of two kinds of interactions: (i) Contact interaction, and (ii) Dipole interaction. The former gives isotropic contribution to $\underline{\underline{A}}^n$, and the latter is responsible for the anisotropic part.

(i) Contact Interaction

The one-electron Hamiltonian for this interaction is

$$H_s(k) = \sum_n 2\beta_e g_n \beta_N \frac{8\pi}{3} \delta(r_{kn}) \underline{s}_k \cdot \underline{I}_n \qquad (4\text{-}15)$$

According to Wigner-Echart theorem, we can relate the one-electron spin operator $\underline{s}_k$ to the total spin operator $\underline{S}$ as, (within the manifold of fixed $\mathcal{S}$)

$$\underline{s}_k = \underline{S}/2\mathcal{S} \qquad (4\text{-}16)$$

where $\mathcal{S}$ (=5/2) is the eigenvalue of $\underline{S}$. Thus Equation (4-15) reads,

$$H_s(k) = \frac{1}{2\mathcal{S}} \sum_n 2\beta_e g_n \beta_N \frac{8\pi}{3} \delta(r_{kn}) \underline{S} \cdot \underline{I}_n \qquad (4\text{-}17)$$

and from

$$\sum_i \langle D_i | H_s | D_i \rangle = \sum_n \underline{S} \cdot \underline{\underline{A}}_s^n \cdot \underline{I}_n = \sum_n A_s^n \underline{S} \cdot \underline{I}_n \qquad (4\text{-}18)$$

we have, for the isotropic SHF interaction,

$$A_s^n = \frac{1}{2s} 2\beta_e g_n \beta_n \frac{8\pi}{3} \sum_{\nu}' \langle D_i | \delta(r_{in}) | D_i \rangle \qquad (4\text{-}19)$$

The last factor $\sum_{\nu}' \langle D_i | \delta(r_{in}) | D_i \rangle$ is the density of unpaired electron spin at the nucleus n. The contributions from the various AO's in D_i to this density are estimated as follows:

Using the Slater radial functions for Mn 3d and Te 5s, 5p,*

$$R_{3d}(\mathrm{Mn}) = \frac{2\sqrt{2}}{3\sqrt{5}} (1.867)^{7/2} r^2 \exp(-1.867 r) \qquad (4\text{-}20)$$

$$R_{5sp}(\mathrm{Te}) = \frac{2}{3\sqrt{35}} (1.56)^{7/2} r^3 \exp(-1.56 r) \qquad (4\text{-}21)$$

and Hydrogenlike wave function for Cd 5s,

$$R_{5s}(\mathrm{Cd}) = \frac{(4.35)^{3/2}}{300\sqrt{5}} [120 - 240(1.74r) + 120(1.74r)^2 - 20(1.74r)^3 + (1.74r)^4] \exp(-0.87 r) \qquad (4\text{-}22)$$

we obtain

$|R_{3d}(\mathrm{Mn})|^2$ at Mn-Cd distance (8.58 at. units) = 1.09×10^{-9} a.u.

$|R_{5sp}(\mathrm{Te})|^2$ at Te-Cd distance (5.25 at. units) = 1.08×10^{-4} a.u.

$|R_{5s}(\mathrm{Cd})|^2$ at Cd nucleus = 1.63 a.u.

From this result we see that even if the probability of an electron being found in cadmium 5s orbital is as small as 0.1%,** practically the contributions from tellurium and manganese orbitals are negligible. Thus finally we have the expression

---

*Slater radial functions are used because they are more extended than Hartree-Fock functions and hence give the upper limit of the estimation.

**This percentage is estimated from Lambe and Kikuchi's experimental value $A_s^n = 2.6 \times 10^{-4}$ cm^{-1} by comparing to Jones' $A_{Cd} = 0.11$ Cm^{-1}.

$$A_s^n = \frac{1}{2S} \beta_e g_n \beta_N \frac{8\pi}{3} |R_s(0)|^2 \left\{ \frac{1}{6} \gamma_{cs}^2 + \frac{1}{4} \gamma_{ts}^2 \right\} \tag{4-23}$$

where $R_s(0)$ represents the value of cadmium 5s orbital at its nucleus, and γ_{cs}, γ_{ts} are the mixing coefficients introduced in Equations (4-5) through (4-9).

We have not taken into account the effect of spin polarization in deriving the above formula. This effect can be included simply by replacing $|R_s(0)|^2$ by $\rho_s(0)$, the density of unpaired spin at the nucleus when there is one electron in the orbit R_s. Thus

$$A_s^n = \frac{2}{5} \beta_e g_n \beta_N \frac{8\pi}{3} \rho_s(0) \left\{ \frac{1}{6} \gamma_{cs}^2 + \frac{1}{4} \gamma_{ts}^2 \right\} \tag{4-24}$$

$\rho_s(0)$ can be estimated from the hyperfine structure constant (isotropic part) A_{Cd} of cadmium,

$$A_{Cd} = 2 S g_n \beta_N \frac{8\pi}{3} \rho_s(0) \tag{4-25}$$

Jones[34] has reported the value $A_{Cd} = 0.11$ cm^{-1} obtained from optical measurement.

(ii) Dipole Interaction

The one-electron Hamiltonian for the dipole interaction is the first two terms in Equation (4-11)

$$H_D(k) = \sum_n 2\beta_e g_n \beta_N \left[\frac{(\underline{l}_{kn} - \underline{s}_k) \cdot \underline{I}_n}{r_{kn}^3} + \frac{3(\underline{r}_{kn} \cdot \underline{I}_n)(\underline{r}_{kn} \cdot \underline{s}_k)}{r_{kn}^5} \right] \tag{4-26}$$

The SHF interaction tensor due to this interaction, $\underline{\underline{A}}_D^n$ can be obtained from the equation

$$= \sum_i \langle D_i(k) | H_D(k) | D_i(k) \rangle$$

$$= \sum_i \langle D_i(k) | \sum_n \underline{S}_k \cdot \underline{\underline{\Omega}}^n_k \cdot \underline{I}_n | D_i(k) \rangle$$

$$= \frac{1}{2S} \sum_i \langle D_i(k) | \sum_n \underline{S} \cdot \underline{\underline{\Omega}}^n_k \cdot \underline{I}_n | D_i(k) \rangle$$

$$= \frac{1}{2S} \sum_n \underline{S} \cdot \left(\sum_i \langle D_i(k) | \underline{\underline{\Omega}}^n_k | D_i(k) \rangle \right) \cdot \underline{I}_n \qquad (4\text{-}27)$$

where $\underline{\underline{\Omega}}^n_k$ is a tensor operator

$$\underline{\underline{\Omega}}^n_k = 2\beta_e g_n \beta_N \left[\frac{-\mathbb{1}}{r^3_{kn}} + \frac{3\, \underline{r}_{kn} : \underline{r}_{kn}}{r^5_{kn}} \right] \qquad (4\text{-}28)$$

Thus,

$$\underline{\underline{A}}^n_D = \frac{1}{2S} \sum_i \langle D_i | \underline{\underline{\Omega}}^n_k | D_i \rangle \qquad (4\text{-}29)$$

Since D_i is a linear combination of manganese, tellurium and cadmium orbitals, we can expand the matrix element as

$$\underline{\underline{A}}^n_D = \frac{1}{2S} \sum_i \left\{ \alpha_i^2 \langle d_i | \underline{\underline{\Omega}}^n | d_i \rangle + \beta_i^2 \langle \varphi_i | \underline{\underline{\Omega}}^n | \varphi_i \rangle + \gamma_i^2 \langle \gamma_i | \underline{\underline{\Omega}}^n | \gamma_i \rangle \right\} \qquad (4\text{-}30)$$

where α_i^2, β_i^2, and γ_i^2 stand for the total fractions of electron in manganese 3d orbitals, tellurium orbitals, and cadmium orbitals respectively. We have neglected the cross product terms in the expansion.

The first two terms in Equation (4-30) are the contributions from the electron densities centered at manganese and tellurium atoms. We can consider these densities as concentrated at the nuclei and calculate their interaction with cadmium nucleus as point dipole-dipole interaction. Further, in the second term we consider only the interaction with the electron density centered at the tellurium which is nearest to cadmium n.

Thus from the first term we have

$$\frac{2}{5}\beta_e g_n \beta_N R_{MC}^{-3}(3\cos^2\theta_\xi - 1)\sum_i \alpha_i^2 \qquad (4\text{-}31)$$

for the diagonal component $A^n_{\xi\xi}$, $\xi = x, y, z$; and

$$\frac{2}{5}\beta_e g_n \beta_N R_{MC}^{-3}(3\cos\theta_\xi \cos\theta_\eta)\sum_i \alpha_i^2 \qquad (4\text{-}32)$$

for the off-diagonal component $A^n_{\xi\eta}$, $\xi, \eta = x, y, z$; where R_{MC} is the distance from the manganese ion to cadmium n, and θ_ξ is the angle between $\underline{R}_{MC}$ and ξ axis.

Similarly from the second term, we have,

$$\frac{2}{5}\beta_e g_n \beta_N R_{TC}^{-3}(3\cos^2\phi_\xi - 1)\left\{\frac{1}{2}\beta_{t\pi}^2 + \frac{1}{4}\beta_{ts}^2 + \frac{1}{4}\beta_{tz}^2 + \frac{3}{4}\beta_{t\pi}^2\right\} \qquad (4\text{-}33)$$

for the diagonal component $A^n_{\xi\xi}$, and

$$\frac{2}{5}\beta_e g_n \beta_N R_{TC}^{-3}(3\cos\phi_\xi \cos\phi_\eta)\left\{\frac{1}{2}\beta_{e\pi}^2 + \frac{1}{4}\beta_{ts}^2 + \frac{1}{4}\beta_{tz}^2 + \frac{3}{4}\beta_{t\pi}^2\right\} \qquad (4\text{-}34)$$

for the off-diagonal component $A^n_{\xi\eta}$; where R_{TC} is the distance from tellurium ion to cadmium ion n, and ϕ_ξ is the angle between $\underline{R}_{TC}$ and ξ axis, $\xi = x, y, z$.

In the third term of Equation (4-30), only the p orbital of the cadmium n has to be considered. By operator equivalence technique $H_D(k)$ can be rewritten as

$$H_D(k) = \frac{2}{5}\sum_n g_n \beta_N \frac{\zeta}{r_n^3}\left[\ell_n(\ell_n+1)\underline{S} - \frac{3}{2}(\underline{S}\cdot\underline{\ell}_n)(\underline{\ell}_n\cdot\underline{I}_n) - \frac{3}{2}(\underline{I}_n\cdot\underline{\ell}_n)(\underline{\ell}_n\cdot\underline{S})\right] \qquad (4\text{-}35)$$

where $\zeta = 2/(2\ell_n - 1)(2\ell_n + 3)$, and $\underline{\ell}_n$ is the orbital angular momentum of electron with respect to the nucleus n. Thus the p_z orbital of the

ion n contributes

$$\frac{2}{5}\beta_e g_n \beta_N \zeta \langle r^{-3} \rangle_{5p} \langle P_z | l(l+1) - 3l_\zeta^2 | P_z \rangle \left\{ \frac{1}{6}\gamma_{ez}^2 + \frac{1}{4}\gamma_{tz}^2 \right\} \qquad (4\text{-}36)$$

to diagonal component $A^n_{\xi\xi}$, and

$$\frac{2}{5}\beta_e g_n \beta_N \zeta \langle r^{-3} \rangle_{5p} \langle P_z | -\frac{3}{2}(l_\xi l_\eta + l_\eta l_\xi) | P_z \rangle \left\{ \frac{1}{6}\gamma_{ez}^2 + \frac{1}{4}\gamma_{tz}^2 \right\} \qquad (4\text{-}37)$$

to off-diagonal component $A^n_{\xi\eta}$.

In applying these general formulae to cadmium ions at different sites, we note that if the components of $\underline{\underline{A}}^n_D$ tensor are referred to the coordinate system (X_o, Y_o, Z_o) of the central (manganese) ion, the expressions will be different for different sites of cadmium. However, if we refer the components to the coordinates (X_n, Y_n, Z_n) at the ion n as defined in Equations (4-2), (4-3), and (4-4), then the expressions will be the same for all the cadmium sites. Therefore we shall first derive the expressions for the components with respect to this set of coordinates and then transform the results into the coordinates of the central ion. The latter coordinates is the one which experimental results are referred to.

For the simplicity of notation, we use (π, μ, σ) for (X_n, Y_n, Z_n) and reserve (X, Y, Z) for (X_o, Y_o, Z_o).

The angles θ, ϕ in the general formulae, Equations (4-31) through (4-34) are

$$\begin{aligned} \theta_\pi &= 90^\circ \\ \theta_\mu &= 90^\circ \\ \theta_\sigma &= 0^\circ \end{aligned} \qquad (4\text{-}38)$$

$$\cos^2\phi_\pi = 1/3$$
$$\cos^2\phi_\mu = 0$$
$$\cos^2\phi_\sigma = 2/3$$
$$\cos\phi_\pi \cos\phi_\sigma = \sqrt{2}/3 \qquad (4\text{-}39)$$

for all of the twelve sites.

Introducing the following abbreviations:

$$A_M = \frac{2}{5}\beta_e g_n \beta_N R_{MC}^{-3} \{ 2\alpha_z^2 + \beta_{tz}^2 \} \qquad (4\text{-}40)$$

$$A_T = \frac{2}{5}\beta_e g_n \beta_N R_{TC}^{-3} \{ \frac{1}{2}\beta_{t\pi}^2 + \frac{1}{4}\beta_{t\sigma}^2 + \frac{1}{4}\beta_{tz}^2 + \frac{3}{4}\beta_{t\pi}^2 \} \qquad (4\text{-}41)$$

$$A_C = \frac{2}{5}\beta_e g_n \beta_N \zeta \langle r^{-3} \rangle_{5p} \{ \frac{1}{6}\gamma_{z\sigma}^2 + \frac{1}{4}\gamma_{t\pi}^2 \} \qquad (4\text{-}42)$$

We have, for the components of A^n tensor, including the isotropic part,

$$A_{\pi\pi} = A_S - A_M - A_C \qquad (4\text{-}43)$$

$$A_{\mu\mu} = A_S - A_M - A_C - A_T \qquad (4\text{-}44)$$

$$A_{\sigma\sigma} = A_S + 2A_M + 2A_C + A_T \qquad (4\text{-}45)$$

$$A_{\pi\sigma} = A_{\sigma\pi} = \sqrt{2}\, A_T \qquad (4\text{-}46)$$

Other components are zero.

The components of A^n tensor in the coordinate system of the central ion, (X, Y, Z) can be obtained by the transformation

$$A^n_{\xi\eta} = \sum_{i,j} a^n_{\xi i} a^n_{\eta j} A_{ij} \qquad (4\text{-}47)$$

$$i, j = \pi, \mu, \sigma \; ; \quad \xi, \eta = X, Y, Z$$

with the transformation matrix ($a^n_{\xi i}$) given in Equations (4-2), (4-3) and (4-4). The results are the following:

For a-type cadmium sites

$$
\begin{aligned}
A_{XX} &= A_{\pi\pi} \\
A_{YY} &= \tfrac{1}{2}\left(A_{\mu\mu} + A_{\sigma\sigma}\right) \\
A_{ZZ} &= \tfrac{1}{2}\left(A_{\mu\mu} + A_{\sigma\sigma}\right) \\
A_{XY} &= (+)(-)(-)(+)\left(\tfrac{-1}{\sqrt{2}} A_{\pi\sigma}\right) \\
A_{YZ} &= (+)(+)(-)(-)\ \tfrac{1}{2}\left(-A_{\mu\mu} + A_{\sigma\sigma}\right) \\
A_{ZX} &= (+)(-)(+)(-)\left(\tfrac{-1}{\sqrt{2}} A_{\pi\sigma}\right)
\end{aligned}
\qquad (4\text{-}48)
$$

For b-type cadmium sites

$$
\begin{aligned}
A_{XX} &= \tfrac{1}{2}\left(A_{\mu\mu} + A_{\sigma\sigma}\right) \\
A_{YY} &= A_{\pi\pi} \\
A_{ZZ} &= \tfrac{1}{2}\left(A_{\mu\mu} + A_{\sigma\sigma}\right) \\
A_{XY} &= (+)(-)(-)(+)\left(\tfrac{-1}{\sqrt{2}} A_{\pi\sigma}\right) \\
A_{YZ} &= (+)(+)(-)(-)\left(\tfrac{-1}{\sqrt{2}} A_{\pi\sigma}\right) \\
A_{ZX} &= (+)(-)(+)(-)\ \tfrac{1}{2}\left(-A_{\mu\mu} + A_{\sigma\sigma}\right)
\end{aligned}
\qquad (4\text{-}49)
$$

For c-type cadmium sites

$$A_{XX} = \frac{1}{2}(A_{\mu\mu} + A_{\sigma\sigma})$$

$$A_{YY} = \frac{1}{2}(A_{\mu\mu} + A_{\sigma\sigma})$$

$$A_{ZZ} = A_{\pi\pi}$$

$$A_{XY} = (+)(-)(-)(+)\frac{1}{2}(-A_{\mu\mu} + A_{\sigma\sigma}) \qquad (4\text{-}50)$$

$$A_{YZ} = (+)(+)(-)(-)\left(\frac{-1}{\sqrt{2}} A_{\pi\sigma}\right)$$

$$A_{ZX} = (+)(-)(+)(-)\left(\frac{-1}{\sqrt{2}} A_{\pi\sigma}\right)$$

The four ± signs preceding the off-diagonal elements are for 1a, 2a, 3a, 4a, etc. respectively.

Introducing the abbreviations

$$A_+ = \frac{1}{2}(A_{\sigma\sigma} + A_{\mu\mu}) - A_S = \frac{1}{2}(A_M + A_C) \qquad (4\text{-}51)$$

$$A_- = \frac{1}{2}(A_{\sigma\sigma} - A_{\mu\mu}) = \frac{3}{2}(A_M + A_C) + A_T \qquad (4\text{-}52)$$

we can express the components in more compact form as:

For a-type cadmium,

$$A_{XX} = A_S - 2A_+$$

$$A_{YY} = A_S + A_+$$

$$A_{ZZ} = A_S + A_+ \qquad (4\text{-}53)$$

$$A_{XY} = (+)(-)(-)(+)(3A_+ - A_-)$$

$$A_{YZ} = (+)(+)(-)(-)\,A_-$$

$$A_{ZX} = (+)(-)(+)(-)(3A_+ - A_-)$$

For b-type cadmium,

$$
\begin{aligned}
A_{xx} &= A_s + A_+ \\
A_{yy} &= A_s - 2A_+ \\
A_{zz} &= A_s + A_+ \\
A_{xy} &= (+)(-)(-)(+)(3A_+ - A_-) \\
A_{yz} &= (+)(+)(-)(-)(3A_+ - A_-) \\
A_{zx} &= (+)(-)(+)(-)\, A_-
\end{aligned}
\tag{4-54}
$$

For c-type cadmium,

$$
\begin{aligned}
A_{xx} &= A_s + A_+ \\
A_{yy} &= A_s + A_+ \\
A_{zz} &= A_s - 2A_+ \\
A_{xy} &= (+)(-)(-)(+)\, A_- \\
A_{yz} &= (+)(+)(-)(-)(3A_+ - A_-) \\
A_{zx} &= (+)(-)(+)(-)(3A_+ - A_-)
\end{aligned}
\tag{4-55}
$$

In total we have three independent parameters A_s, A_+ and A_-. We shall discuss the relations between these parameters and the experimental quantities in the following sections.

C. SHF Structure in EPR Spectrum

In natural cadmium only about 25% of nuclei (Cd^{111}, Cd^{113}) have non-zero spin I = 1/2. The magnetic moments of Cd^{111}($-0.5922\ \beta_N$) and Cd^{113}($-0.6195\ \beta_N$) are nearly equal. We shall treat them as identical in the following discussion.

The spin-Hamiltonian describing the interaction of cadmium nuclear spins I_n's with the unpaired electrons and external magnetic field $\underline{H}_o$ is

$$\mathcal{H} = \sum_n \left\{ \underline{S} \cdot \underline{\underline{A}}^n \cdot \underline{I}_n - g_n \beta_N \underline{I}_n \cdot \underline{H}_0 \right\} \tag{4-56}$$

where the summation is over the cadmium nuclei with non-zero spins. By introducing an effective magnetic field

$$\underline{H}^n_{eff} = \underline{H}_0 - \frac{M_S}{g_n \beta_N} \underline{\underline{A}}^n \cdot \underline{h} \tag{4-57}$$

where $\underline{h}$ is the unit vector in the direction of $\underline{H}_o$, and M_S is the projection of $\underline{S}$ along $\underline{h}$, the Hamiltonian (4-56) can be rewritten as

$$\mathcal{H} = - \sum_n g_n \beta_N \underline{I}_n \cdot \underline{H}^n_{eff} \tag{4-58}$$

In EPR experiments we observe the transitions with $\Delta M_s = \pm 1$, $\Delta M_I = 0$. Therefore, the direction of $\underline{H}^n_{eff}$ changes after the transition. Thus it is convenient to describe the nuclear spin states of the ligands with the direction of crystal Z axis as quantization axis.

Consider the case $\underline{H}_o$//Z axis, [001]: The effective magnetic field can be written as

$$\underline{H}^{n}_{eff} = \begin{bmatrix} 0 \\ 0 \\ H_0 \end{bmatrix} - \frac{M_s}{g_n \beta_N} \begin{bmatrix} A^n_{xx} & A^n_{xy} & A^n_{xz} \\ A^n_{yx} & A^n_{yy} & A^n_{yz} \\ A^n_{zx} & A^n_{zy} & A^n_{zz} \end{bmatrix} \begin{bmatrix} 0 \\ 0 \\ 1 \end{bmatrix}$$

$$= \begin{bmatrix} -(M_s/g_n\beta_N) A^n_{xz} \\ -(M_s/g_n\beta_N) A^n_{yz} \\ H_0 - (M_s/g_n\beta_N) A^n_{zz} \end{bmatrix} \qquad (4\text{-}59)$$

Thus the Hamiltonian (4-58) reads

$$\mathcal{H} = \sum_n \left\{ M_s A^n_{xz} I_{nx} + M_s A^n_{yz} I_{ny} + (-g_n\beta_N H_0 + M_s A^n_{zz}) I_{nz} \right\}$$

$$= \sum_n \left\{ \frac{M_s}{2}(A^n_{xz} - i A^n_{yz}) I_{n+} + \frac{M_s}{2}(A^n_{xz} + i A^n_{yz}) I_{n-} + (-g_n\beta_N H_0 + M_s A^n_{zz}) I_{nz} \right\} \qquad (4\text{-}60)$$

The electronic states specified by a set of quantum numbers (M_s, M_I, m_{1a}, m_{1b}, $\cdots$ m_{4b}, m_{4c}) with the same M_s and M_I (z component of impurity ion nuclear spin) but different m_n's (z components of ligand nuclear spins) are degenerate before this perturbation is taken into consideration. Splitting due to this perturbation can be calculated by degenerate perturbation theory. However, for natural cadmium, even for the most probable case of three non-zero spin nuclei out of twelve, the perturbation theory leads to 8 x 8 secular determinant. Moreover, the probabilities of having four and five non-zero spin ligands are 3/4 and 2/5, respectively, of the most probable case and hence cannot be ignored. These cases will lead to secular determinants of 16 x 16 and 32 x 32 respectively. It is quite complicated to analyize such a spectrum. However, we can make use of the fact that each ligand nuclear spin is quite independent and first treat the

splitting due to each ligand spin separately, and then sum up the results.

For a and b type cadmium, the 2 x 2 secular determinant has the form:

$$\begin{vmatrix} \frac{1}{2}[-g_n\beta_N H_0 + M_S(A_S + A_+)] - \Delta E_{ab} & \frac{M_S}{2}[\pm(3A_+ - A_-) \mp i A_-] \\ \frac{M_S}{2}[\pm(3A_+ - A_-) \pm i A_-] & -\frac{1}{2}[-g_n\beta_N H_0 + M_S(A_S + A_+)] - \Delta E_{ab} \end{vmatrix} = 0 \qquad (4\text{-}61)$$

Solving this equation, we have

$$\begin{aligned} \Delta E_{ab} &= \frac{1}{2}\left\{[-g_n\beta_N H_0 + M_S(A_S + A_+)]^2 + M_S^2[(3A_+ - A_-)^2 + A_-^2]\right\}^{1/2} \\ &\approx \frac{1}{2}\left|-g_n\beta_N H_0 + M_S(A_S + A_+)\right| \end{aligned} \qquad (4\text{-}62)$$

For c-type cadmium, the secular determinant is

$$\begin{vmatrix} \frac{1}{2}[-g_n\beta_N H_0 + M_S(A_S - 2A_+)] - \Delta E_c & \frac{M_S}{2}(3A_+ - A_-)(\pm 1 \mp i) \\ \frac{M_S}{2}(3A_+ - A_-)(\pm 1 \pm i) & -\frac{1}{2}[-g_n\beta_N H_0 + M_S(A_S - 2A_+)] - \Delta E_c \end{vmatrix} = 0 \qquad (4\text{-}63)$$

hence,

$$\begin{aligned} \Delta E_c &= \frac{1}{2}\left\{[-g_n\beta_N H_0 + M_S(A_S + A_+)]^2 + M_S^2[(3A_+ - A_-)^2 + A_-^2]\right\}^{1/2} \\ &\approx \frac{1}{2}\left|-g_n\beta_N H_0 + M_S(A_S - 2A_+)\right| \end{aligned} \qquad (4\text{-}64)$$

Let us introduce a set of new quantum numbers for the ligand nuclear spins, μ_{1a}, μ_{1b}, μ_{1c}, etc., $\mu_n = +1/2$ for the state whose energy is shifted by $+\Delta E$ of Equation (4-62) or (4-64) by the perturbation, and $\mu_n = -1/2$ for the state whose energy is shifted by $-\Delta E$.

The eight a and b type cadmium ions are equivalent with magnetic field in [001] direction, and contribute equal amount of

energy shift $\pm \Delta E_{ab}$. We can introduce the "total μ quantum number of a, b type ligands" μ^{ab} by

$$\mu^{ab} = \sum_{n=a,b} \mu_n$$

Depending on the number of odd cadmium nuclei and the values of individual μ_n, μ^{ab} can have the seventeen values $\mu^{ab} = 0, \pm 1/2, \pm 1, \ldots, \pm 3, \pm 7/2, \pm 4$. Similarly the four c type cadmium ions are equivalent and all shift the energy level by $\pm \Delta E_c$. We define the "total μ quantum number of c type ligands" μ^c by

$$\mu^c = \sum_{n=c} \mu_n$$

which can have the nine values $\mu^c = 0, \pm 1/2, \ldots, \pm 2$.

Thus the energy of the state specified by $(M_S, M_I, \mu^{ab}, \mu^c)$ is

$$E(M_s, M_I, \mu^{ab}, \mu^c) = E(M_s, M_I, 0, 0) + 2\mu^{ab}\Delta E_{ab} + 2\mu^c \Delta E_c \qquad (4\text{-}65)$$

and the frequency of transition $\Delta M_S = \pm 1$, $\Delta M_I = 0$, is given by

$$\begin{aligned} h\nu_{\mu^{ab},\mu^c} &= h\nu_0 + 2\mu^{ab}(\Delta E_{ab} - \Delta E'_{ab}) + 2\mu^c(\Delta E_c - \Delta E'_c) \\ &\approx h\nu_0 + \mu^{ab}(A_S + A_+) + \mu^c(A_S - 2A_+) \end{aligned} \qquad (4\text{-}66)$$

where $\Delta E'_{ab}$, $\Delta E'_c$ are the values of ΔE_{ab}, ΔE_c for $M'_S = M_S \pm 1$. A schematic diagram of energy levels and transitions is given in Figure 4-2.

The above result shows that the HF structure line $h\nu_0$ is split into 17 x 9 = 153 lines. However, because of the high abundance of spinless nuclei, the higher values of μ^{ab}, μ^c are less probable and the intensities of these lines are not strong enough to be observable.

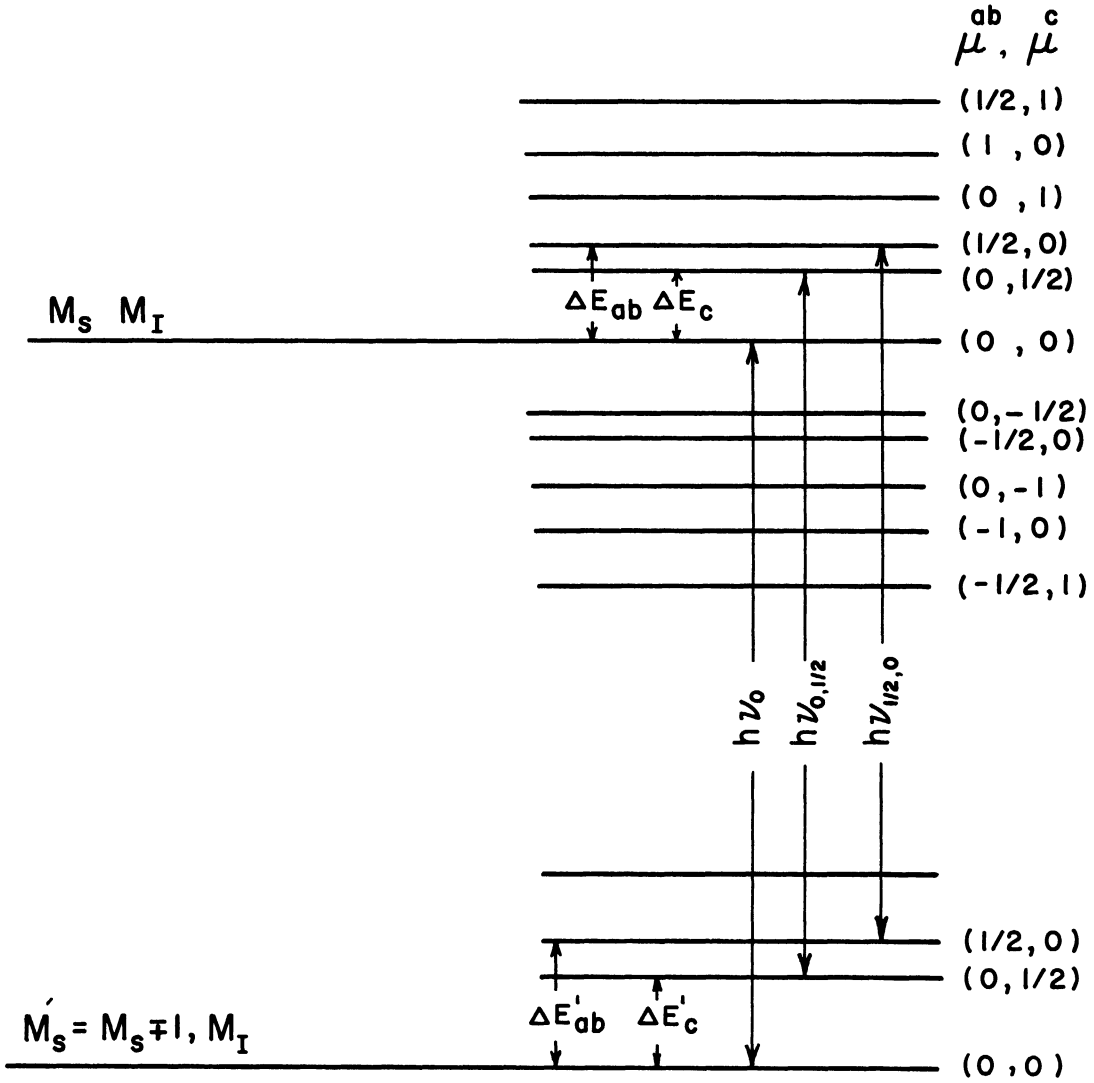

Figure 4-2. SHF Levels and EPR Transitions.

The relative intensity of the line (μ^{ab}, μ^{c}) can be expressed as

$$I(\mu^{ab}, \mu^{c}) = \sum_{\substack{n=2|\mu^{ab}| \\ +2|\mu^{c}|}}^{12} \sum_{k} \frac{W(n)\,P(n,k)}{2^{n}} \frac{k!}{(\frac{k}{2}+\mu^{ab})!(\frac{k}{2}-\mu^{ab})!} \frac{(n-k)!}{(\frac{n-k}{2}+\mu^{c})!(\frac{n-k}{2}-\mu^{c})!} \quad (4\text{-}67)$$

where

$$W(n) = f^{n}(1-f)^{12-n} \frac{12!}{n!\,(12-n)!} \quad (4\text{-}68)$$

is the probability of having n non-zero spin nuclei out of twelve, f is the natural abundance of non-zero spin cadmium, and

$$P(n,k) = \left(\frac{2}{3}\right)^{k}\left(\frac{1}{3}\right)^{n-k} \frac{n!}{k!\,(n-k)!} \quad (4\text{-}69)$$

is the probability of having k nuclei of ab type and n-k nuclei of c type out of n non-zero spin nuclei in total. The summation over k is to be taken from $k = 2|\mu^{ab}|$ to the lesser of 8 and $n-2|\mu^{c}|$, in steps of 2. The numerical values of $I(\mu^{ab}, \mu^{c})$ are given in Table 4-6.

If the anisotropic part of A^{n} tensor, A_{+} and A_{-} are too small to be observable, as in Lambe and Kikuchi's experiment, then $\Delta E_{ab} = \Delta E_{c}$, and we can describe the SHF lines by "total μ quantum number of ligands" μ^{L}. In this case the intensity ratio can be calculated by a simpler formula[16]:

$$I(\mu^{L}) = \sum_{n=2|\mu^{L}|}^{11\text{ or }12} \frac{W(n)}{2^{n}} \frac{n!}{(\frac{n}{2}+\mu^{L})!(\frac{n}{2}-\mu^{L})!} \quad (4\text{-}70)$$

where W(n) is given by Equation (4-68), and the summation over n is to be taken from $n = 2|\mu^{L}|$ to 11 or 12 in step of 2. The same result can

be obtained from Table 4-6 by adding the intensities of possible combinations, for example:

μ^L	μ^{ab}	μ^c	$I(\mu^{ab}, \mu^c)$	$I(\mu^L)$
0	0	0	.202	
	$\pm$ 1/2	$\mp$ 1/2	2 x .070	
	$\pm$ 1	$\mp$ 1	2 x .0066	.3557
	$\pm$ 3/2	$\mp$ 3/2	2 x .0002	
	$\pm$ 2	$\mp$ 2	2 x .000002	
1/2	0	1/2	.097	
	1/2	0	.150	
	1	- 1/2	.030	
	3/2	- 1	.00172	.2961
	2	- 3/2	.00003	
	5/2	- 2	.000000	
	- 1/2	1	.016	
	- 1	3/2	.00088	
	- 3/2	2	.0000156	

This result agrees with that calculated by Equation (4-70), and also with Lambe and Kikuchi's experiment. This shows that Lambe and Kikuchi's experiment is one special case of the general formulation given above.

TABLE 4-4

RELATIVE INTENSITIES OF SHF LINES IN CdTe:Mn

μ^c \ μ^{ab}	0	$\pm$ 1/2	$\pm$1	$\pm$ 3/2	$\pm$ 2	$\pm$ 5/2	$\pm$ 3	$\pm$ 7/2	$\pm$ 4
0	.202	.150	.068	.02085	.0045	.0007	8×10^{-5}	7.1×10^{-6}	4.6×10^{-7}
$\pm$ 1/2	.097	.070	.030	.00865	.0017	.0002	2.5×10^{-5}	1.8×10^{-6}	9.5×10^{-8}
$\pm$ 1	.0235	.016	.0066	.00172	.0003	.00004	3.2×10^{-6}	1.9×10^{-7}	7.5×10^{-9}
$\pm$ 3/2	.0035	.0024	.0009	.0002	.00003	3×10^{-6}	2.2×10^{-7}	1.0×10^{-8}	2.6×10^{-10}
$\pm$ 2	.00037	.00023	.00008	.00001	2×10^{-6}	1.6×10^{-7}	8.8×10^{-9}	2.6×10^{-10}	3.5×10^{-12}

It will be shown in the next section that A_+ is much smaller than A_-, so that [001] is not a good direction to observe the anisotropy of $\underline{\underline{A}}^n$, since only A_+, but not A_-, appears in the energy shift ΔE. Observation with external magnetic field in other directions (e.g. [110]) may show the anisotropy.

D. SHF Interaction in ENDOR Experiment

In electron-nuclear double resonance experiment (ENDOR) we observe the transition $\Delta M_S = 0$, $\Delta M_I = 1$, where I may be either the impurity ion nuclear spin or ligand nuclear spin. For the latter case, the transitions between SHF levels (Figure 4-3) are observed.

Since M_S does not change in such transitions, the direction of effective magnetic field $\underline{H}^n_{eff}$, Equation (4-57), unlike the case of EPR, does not change after the transition. Therefore, we can describe the ligand nuclear spin states by taking the direction of the effective magnetic field as the direction of quantization axis Z'. Then the Hamiltonian (4-58) reduces into the form:

$$\mathcal{H} = -\sum_n g_n \beta_N I_{nz'} |\underline{H}^n_{eff}| = -\sum_n g_n \beta_N m_n |\underline{H}^n_{eff}| \qquad (4\text{-}71)$$

Case I: $\underline{H}_0 // [001]$

The effective field has the components (4-59) and the magnitude:

$$|\underline{H}^n_{eff}| = \left\{ \left(H_0 - \frac{M_S}{g_n \beta_N} A^n_{zz}\right)^2 + \left(\frac{M_S}{g_n \beta_N}\right)^2 \left(A^{n\,2}_{xz} + A^{n\,2}_{yz}\right) \right\}^{1/2} \qquad (4\text{-}72)$$

Line A: Central Ion ENDOR
Line B: Ligand ENDOR
Line C: Microwave Pumping Frequency

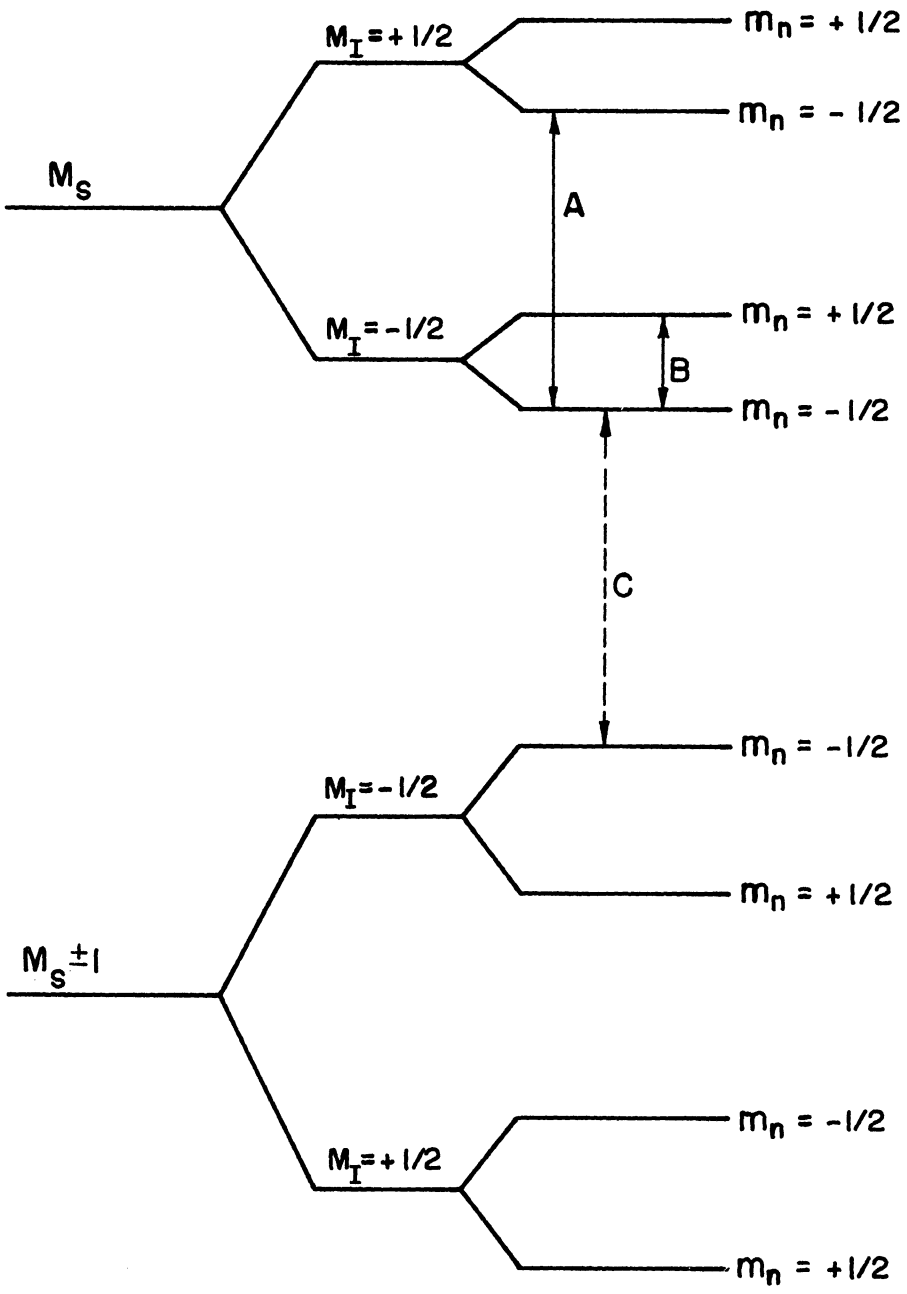

Figure 4-3. SHF Levels and ENDOR Transitions.

The frequency of transition between the states (M_S, M_I, ... m_n ...) and (M_S, M_I, ... m_n', ...) where $m_n' = m_n \pm 1$, is given by the following formula

$$h\nu_n = g_n \beta_N | \underline{H}^n_{eff} | \tag{4-73}$$

Using the expressions for the components A^n_{ij}, Equations (4-53), (4-54), and (4-55) we obtain two frequencies:

$$h\nu_{ab} = \left\{ [g_n \beta_N H_0 - M_S(A_S + A_+)]^2 + M_S^2 [A_-^2 + (3A_+ - A_-)^2] \right\}^{1/2}$$

$$\approx | g_n \beta_N H_0 - M_S (A_S + A_+) | \tag{4-74}$$

$$h\nu_c = \left\{ [g_n \beta_N H_0 - M_S(A_S - 2A_+)]^2 + 2 M_S^2 (3A_+ - A_-)^2 \right\}^{1/2}$$

$$\approx | g_n \beta_N H_0 - M_S (A_S - 2A_+) | \tag{4-75}$$

The first one corresponds to the transition $\Delta m_n = \pm 1$, where n is one of the eight a and b type cadmium. The second frequency corresponds to the change in the nuclear spin state of one of the four c type cadmium. The intensity ratio of the two lines is 2:1.

Case II: $\underline{H}_0 // [110]$

The effective magnetic field is given by

$$| \underline{H}^n_{eff} | = \frac{1}{\sqrt{2}} \left\{ \left[H_0 - \frac{M_S}{g_n \beta_N} (A^n_{xx} + A^n_{xy}) \right]^2 + \left[H_0 - \frac{M_S}{g_n \beta_N} (A^n_{yx} + A^n_{yy}) \right]^2 + \left[\frac{M_S}{g_n \beta_N} (A^n_{zx} + A^n_{zy}) \right]^2 \right\}^{1/2} \tag{4-76}$$

In this case, there are four non-equivalent sets of ligands, and hence, four different frequencies. For the transition of the set(1a, 1b, 4a, 4b)

$$h\nu_1 = \left\{ g_n^2\beta_N^2 H_0^2 + \frac{M_S^2}{2}\left[(A_S+A_+-A_-)^2+(A_S+4A_+-A_-)^2+9A_+^2\right] - g_n\beta_N H_0 M_S(2A_S+5A_+-2A_-)\right\}^{1/2}$$

$$\approx \left| g_n\beta_N H_0 - M_S\left(A_S + \frac{3}{2}A_+ - A_-\right)\right| \qquad (4\text{-}77)$$

for the set (2a, 2b, 3a, 3b)

$$h\nu_2 = \left\{ g_n^2\beta_N^2 H_0^2 + \frac{M_S^2}{2}\left[(A_S-5A_+ + A_-)^2+(A_S-2A_+ + A_-)^2+(3A_+-2A_-)^2\right]\right.$$

$$\left. - g_n\beta_N H_0 M_S(2A_S-7A_+ + 2A_-)\right\}^{1/2}$$

$$\approx \left| g_n\beta_N H_0 - M_S\left(A_S - \frac{7}{2}A_+ + A_-\right)\right| \qquad (4\text{-}78)$$

for the set (1c, 4c)

$$h\nu_3 = \left\{ g_n^2\beta_N^2 H_0^2 + M_S^2\left[(A_S+A_++A_-)^2+2(A_+-A_-)^2\right] - 2g_n\beta_N H_0 M_S(A_S+A_++A_-)\right\}^{1/2}$$

$$\approx \left| g_n\beta_N H_0 - M_S(A_S+A_++A_-)\right| \qquad (4\text{-}79)$$

and for the set (2c, 3c)

$$h\nu_4 = \left| g_n\beta_N H_0 - M_S(A_S+A_+-A_-)\right| \qquad (4\text{-}80)$$

The relative intensity is 2:2:1:1.

Case III: $\underline{H}_0 // [111]$

In this case the effective magnetic field has the magnitude

$$\left|\underline{H}_{eff}^n\right| = \frac{1}{\sqrt{3}}\left\{\left[H_0 - \frac{M_S}{g_n\beta_N}(A_{XX}^n + A_{XY}^n + A_{XZ}^n)\right]^2 + \left[H_0 - \frac{M_S}{g_n\beta_N}(A_{YX}^n + A_{YY}^n + A_{YZ}^n)\right]^2\right.$$

$$\left. + \left[H_0 - \frac{M_S}{g_n\beta_N}(A_{ZX}^n + A_{ZY}^n + A_{ZZ}^n)\right]^2\right\}^{1/2} \qquad (4\text{-}81)$$

There are three sets of non-equivalent ligands, and the frequencies are, for the set (1a, 1b, 1c)

$$h\nu_1 = \frac{1}{\sqrt{3}}\left\{\left[g_n\beta_N H_0 - M_S(A_S + 4A_+ - 2A_-)\right]^2 + 2\left[g_n\beta_N H_0 - M_S(A_S + 4A_+)\right]^2\right\}^{1/2} \qquad (4\text{-}82)$$

for the set (2b, 2c, 3a, 3c, 4a, 4b)

$$h\nu_2 = \frac{1}{\sqrt{3}}\left\{\left[g_n\beta_N H_0 - M_S(A_S + 4A_+ - 2A_-)\right]^2 + 2\left[g_n\beta_N H_0 - M_S(A_S - 2A_+)\right]^2\right\}^{1/2} \qquad (4\text{-}83)$$

for the set (2a, 3b, 4c)

$$h\nu_3 = \frac{1}{\sqrt{3}}\left\{\left[g_n\beta_N H_0 - M_S(A_S - 8A_+ + 2A_-)\right]^2 + 2\left[g_n\beta_N H_0 - M_S(A_S - 2A_+ + 2A_-)\right]^2\right\}^{1/2} \qquad (4\text{-}84)$$

The intensity ratio is 1:2:1.

Ludwig and Lorenz[21] have observed the SHF interaction between the unpaired electrons and cadmium nuclear spins in CdTe containing Cr^+ ion impurity by ENDOR. With magnetic field in $[\bar{1}10]$ direction (which is equivalent to Case II above) they observed, for $M_S = -3/2$, four lines with relative intensities 2:2:1:1 as expected in the discussion under Case II.

From the frequencies they obtained the three principal values of the A^n tensor and found that the interaction is anisotropic. The three principal values are (using their notation)

$$T_1 = (5.82 \pm 0.05) \times 10^{-4} \quad cm^{-1}$$

$$T_2 = (5.63 \pm 0.05) \times 10^{-4} \quad cm^{-1}$$

$$T_3 = (5.61 \pm 0.05) \times 10^{-4} \quad cm^{-1}$$

Isotropic part (contact term) of the SHF tensor A_s^n is given by

$$A_s^n = (T_1 + T_2 + T_3)/3 = (5.69 \pm 0.05) \times 10^{-4} \text{ cm}^{-1} .$$

This value is of the same order of, but twice larger than, the value 2.6×10^{-4} cm^{-1}, obtained by Lame and Kikuchi for CdTe:Mn . This means chromium d electrons are more delocalized than manganese d electrons. This is in the right direction as nuclear charges are compared. From the relations (4-24) and (4-25) we have, for the average probability of an electron being found at the 5s orbital of cadmium ion

$$\frac{1}{5}\left(\frac{1}{6}\gamma_{es}^2 + \frac{1}{4}\gamma_{ts}^2\right) = 0.51 \times 10^{-2} \qquad (4\text{-}85)$$

which is comparable to what a simplified MO calculation gives (see Appendix C).

Equating the observed transition frequencies to the expressions (4-77), (4-78), (4-79), and (4-80), with $M_s = -3/2$,

$$h\nu_1 = g_n\beta_N H_0 + \frac{3}{2}(A_s + \frac{5}{2}A_+ - A_-) = 20.51 \quad \text{MC/sec}$$

$$h\nu_2 = g_n\beta_N H_0 + \frac{3}{2}(A_s - \frac{7}{2}A_+ + A_-) = 21.12$$

$$h\nu_3 = g_n\beta_N H_0 + \frac{3}{2}(A_s + A_+ + A_-) = 21.04$$

$$h\nu_4 = g_n\beta_N H_0 + \frac{3}{2}(A_s + A_+ - A_-) = 20.42$$

From the higher intensity lines ($h\nu_1$ and $h\nu_2$), we have

$$A_- - 3A_+ = A_T = 0.2 \text{ MC/sec}$$

and from the two lines ($h\nu_3$ and $h\nu_4$) of lower intensity,

$$A_- = 0.21 \text{ MC/sec}$$

The observed values of frequencies are very close to each other, hence the above calculations are subject to large errors. We can only say that the above results show that $A_+ = 1/2(A_M + A_C)$ is very small compared to $A_- = 3/2(A_M + A_C) + A_T$ which essentially equals to A_T, the contribution from tellurium orbitals. From Equation (4-41) and $g_{Cd} \approx 1.2$, $R_{TC} = 5.25$ a.u., we have

$$A_T = \frac{2}{5}\beta_e g_n \beta_N R_{TC}^{-3}\left\{\frac{1}{2}\beta_{e\pi}^2 + \frac{1}{4}\beta_{ts}^2 + \frac{1}{4}\beta_{tz}^2 + \frac{3}{4}\beta_{t\pi}^2\right\}$$

$$= (0.8)\frac{1}{5}\left\{\frac{1}{2}\beta_{e\pi}^2 + \frac{1}{4}\beta_{ts}^2 + \frac{1}{4}\beta_{tz}^2 + \frac{3}{4}\beta_{t\pi}^2\right\} \quad \text{MC/sec}$$

which gives for the probability of an electron being found at tellurium orbitals

$$\frac{1}{5}\left\{\frac{1}{2}\beta_{e\pi}^2 + \frac{1}{4}\beta_{ts}^2 + \frac{1}{4}\beta_{tz}^2 + \frac{3}{4}\beta_{t\pi}^2\right\} = 0.25 \qquad (4\text{-}86)$$

From the fact that no SHF structure of nearest ligand is observed, we can conclude that most part of this probability is due to the p orbitals and not the s orbital of tellurium. This probability is much larger than that obtained by simplified MO calculations as shown in Appendix C.

The fact that A_T is the largest component among the three (A_M, A_T, and A_C) components of dipole-dipole interaction has an important meaning. It can be seen from Equation (4-46) that this component makes the σ axis (Mn-Cd direction) not one of the principal axes of A^n tensor, and also it makes π axis not equivalent to μ axis. The latter is one of the principal axes.

The fact that A_+ is very small explains why the anisotropy of $\underline{\underline{A}}^n$ is not observed in Lambe and Kikuchi's EPR experiment. Equation (4-66) shows that A_+ appears in the expression of transition energy, but not A_-.

CHAPTER V

SUPERHYPERFINE STRUCTURE IN $SnO_2:V^{4+}$

A. Structure of the "Complex"

The crystal structure of tin oxide (SnO_2) belongs to tetragonal D_{4h} group. In this structure atoms are located at the following positions: (Figure 5-1)

Sn : (0,0,0), (1/2, 1/2, 1/2)

O : $\pm$(u,u,0), $\pm$(u + 1/2, 1/2 - u, 1/2)

The lattice parameters a, c, and u are given in Figure 5-1.

The symmetry of the substitutional site in this crystal is, however, orthorhombic D_{2h}, (Figure 5-2). Using the coordinate system of Figures 5-1 and 5-2, (following From, Kikuchi, and Dorain[18]) the six nearest ligands, oxygen ions, are located in x-y plane (1,2,3,4) and on z axis (5,6). Ten next nearest ligands, tin, are classified into three types: (i) two "a" tins, (15,16) which are closest to the impurity ion and lie on the y-axis; (ii) four "b" tins (7,8,9,10) which lie in the x-y plane; and (iii) four "c" tins (11,12,13,14) which lie in the y-z plane and at the same distance as "b" tins from the impurity ion. The distances and bond angles are given in Figure 5-2.

Symmetry characters of vanadium orbitals and linear combinations of ligand orbitals in D_{2h} group are given in Table 5-1.

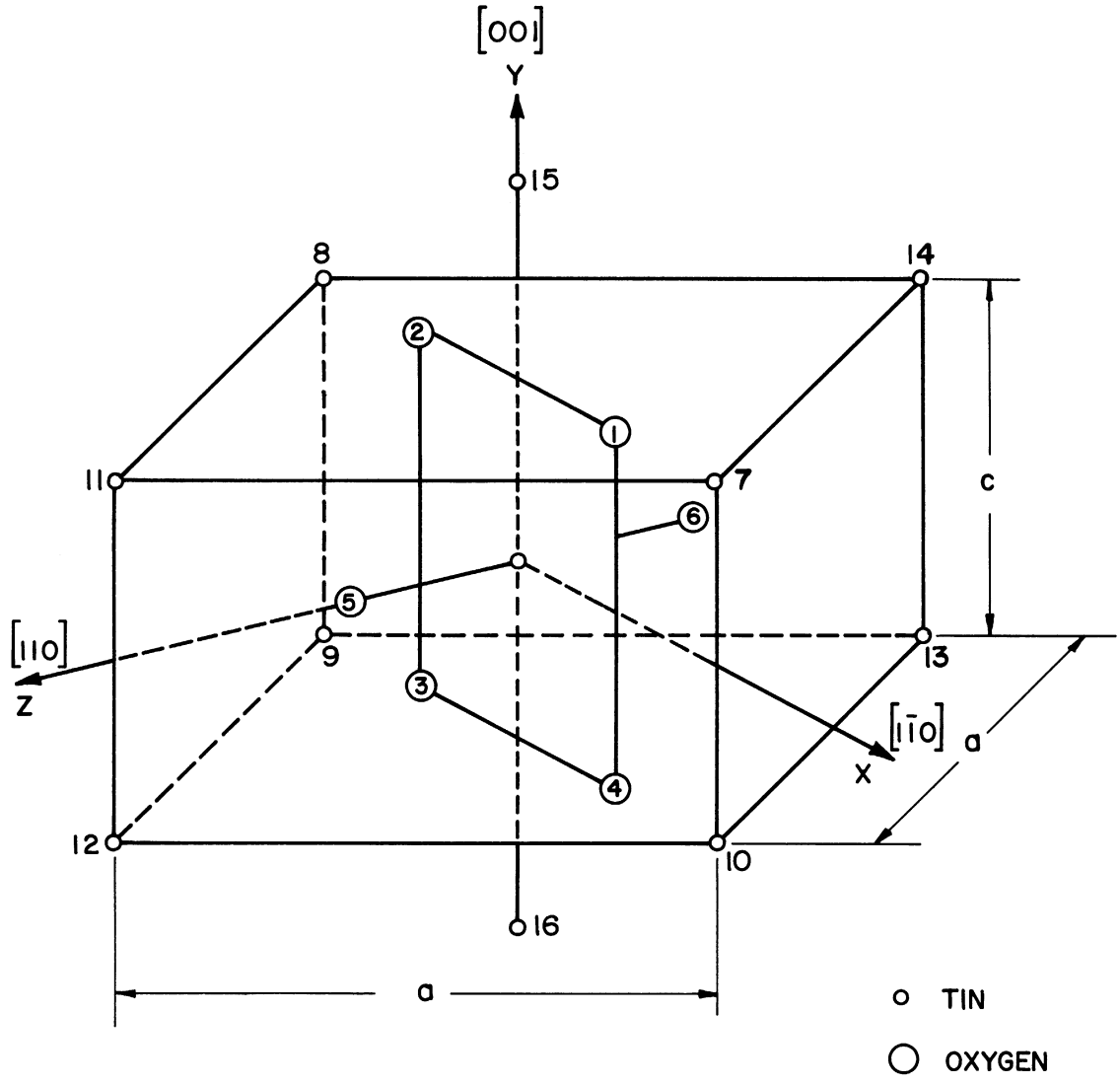

Lattice Parameter	a(A)	c(A)	u	c/a
SnO_2	4.737	3.185	0.307	.6724
TiO_2	4.594	2.959	0.306	.6441

Figure 5-1. Unit Cell of SnO_2 (TiO_2).

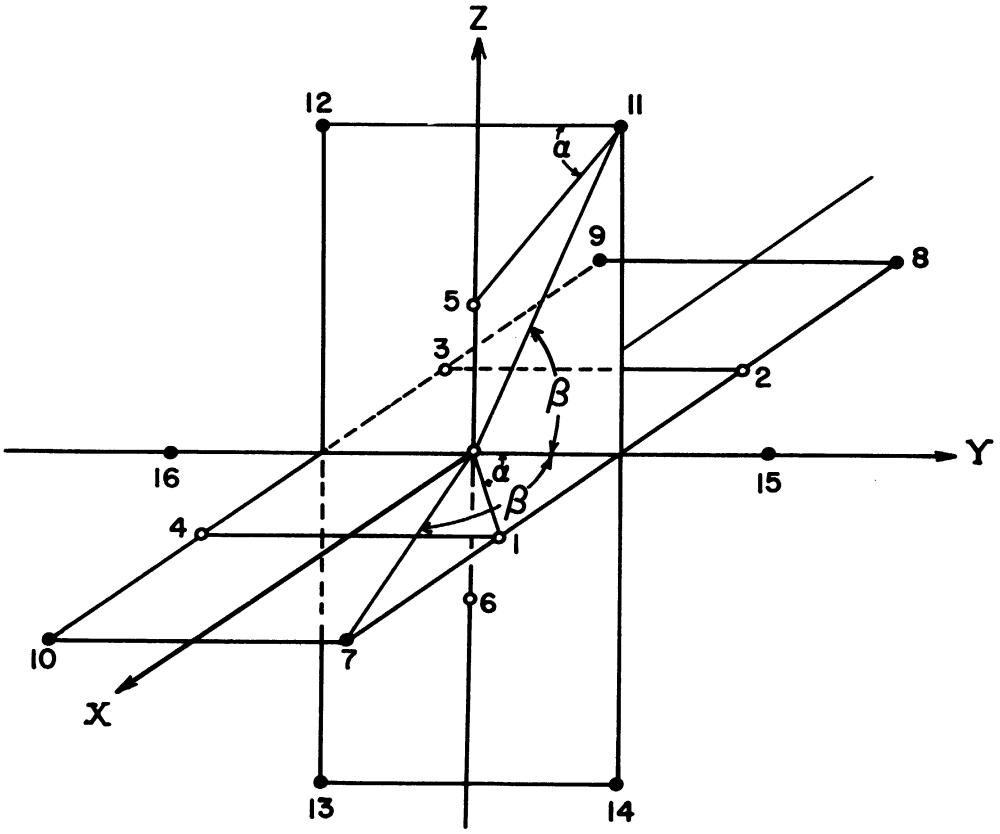

Distance and Angles	SnO_2	TiO_2
$d_{1,4} = d_{0.15} = C$	3.185 A°	2.959 A°
$d_{1,2} = \sqrt{2}(1-2u)a$	2.586	2.521
$d_{7,8} = d_{11,14} = \sqrt{2}a$	6.699	6.497
$d_{0,5} = \sqrt{2}\ ua$	2.057	1.988
$d_{0,1} = [2(\frac{1}{2} -u)^2a^2 + c^2/4]^{1/2}$	2.051	1.944
$d_{0,7} = d_{0,11} = \frac{1}{2}(c^2 + 2a^2)^{1/2}$	3.709	3.569
Cosα	.7763	.7612
Sinα	.6303	.6485
Cosβ	.4294	.4145
Sinβ	.9031	.9102

Figure 5-2. Nearest and Next Nearest Ligands of V^{4+} in SnO_2 (TiO_2).

TABLE 5-1

SYMMETRY CHARACTERS OF ORBITALS IN SnO_2:V

Ir. Rep.	V Orbital	O in x-y Plane	O on z Axis	a Tins	b Tins	c Tins
N_1	4s	$s_1 + s_2 + s_3 + s_4$	$s_5 + s_6$	$s_{15} + s_{16}$	$s_7 + s_8 + s_9 + s_{10}$	$s_{11} + s_{12} + s_{13} + s_{14}$
	$3z^2-r^2$	$x_1 - x_2 - x_3 + x_4$	$z_5 - z_6$	$y_{15} - y_{16}$	$x_7 - x_8 - x_9 + x_{10}$	$y_{11} - y_{12} - y_{13} + y_{14}$
	x^2-y^2	$y_1 + y_2 - y_3 - y_4$			$y_7 + y_8 - y_9 - y_{10}$	$z_{11} + z_{12} - z_{13} - z_{14}$
N_2	zx	$z_1 - z_2 - z_3 + z_4$	$x_5 - x_6$		$z_7 - z_8 - z_9 + z_{10}$	$x_{11} + x_{12} - x_{13} - x_{14}$
N_3	xy	$x_1 + x_2 - x_3 - x_4$		$x_{15} - x_{16}$	$x_7 + x_8 - x_9 - x_{10}$	$x_{11} - x_{12} - x_{13} + x_{14}$
		$y_1 - y_2 - y_3 + y_4$			$y_7 - y_8 - y_9 + y_{10}$	
		$s_1 - s_2 + s_3 - s_4$			$s_7 - s_8 + s_9 - s_{10}$	
N_4	yz	$z_1 + z_2 - z_3 - z_4$	$y_5 - y_6$	$z_{15} + z_{16}$	$z_7 + z_8 - z_9 - z_{10}$	$s_{11} - s_{12} + s_{13} - s_{14}$
						$y_{11} + y_{12} - y_{13} - y_{14}$
						$z_{11} - z_{12} - z_{13} + z_{14}$

B. Ground State of V^{4+} in SnO_2

According to point charge model crystal field theory, and using the coordinate system of Figure 5-2, the splitting of d electron levels in rhombic crystal field of SnO_2 is as shown in the following figure (Figure 5-3).

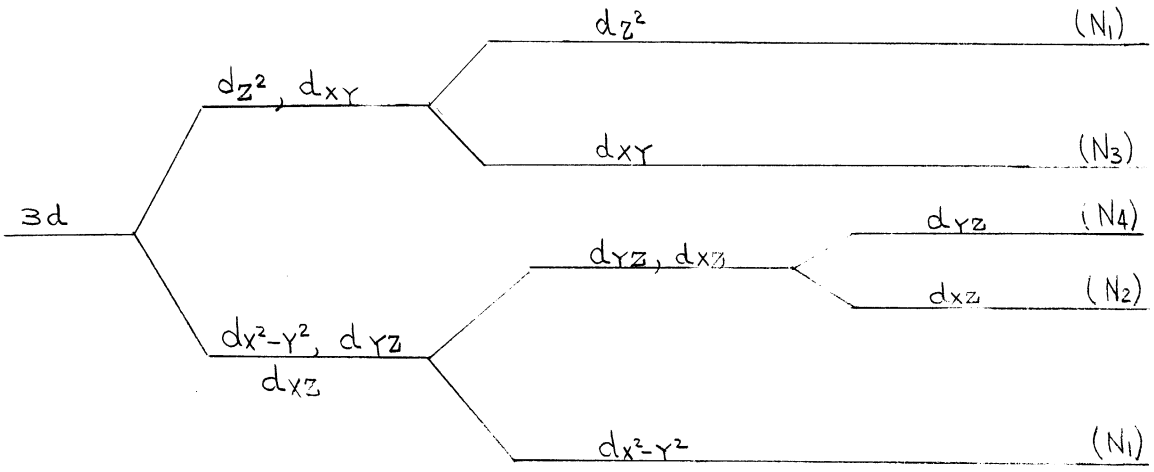

Figure 5-3. Splitting of d Levels in Crystalline Field of SnO_2.

The relative positions of d_{xz}, d_{yz} and $d_{x^2-y^2}$ cannot be determined intuitively based on point charge model. In the EPR experiment on $SnO_2:V^{4+}$, From, et al.[18] observed (see Table 5-2): (i) large Δg_y; (ii) large $\Delta A_z = A_z - A_s$, ΔA_x and ΔA_y have opposite signs to ΔA_z; (iii) large superhyperfine interaction with "a" tins. These results suggest that $d_{x^2-y^2}$ lies lowest. Thus the ground state consists of mainly $d_{x^2-y^2}$and small amount of d_{xz} admixed through spin-orbit interaction.

TABLE 5-2

RESULTS OF EPR EXPERIMENT ON $S_nO_2:V^{4+}$(18)

		x	y	z
g		1.939	1.903	1.943
HFS	A (gauss)	23.3	47.03	154.4
SHFS	a (gauss)	~166.	172.6	165.2
SHFS	b (gauss)	~ 28	28	28

C. Mechanism of SHF Interaction[35]

In this section we shall discuss the mechanism of SHF interaction as inferred from the large and small SHF structure observed by From, et al. in the EPR spectrum of $SnO_2:V^{4+}$. (Table 5-2)

SHF interaction is proportional to the density of unpaired electron at the ligand nucleus. We shall apply molecular orbital theory to obtain an expression for this density and compare the result with experimental observation.

Consider three orbitals: (i) vanadium d orbital U_v, (ii) nearest ligand oxygen orbital, U_o, and (iii) next nearest ligand tin orbitals U_s. We can construct three orthogonal molecular orbitals from the linear combinations of these three orbitals. They are:

$$\psi_a = U_v + \beta_a U_o + \gamma_a U_s \tag{5-1}$$

$$\psi_b = \alpha_b U_v + U_o + \gamma_b U_s \tag{5-2}$$

$$\psi_c = \alpha_c U_v + \beta_c U_o + U_s \tag{5-3}$$

where the coefficients (assumed to be real) α, β, γ, and the overlap integrals

$$S_{vo} = \int U_v^* U_o \, d\tau \tag{5-4}$$

etc., are small quantities of the same order and if small quantities of higher order than this are neglected the MO's are normalized.

A schematic diagram of the energy levels of MO's and AO's is shown in Figure 5-4.

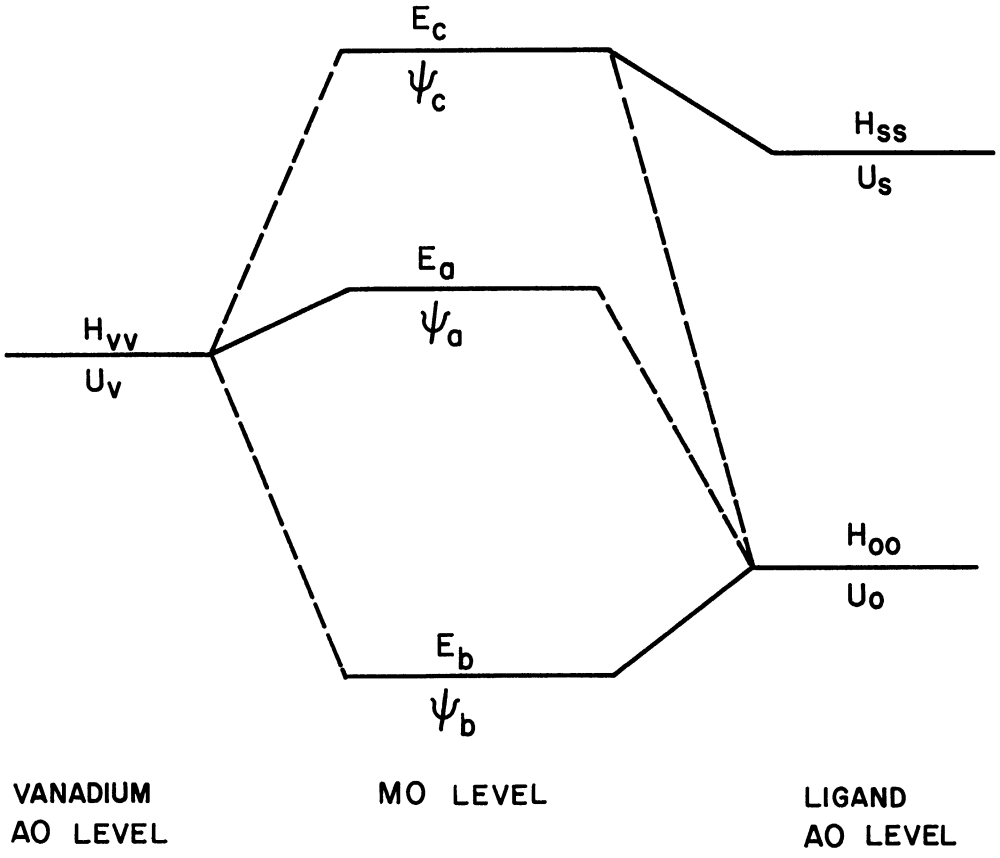

Figure 5-4. Schematic Energy Level Diagram for $SnO_2:V^{4+}$.

From the orthogonality relations

$$\int \psi_i^* \psi_j \, d\tau = 0, \quad i \neq j, \quad i, j = a, b, c \tag{5-5}$$

we have,

$$\beta_a = -(S_{V0} + \alpha_b) \tag{5-6}$$

$$\gamma_a = -(S_{VS} + \alpha_c) \tag{5-7}$$

$$\gamma_b = -(S_{0S} + \beta_c) \tag{5-8}$$

The coefficients α_b, α_c and β_c can be obtained from the secular equation (2-7),

$$\sum_{\nu}(H_{\mu\nu} - E_i S_{\mu\nu}) C_{i\nu} = 0, \quad \begin{matrix} \mu, \nu = V, 0, S \\ i = a, b, c \end{matrix} \tag{5-9}$$

where $H_{\mu\nu}$ is the matrix element of the effective one-electron Hamiltonian between two AO's U_μ and U_ν; $C_{i\nu}$ is the coefficient of AO U_ν in MO ψ_i. Let $E_i = E_b$, the energy of MO ψ_b, and $\mu = V$, we have

$$(H_{VV} - E_b)\alpha_b + (H_{V0} - E_b S_{V0}) + (H_{VS} - E_b S_{VS})\gamma_b = 0 \tag{5-10}$$

In Wolfsberg and Helmholz's semi-empirical MO method,[26] the off-diagonal elements $H_{\mu\nu}$'s are approximated by, (Equation 2-10),

$$H_{\mu\nu} = K_{\mu\nu} S_{\mu\nu} \tag{5-11}$$

where $K_{\mu\nu}$ is a factor depending on the energies of AO's U_μ and U_ν only. Hence the last term in Equation (5-10) is one order of magnitude smaller than the other two terms. By neglecting this term, we have,

$$\alpha_b = (S_{V0} E_b - H_{V0})/(H_{VV} - E_b) \tag{5-12}$$

Similarly, for $E_i = E_c$, $\mu = V$, we get

$$\alpha_c = (S_{VS} E_c - H_{VS})/(H_{VV} - E_c) \tag{5-13}$$

and for $E_i = E_c$, $\mu = 0$, we have

$$\beta_c = (S_{0S} E_c - H_{0S})/(H_{00} - E_c) \tag{5-14}$$

The lowest and next lowest energy configurations of this three-electron system are, respectively

$$\Psi_1 = \{ \psi_a^+, \psi_b^+, \psi_b^- \} \tag{5-15}$$

and

$$\Psi_2 = \{ \psi_a^+, \psi_b^+, \psi_a^- \} \tag{5-16}$$

where $\{\ \}$ represents Slater determinant and $\pm$ signs superscript the MO represent the spin functions. In the second configuration an electron is transferred from the filled MO ψ_b to unpaired MO ψ_a. The ground state wave function of this system can be written as the linear combination of these two configurations:

$$\begin{aligned} \Psi &= \Psi_1 + \lambda \Psi_2 \\ &= \{ \psi_a^+, \psi_b^+, (\psi_b^- + \lambda \psi_a^-) \} \end{aligned} \tag{5-17}$$

The unpaired spin density ρ_s can be obtained by

$$\rho_s(r) = \int \Psi^* \sum_{k=1}^{3} \sigma_z(k) \Psi \, d\tau'_k \tag{5-18}$$

where $\sigma_z(k)$ is the third component of Pauli spin matrices for electron k, and

$$d\tau'_k = d\tau_1 d\tau_2 d\tau_3 / d\tau_k \qquad k = 1, 2, 3. \tag{5-19}$$

Carrying out the integration, we have

$$\begin{aligned} \rho_s(r) &= \sum_i \psi_i^* \sigma_z \psi_i \\ &= |\psi_a(r)|^2 + |\psi_b(r)|^2 - |\psi_b(r) + \lambda \psi_a(r)|^2 \end{aligned} \tag{5-20}$$

At the nucleus of the next nearest ligand $\underline{r}_s$,

$$\psi_a(r_s) \approx \gamma_a U_s(0) \ , \quad \psi_b(r_s) \approx \gamma_b U_s(0) \tag{5-21}$$

hence,

$$\begin{aligned} \rho_s(r_s) &= |U_s(0)|^2 \{ \gamma_a^2 + \gamma_b^2 - (\gamma_b + \lambda \gamma_a)^2 \} \\ &\approx |U_s(0)|^2 (\gamma_a - \lambda \gamma_b)^2 \end{aligned} \tag{5-22}$$

Substituting the relations (5-7), (5-8), (5-13), (5-14), we have

$$\begin{aligned} \rho_s(r_s) &= |U_s(0)|^2 \left\{ S_{vs} + \frac{S_{vs}E_c - H_{vs}}{H_{vv} - E_c} - \lambda \left(S_{os} + \frac{S_{os}E_c - H_{os}}{H_{oo} - E_c} \right) \right\}^2 \\ &= |U_s(0)|^2 \left\{ S_{vs} \left(\frac{H_{vv} - K_{vs}}{H_{vv} - E_c} \right) - \lambda S_{os} \left(\frac{H_{oo} - K_{os}}{H_{oo} - E_c} \right) \right\}^2 \end{aligned} \tag{5-23}$$

This result shows that there are two electron transfer processes which cause the SHF interaction. The first, which is represented by the

term γ_a in Equation (5-22), comes from the transfer of impurity d electron to the ligand orbital, or in other words, formation of anti-bonding MO ψ_a. The second process, which is represented by the term $\lambda\gamma_b$ in Equation (5-22), comes from the transfer of ligand electron into impurity ion orbital, or in other words, the mixture of higher energy configuration Ψ_2.

The quantity λ can be obtained by perturbation theory:

$$\lambda = \frac{\langle \Psi_1 | \mathcal{H} | \Psi_2 \rangle}{\langle \Psi_1 | \mathcal{H} | \Psi_1 \rangle - \langle \Psi_2 | \mathcal{H} | \Psi_2 \rangle} \tag{5-24}$$

where $\mathcal{H}$ is the system Hamiltonian. If we assume that it can be approximated by a sum of effective one-electron Hamiltonian H, then we have

$$\lambda = \frac{\langle \psi_a | H | \psi_b \rangle}{\langle \psi_b | H | \psi_b \rangle - \langle \psi_a | H | \psi_a \rangle} = \frac{\alpha_b H_{VV} + \beta_a H_{OO} + H_{VO}}{E_b - E_a}$$

$$= \frac{(S_{VO} H_{VV} - H_{VO})(E_b - H_{OO})}{(H_{VV} - E_b)(E_b - E_a)}$$

$$= S_{VO} \left\{ \left(\frac{H_{VV} - K_{VO}}{H_{VV} - E_b} \right) \left(\frac{E_b - H_{OO}}{E_b - E_a} \right) \right\} \tag{5-25}$$

to first order in small quantities α, β, etc. We have used the relations (5-6), (5-11) and (5-12) in obtaining Equation (5-25). This equation shows that λ is a quantity of the order of overlap integral S_{VO}. Thus the second process of electron transfer is less important than the first one. Also we see from Equation (5-23) that the first process is proportional to the square of the overlap integral S_{VS}.

In order to compare this result with the experimental observation, calculations of overlap intergrals are made by using the following Slater radial functions and Hartree-Fock radial function obtained by Watson[25]:

Vanadium 3d

$$\psi_{Slater}(V3d) = \phi_3(1.43) \tag{5-26}$$

$$\psi_{HF}(V3d) = .5243\,\phi_3(1.83) + .4989\,\phi_3(3.61) + .1131\,\phi_3(6.80) + .0055\,\phi_3(12.43) \tag{5-27}$$

V^{4+} 3d

$$\psi_{Slater}(V^{4+}3d) = \phi_3(1.67) \tag{5-28}$$

Tin 5s

$$\psi_{Slater}(Sn\,5s) = \phi_4(1.412) \tag{5-29}$$

where

$$\phi_n(\mu) = N_{n\mu}\, r^{n-1} e^{-\mu r} \tag{5-30}$$

and

$$N_{n\mu} = \left[(2\mu)^{2n+1} / (2n)! \right]^{1/2} \tag{5-31}$$

The overlap integrals between $3d_{x^2-y^2}$ orbital and the 5s orbitals of "a" tins and "b" tins are given in Table 5-3. We have used the radial functions of neutral atoms based on the electroneutrality principle of Pauling.[36] However, we have also considered the 3d orbital of V^{4+} ion. For all cases, the square of the ratio of overlap integrals is in

TABLE 5-3

VANADIUM-TIN OVERLAP INTEGRALS

	S_{vs} (Slater 3d Orbital) V^o (Neutral)	V^{4+}	S_{vs} (HF 3d orbital)
a Sn	-0.1313	-0.0910	-0.04212
b Sn	0.0583	0.0379	0.01640
$\left[\frac{S_{vs}(a)}{S_{vs}(b)}\right]^2$	5.08	5.76	6.60

TABLE 5-4

VANADIUM-OXYGEN OVERLAP INTEGRALS*

$< 3d_{x^2-y^2} \mid 2S >$	- 0.01932
$< 3d_{x^2-y^2} \mid 2P_x >$	0.06652
$< 3d_{x^2-y^2} \mid 2P_y >$	- 0.02805

* Vanadium 3d orbital is the Hartree-Fock function given in Equation (5-27). Oxygen functions are

$$R(2S) = 0.5459\ \phi_2\ (1.80) + 0.4839\ \phi_2\ (2.80)$$

$$R(2P) = 0.6804\ \phi_2\ (1.55) + 0.4038\ \phi_2\ (3.43)$$

obtained by fitting the numerical Hartree-Fock functions.(27)

good agreement with the ratio of the experimentally observed SHF structure constants, which is 6.

The overlap integrals between vanadium orbital and nearest ligand oxygen orbitals are given in Table 5-4. The results show that for this complex, the assumption that all overlap integrals are of the same order is justified.

D. Anisotropic Component of SHF Tensor

The dipole-dipole interaction which contributes to the anisotropic part of SHF tensor can be treated in the same way as we did in Chapter IV, Section B. The result is

$$\Delta A_x^n = A_x^n - A_s^n = 2\beta_e g_n \beta_N \{ R_{vn}^{-3}(3\cos^2\theta_x - 1) + \sum_m R_{mn}^{-3}(3\cos^2\theta_{mx} - 1)\beta_m^2 + \zeta \langle r^{-3} \rangle_{5p} \langle p|l(l+1) - 3l_x^2|p\rangle \gamma_{np}^2 \} \quad (5\text{-}32)$$

where $\underline{R}_{vn}$, $\underline{R}_{mn}$ are the distances from vanadium and oxygen m to tin n respectively: θ_x, θ_{mx}, are the angles between $\underline{R}_{vn}$, $\underline{R}_{mn}$ and x axis respectively. β_m^2 , γ_{np}^2 are respectively the probabilities that the unpaired electron being found in orbitals of oxygen m, and 5p orbital of tin n. ζ is given by Equation (4-35). With the subscript x replaced by y and z respectively, we can obtain ΔA_y^n and ΔA_z^n. Off-diagonal elements A_{xy}^n etc. vanishes in this structure.

In $SnO_2:V^{4+}$, the explicit expressions for the SHF tensor components are,

for "a" tins:

$$\Delta A_x^a = -A_V^a + .192\, A_0^a - A_T^a \quad (5\text{-}33)$$

$$\Delta A_y^a = 2A_V^a + .808A_0^a + 2A_T^a \tag{5-34}$$

$$\Delta A_z^a = -A_V^a - A_0^a - A_T^a \tag{5-35}$$

where

$$A_V^a = 2g_n\beta_e\beta_N(3.185\times10^{-8})^{-3} \tag{5-36}$$

$$A_0^a = 4g_n\beta_e\beta_N(2.051\times10^{-8})^{-3}\beta_1^2 \tag{5-37}$$

$$A_T^a = 2g_n\beta_e\beta_N\zeta\langle r^{-3}\rangle_{5p}\gamma_{15p}^2 \tag{5-38}$$

and for "b" tins:

$$\Delta A_x^b = 1.447A_V^b + 2A_0^b + 2A_{TX}^b - A_{TY}^b \tag{5-39}$$

$$\Delta A_Y^b = -.447A_V^b - A_0^b - A_{TX}^b + 2A_{TY}^b \tag{5-40}$$

$$\Delta A_z^b = -A_V^b - A_0^b - A_{TX}^b - A_{TY}^b \tag{5-41}$$

where

$$A_V^b = 2g_n\beta_e\beta_N(3.709\times10^{-8})^{-3} \tag{5-42}$$

$$A_0^b = 2g_n\beta_e\beta_N(2.057\times10^{-8})^{-3}\beta_1^2 \tag{5-43}$$

$$A_{TX}^b = 2g_n\beta_e\beta_N\zeta\langle r^{-3}\rangle_{5p}\gamma_{7x}^2 \tag{5-44}$$

$$A_{TY}^b = 2g_n\beta_e\beta_N\zeta\langle r^{-3}\rangle_{5p}\gamma_{7Y}^2 \tag{5-45}$$

with γ_{7x}^2, γ_{7y}^2 respectively the fraction of $5p_x$, $5p_y$ orbitals of b tin (e.g., tin-7) in the ground antibonding MO.

Anisotropy is not observed in the SHF structure due to b tins. This can be expected as the parameters A_v^b, A_o^b and A_T^b are smaller than the corresponding parameters for a tins. Also from Equations (5-33), (5-34), and (5-35) we see that ΔA_y^a is positive and the largest; ΔA_z^a is negative and the smallest. This agrees with the experimental results of From, et al. (Table 5-2).

CHAPTER VI

SUMMARY AND CONCLUSION

The purpose of this thesis has been to study the delocalization of d electrons from their interaction with next nearest ligand spins, the so-called superhyperfine (SHF) interaction.

The electrons are described by molecular orbitals (MO) formed from linear combinations of atomic orbitals of the central and ligand (nearest and next nearest) ions.

The Hamiltonian for the interaction between electrons and nuclear spins are derived from the non-relativistic limit of the Dirac relativistic wave equation. This Hamiltonian is used to obtain the SHF interaction tensor A^n in terms of MO parameters (mixing coefficients) and geometry factors (interionic distances and bond angles). The details of derivation are given for the next nearest ligands in cubic $A_{II}B_{VI}$ compounds containing S state iron group ions. However, the formulation is quite general and can be easily applied to complexes of other structures.

Electron spin resonance (ESR) and electron-nuclear double resonance (ENDOR) spectra are related to the components of SHF interaction tensor. An attempt is made to deduce the amount of d electron delocalization from these relations. Unfortunately, existing experimental results are not precise enough to give more than "of the order of magnitude" values.

The delocalization at next nearest ligand s orbital is found to be 0.2 and 0.5%, respectively, for Mn^{++} and Cr^{+} in CdTe. The values are obtained by comparing the measured isotropic SHF structures with the isotropic hyperfine structure constant of atomic cadmium. Rigorously, we should use the value for cadmium in crystal. However, this has not been obtained either experimentally or theoretically. Watson and Freeman[37] have reported 20% increase in isotropic hyperfine structure constant for Ni^{++} in cubic crystalline field by unrestricted Hartree-Fock calculation. If this trend is also true for cadmium in crystal, it will lead to smaller value for the delocalization and in better agreement with the results of simplified MO calculations (Appendix C), which will be discussed in the following.

Simplified MO calculation of CdTe:Mn^{++} using Slater radial functions and atomic spectroscopic data gives a value 0.1% for the amount of delocalization at cadmium 5s orbital. Similar calculation for ZnS:Mn^{++}, using Hartree-Fock radial functions and one electron orbital energies gives 0.01% for the amount of delocalization at zinc 4s orbital. Experimentally, SHF structures for zinc and cadmium are proportional to their nuclear magnetic moments. Hence if the above mentioned amounts of delocalization (differ by one order of magnitude) are true, then the unpaired spin density at the nucleus of zinc (when there is one electron in 4s orbit) should be one order of magnitude larger than that of cadmium (when there is one electron in 5s). Although this is in the correct direction a factor of ten is by no means obvious. Unrestricted Hartree-Fock calculation can be suggested

for further investigation of this point. The use of two different systems of radial functions is a defect in this analysis. A systematic Hartree-Fock calculations of Groups II and VI elements (for neutral, univalent, and divalent ions) are necessary for further studies of Group II-VI compounds.

Anisotropic SHF structure data are needed to deduce the amount of delocalization at the nearest and next nearest ligand p orbitals. Experimentally observed anisotropies are, in all cases, small and subject to large experimental error. The development of ENDOR technique has already shown the possibility of refined measurement. The molecular orbital formulation of SHF structure as developed in this work, combined with existing experimental data, can be used to guide experimentalists to the best observation as has been pointed out in Chapter IV, Section C.

In spite of the existence of small but finite abundance of odd isotope, no SHF structure due to nearest ligands has been observed. The overlap integral between Mn^{++} 3d orbital and Te 5s is comparable to that between Mn^{++} 3d and Te 5p, and even larger than that between 3d and Cd 5s (see Appendix C). Yet no observation of SHF structure means that the Te 5s level lies far below Mn^{++} 3d, and essentially can be removed from bonding orbitals. From Mössbauer experiment on MnTe crystal, Shikazono[38] also found that no internal magnetic field exists at the Te nucleus in MnTe. Further confirmation may be obtained by investigating the ESR of odd isotope enriched samples.

The unpaired spin density at next nearest ligand nucleus derived in Chapter V has also included the mechanism of charge transfer

from ligand to central ion, although this mechanism has been shown to be less important for $SnO_2:V^{4+}$. The more important mechanism: - direct interaction between central and next nearest ligand ions has been shown to be proportional to the square of overlap integral. This is a generalization of the Heitler-London model used by Marshall and Stuart.[12] Further investigation of this proportionality can be attained by pressure experiments in which overlap integrals are largely affected while the second factor - energy difference - varies rather slowly, Equation (5-23).

As we have seen, the deduction of d electron delocalization from SHF structure data necessitates further information, both experimental and theoretical. The development of ENDOR technique and electronic computational facility casts delightful future on this approach.

APPENDIX A

OVERLAP INTEGRALS

In this appendix we describe the method of computing the overlap integrals appeared in the discussions of Chapter II, IV and V. Some formulae of the diatomic overlap integrals and IBM 7090 computer programs for the evaluation of the numerical values of overlap integrals are also given.

The first step in the evaluation of the overlap integral between two atomic orbitals in a complex is to transform the coordinates of the two centers (ions) such that they are related to each other in the same way as the "a" and "b" coordinates of Mulliken, et al.[39] in their calculations of diatomic overlap integrals (see Figure A-1)

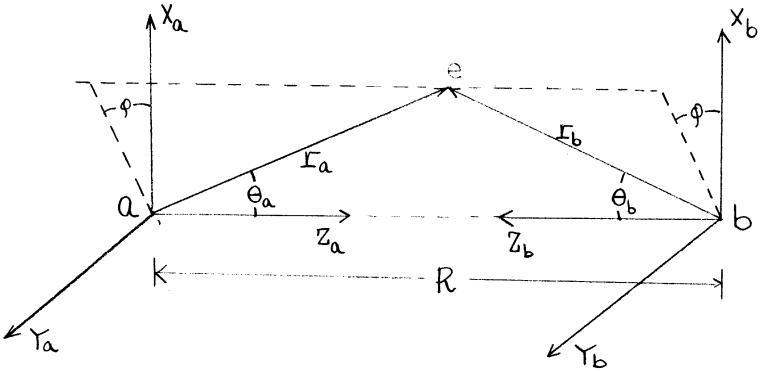

Figure A-1. Coordinates for Overlap Integral Calculations.

In this set of coordinates, the z axes (z_a and z_b) are pointing toward each other, and the two x axes and two y axes are parallel. Thus if the "a" coordinates is a right handed system, then "b" coordinates is a left handed system, and vice versa. We use the former choice. Examples of transformation matrices are given in Table A-1, A-2, and A-3.

The next step is to introduce the ellipsoidal coordinates (ξ, η, φ) defined by

$$\xi = (r_a + r_b)/R \quad , \qquad 1 \leq \xi \leq \infty \tag{A-1}$$

$$\eta = (r_a - r_b)/R \quad , \qquad -1 \leq \eta \leq 1 \tag{A-2}$$

$$\varphi = \varphi_a = \varphi_b \quad , \qquad 0 \leq \varphi \leq 2\pi \tag{A-3}$$

$$d\tau = \left(\frac{R}{2}\right)^3 (\xi^2 - \eta^2)\, d\xi\, d\eta\, d\varphi \tag{A-4}$$

where R is the interionic distance. Some other useful relations between a, b coordinates and (ξ, η, φ) are:

$$r_a \cos\theta_a = R(1 + \xi\eta)/2 \tag{A-5}$$

$$r_b \cos\theta_b = R(1 - \xi\eta)/2 \tag{A-6}$$

$$r_a \sin\theta_a = r_b \sin\theta_b = R(\xi^2 - 1)^{\frac{1}{2}}(1 - \eta^2)^{\frac{1}{2}} \tag{A-7}$$

The two orbitals for which the overlap integral is to be evaluated are written as Slater type orbitals (STO) (in atomic unit), for example:

$$|n_a d\sigma\rangle = N_a r_a^{n_a^* - 1} \exp(-Z_a^* r_a / n_a^*)\, Y_{20}(\theta_a, \varphi_a) \tag{A-8}$$

$$|n_b p\sigma\rangle = N_b r_b^{n_b^*-1} \exp\left(-Z_b^* r_b/n_b^*\right) Y_{10}(\theta_b, \varphi_b) \qquad \text{(A-9)}$$

where Z^* and n^* are effective nuclear charge and effective principal quantum number respectively of the orbital. The normalization factor N is given by

$$N = \left(2Z^*/n^*\right)^{n^*+\frac{1}{2}} \Big/ \sqrt{(2n^*)!} \qquad \text{(A-10)}$$

Using the relations (A-1, ...7), the integral $\langle n_a d\sigma | n_b p\sigma\rangle$ can be written in terms of (ξ, η, φ) as follows:

$$\begin{aligned}\langle n_a d\sigma | n_b p\sigma\rangle &= N_a N_b \int \exp\left(-\frac{Z_a^*}{n_a^*} r_a - \frac{Z_b^*}{n_b^*} r_b\right) r_a^{n_a^*-1} \sqrt{\frac{5}{16\pi}}(3\cos^2\theta_a - 1) \\ &\quad \times r_b^{n_b^*-1} \sqrt{3/4\pi}\cos\theta_b \, d\tau \\ &= N_a N_b \frac{\sqrt{15}}{8\pi}\left(\frac{R}{2}\right)^{n_a^*+n_b^*+1} \int_1^\infty d\xi \int_{-1}^1 d\eta \int_0^{2\pi} d\varphi \left\{\left[\exp(-p\xi - q\eta)\right](\xi+\eta)^{n_a^*-3}\right. \\ &\quad \left. \times \left[3(1+\xi\eta)^2 - (\xi+1)^2\right](\xi-1)^{n_b^*-2}(1-\xi\eta)(\xi^2-\eta^2)\right\} \\ &= N_a N_b \frac{\sqrt{15}}{4}\left(\frac{R}{2}\right)^{n_a^*+n_b^*+1} \sum_{i\,j} C_{ij} A_i(p) B_j(q) \end{aligned} \qquad \text{(A-11)}$$

where

$$p = \frac{R}{2}\left\{Z_a^*/n_a^* + Z_b^*/n_b^*\right\} \qquad \text{(A-12)}$$

$$q = \frac{R}{2}\left\{Z_a^*/n_a^* - Z_b^*/n_b^*\right\} \qquad \text{(A-13)}$$

$$A_i(p) = \int_1^\infty \xi^i e^{-p\xi} d\xi \qquad \text{(A-14)}$$

$$B_j(q) = \int_{-1}^1 \eta^j e^{-q\eta} d\eta \qquad \text{(A-15)}$$

and C_{ij} is the coefficient of the term $\xi^i \eta^j$ in the polynomial in the integrand.

The integrals A_i and B_j can be evaluated by the recursion formulae:

$$A_0(p) = \frac{1}{p} \exp(-p) \tag{A-16}$$

$$A_i(p) = A_0(p) + \frac{i}{p} A_{i-1}(p) \tag{A-17}$$

$$B_0(q) = \frac{1}{q}\left[e^{q} - e^{-q}\right] \tag{A-18}$$

$$B_j(q) = \frac{1}{q}\left[(-1)^j e^{q} - e^{-q} + j\, B_{j-1}(q)\right] \tag{A-19}$$

In case $|q|$ is very small ($\sim < 0.25$), the above recursion formulae (A-18), (A-19) break down because of the error introduced by the subtraction of two numbers of almost the same size. Hence in this case we use the following formulae:

$$B_j(q) = \int_{-1}^{1} \eta^j e^{-q\eta} d\eta = \int_{-1}^{1} \eta^j \left[1 - q\eta + \frac{(q\eta)^2}{2!} - \frac{(q\eta)^3}{3!}\right] d\eta$$

$$= \begin{cases} \dfrac{2}{j+1} + \dfrac{q^2}{j+3} & j = \text{even} \qquad \text{(A-20)} \\ \dfrac{-2q}{j+2} + \dfrac{-q^3}{3(j+4)} & j = \text{odd} \; . \qquad \text{(A-20')} \end{cases}$$

In Table A-4 we summarize formulae corresponding to Equations (A-11) for two Slater type orbitals. Some of them have been given elsewhere[39,40], but the formulae given here have the form directly connected with the computer programs which will be given later.

TABLE A-1

TRANSFORMATION OF Mn^{++} COORDINATES INTO "a" COORDINATES WITH RESPECT TO Tel AND Cd la, lb, lc COORDINATES

$$\begin{pmatrix} x_o \\ y_o \\ z_o \end{pmatrix} = \begin{pmatrix} 1/\sqrt{6} & 1/\sqrt{2} & 1/\sqrt{3} \\ -\sqrt{2/3} & 0 & 1/\sqrt{3} \\ 1/\sqrt{6} & -1/\sqrt{2} & 1/\sqrt{3} \end{pmatrix} \begin{pmatrix} x_a \\ y_a \\ z_a \end{pmatrix}$$ With respect to Te-1

$$\begin{pmatrix} x_o \\ y_o \\ z_o \end{pmatrix} = \begin{pmatrix} 1 & 0 & 0 \\ 0 & 1/\sqrt{2} & 1/\sqrt{2} \\ 0 & -1/\sqrt{2} & 1/\sqrt{2} \end{pmatrix} \begin{pmatrix} x_a \\ y_a \\ z_a \end{pmatrix}$$ With respect to Cd-la

$$\begin{pmatrix} x_o \\ y_o \\ z_o \end{pmatrix} = \begin{pmatrix} 0 & -1/\sqrt{2} & 1/\sqrt{2} \\ 1 & 0 & 0 \\ 0 & 1/\sqrt{2} & 1/\sqrt{2} \end{pmatrix} \begin{pmatrix} x_a \\ y_a \\ z_a \end{pmatrix}$$ With respect to Cd-lb

$$\begin{pmatrix} x_o \\ y_o \\ z_o \end{pmatrix} = \begin{pmatrix} 0 & 1/\sqrt{2} & 1/\sqrt{2} \\ 0 & -1/\sqrt{2} & 1/\sqrt{2} \\ 1 & 0 & 0 \end{pmatrix} \begin{pmatrix} x_a \\ y_a \\ z_a \end{pmatrix}$$ With respect to Cd-lc.

$$d_{z^2} \longrightarrow \frac{-1}{2\sqrt{3}} d_{x^2-y^2} - \frac{1}{2} d_{xy} + \frac{1}{\sqrt{6}} d_{xz} - \frac{1}{\sqrt{2}} d_{yz} \qquad \text{w. r. t. Te 1}$$

$$\longrightarrow \frac{1}{4} d_{z^2} - \frac{\sqrt{3}}{4} d_{x^2-y^2} - \frac{\sqrt{3}}{2} d_{yz} \qquad \text{w. r. t. Cd 1a}$$

$$\longrightarrow \frac{1}{4} d_{z^2} - \frac{\sqrt{3}}{4} d_{x^2-y^2} + \frac{\sqrt{3}}{2} d_{yz} \qquad \text{w. r. t. Cd 1b}$$

$$\longrightarrow \frac{-1}{2} d_{z^2} + \frac{\sqrt{3}}{2} d_{x^2-y^2} \qquad \text{w. r. t. Cd 1C}$$

$$d_{yz} \longrightarrow \frac{1}{\sqrt{3}} d_{z^2} - \frac{1}{3} d_{x^2-y^2} - \frac{1}{3\sqrt{2}} d_{xz} + \frac{1}{\sqrt{3}} d_{xy} - \frac{1}{\sqrt{6}} d_{yz} \qquad \text{w. r. t Te 1}$$

$$\longrightarrow \frac{\sqrt{3}}{2} d_{z^2} + \frac{1}{2} d_{x^2-y^2} \qquad \text{w. r. t Cd 1a}$$

TABLE A-2

TRANSFORMATION OF Cd COORDINATES INTO "a" COORDINATES AND Te COORDINATES INTO "b" COORDINATES WITH RESPECT TO EACH OTHER IN CUBIC CdTe

$$\begin{pmatrix} x_1 \\ y_1 \\ x_1 \end{pmatrix} = \begin{pmatrix} -2/3 & 1/\sqrt{3} & -\sqrt{2}/3 \\ 1/\sqrt{3} & 0 & -\sqrt{2/3} \\ -\sqrt{2}/3 & \sqrt{2/3} & -1/3 \end{pmatrix} \cdot \begin{pmatrix} x_b \\ y_b \\ z_b \end{pmatrix}$$ With respect to Cd-1a

$$\begin{pmatrix} x_1 \\ y_1 \\ z_1 \end{pmatrix} = \begin{pmatrix} 1/3 & 0 & 2\sqrt{2}/3 \\ 0 & -1 & 0 \\ 2\sqrt{2}/3 & 0 & -1/3 \end{pmatrix} \begin{pmatrix} x_b \\ y_b \\ z_b \end{pmatrix}$$ With respect to Cd-1b

$$\begin{pmatrix} x_1 \\ y_1 \\ z_1 \end{pmatrix} = \begin{pmatrix} -2/3 & -1/\sqrt{3} & -\sqrt{2}/3 \\ -1/\sqrt{3} & 0 & \sqrt{2/3} \\ -\sqrt{2}/3 & \sqrt{2/3} & -1/3 \end{pmatrix} \begin{pmatrix} x_b \\ y_b \\ z_b \end{pmatrix}$$ With respect to Cd-1c

$$\begin{pmatrix} x_{1a} \\ y_{1a} \\ y_{1a} \end{pmatrix} = \begin{pmatrix} 1/\sqrt{6} & 1/\sqrt{2} & 1/\sqrt{3} \\ \sqrt{3}/2 & -1/2 & 0 \\ -1/2\sqrt{3} & -1/2 & \sqrt{2/3} \end{pmatrix} \begin{pmatrix} x_a \\ y_a \\ z_a \end{pmatrix}$$ With respect to Te-1

$$\begin{pmatrix} x_{1b} \\ y_{1b} \\ z_{1b} \end{pmatrix} = \begin{pmatrix} -\sqrt{2}/3 & 0 & 1/\sqrt{3} \\ 0 & 1 & 0 \\ 1/\sqrt{3} & 0 & \sqrt{2/3} \end{pmatrix} \begin{pmatrix} x_a \\ y_a \\ z_a \end{pmatrix}$$ With respect to Te-1

$$\begin{pmatrix} x_{1c} \\ y_{1c} \\ z_{1c} \end{pmatrix} = \begin{pmatrix} 1/\sqrt{6} & -1/\sqrt{2} & 1/\sqrt{3} \\ \sqrt{3}/2 & -1/2 & 0 \\ -1/2\sqrt{3} & 1/2 & \sqrt{2/3} \end{pmatrix} \begin{pmatrix} x_a \\ y_a \\ z_a \end{pmatrix}$$ With respect to Te-1

TABLE A-3

TRANSFORMATION OF COORDINATES INTO "a", "b" COORDINATES IN SnO_2:V AND TiO_2:V

$$\begin{pmatrix} x_a \\ y_a \\ z_a \end{pmatrix} = \begin{pmatrix} \cos\theta & -\sin\theta & 0 \\ 0 & 0 & -1 \\ \sin\theta & \cos\theta & 0 \end{pmatrix} \begin{pmatrix} x \\ y \\ z \end{pmatrix}$$

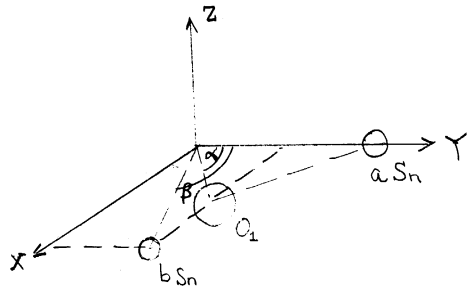

for V - a Sn overlap $\theta = 0$

for V - O_1 overlap $\theta = \tan^{-1}(1-2u)\sqrt{2}a/c = \alpha$

for V - b Sn overlap $\theta = \tan^{-1}\sqrt{2}a/c = \beta$

$$d(z^2) \longrightarrow -\frac{1}{2}\, d(z^2) + \sqrt{3}/2\; d(x^2 - y^2)$$

$$d(x^2 - y^2) \longrightarrow -\sqrt{3}/2 \cos 2\theta\, d(z^2) + 1/2 \cos 2\theta\, d(x^2-y^2) + \sin 2\theta\, d(xz)$$

$$\begin{pmatrix} x_a \\ y_a \\ z_a \end{pmatrix} \begin{pmatrix} \cos\phi & -\sin\phi & 0 \\ 0 & 0 & -1 \\ \sin\phi & \cos\phi & 0 \end{pmatrix} \begin{pmatrix} x \\ y \\ z \end{pmatrix}$$

for O_1 - a Sn overlap $\phi = -\tan^{-1}(1-2\mu)\sqrt{2}\, a/c$

for O_1 - b Sn overlap $\phi = \pi/2$

TABLE A-4

FORMULAE FOR STO OVERLAP INTEGRALS

$$< 3d\sigma | 1S >$$

$$= N_a N_b \frac{\sqrt{5}}{4} \left(\frac{R}{2}\right)^5 \{A_o(-3B_2 + B_4) - 4A_1B_3 + A_2(3B_o - 3B_4) + 4A_3B_1 + A_4(-B_o + 3B_2)\}$$

$$< 3d\sigma | 2S >$$

$$= N_a N_b \frac{\sqrt{5}}{4} \left(\frac{R}{2}\right)^6 \{A_o(3B_3 - B_5) + A_1(-3B_2 + 5B_4) + A_2(-3B_1 - 4B_3 + 3B_5) + A_3(3B_o - 4B_2 - 3B_4) + A_4(5B_1 - 3B_3) + A_5(-B_o + 3B_2)\}$$

$$< 3d\sigma | 3S >$$

$$= N_a N_b \frac{\sqrt{5}}{4} \left(\frac{R}{2}\right)^7 \{A_o(-3B_4 + B_6) + A_1(6B_3 - 6B_5) + A_2(9B_4 - 3B_6) + A_3(-6B_1 + 6B_5) + A_4(3B_o - 9B_2) + A_5(6B_1 - 6B_3) + A_6(-B_o + 3B_2)\}$$

$$< 3d\sigma | 4S >$$

$$= N_a N_b \frac{\sqrt{5}}{4} \left(\frac{R}{2}\right)^8 \{A_o(3B_5 - B_7) + A_1(-9B_4 + 7B_6) + A_2(6B_3 - 15B_5 + 3B_7) + A_3(6B_2 + 9B_4 - 9B_6) + A_4(-9B_1 + 9B_3 + 6B_5) + A_5(3B_o - 15B_2 + 6B_4) + A_6(7B_1 - 9B_3) + A_7(-B_o + 3B_2)\}$$

$$< 3d\sigma | 2p\sigma >$$

$$= N_a N_b \frac{\sqrt{15}}{4} \left(\frac{R}{2}\right)^6 \{A_o(-3B_2 + B_4) + A_1(-B_3 - B_5) + A_2(3B_o + B_4) + A_3(B_1 + 3B_5) + A_4(-B_o - B_2) + A_5(B_1 - 3B_3)\}$$

TABLE A-4 CONT'D

$$< 3d\sigma | 3p\sigma >$$

$$= N_a N_b \frac{\sqrt{15}}{4} \left(\frac{R}{2}\right)^7 \{A_o(3B_3 - B_5) + A_1(-3B_2 + 2B_4 + B_6) + A_2(-3B_1 - B_3 - 2B_5)$$

$$+ A_3(3B_o - B_2 + B_4 - 3B_6) + A_4(2B_1 + B_3 + 3B_5)$$

$$+ A_5(-B_o - 2B_2 + 3B_4) + A_6(B_1 - 3B_3)\}$$

$$< 3d\sigma | 4p\sigma >$$

$$= N_a N_b \frac{\sqrt{15}}{4} \left(\frac{R}{2}\right)^8 \{A_o(-3B_4 + B_6) + A_1(6B_3 - 3B_5 - B_7) + A_2(3B_4 + 3B_6)$$

$$+ A_3(-6B_1 - 3B_5 + 3B_7) + A_4(3B_o - 3B_2 - 6B_6)$$

$$+ A_5(3B_1 + 3B_3) + A_6(-B_o - 3B_2 + 6B_4) + A_7(B_1 - 3B_3)\}$$

$$< 3d\pi | 2p\pi >$$

$$= N_a N_b \frac{3\sqrt{5}}{4} \left(\frac{R}{2}\right)^6 \{A_o(B_2 - B_4) + A_1(B_3 - B_5) + A_2(-B_o + B_4)$$

$$+ A_3(-B_1 + B_5) + A_4(B_o - B_2) + A_5(B_1 - B_3)\}$$

$$< 3d\pi | 3p\pi >$$

$$= N_a N_b \frac{3\sqrt{5}}{4} \left(\frac{R}{2}\right)^7 \{A_o(-B_3 + B_5) + A_1(B_2 - 2B_4 + B_6) + A_2(B_1 + B_3 - 2B_5)$$

$$+ A_3(-B_o + B_2 + B_4 - B_6) + A_4(-2B_1 + B_3 + B_5)$$

$$+ A_5(B_o - 2B_2 + B_4) + A_6(B_1 - B_3)\}$$

$$< 3d\pi | 4p\pi >$$

$$= N_a N_b \frac{3\sqrt{5}}{4} \left(\frac{R}{2}\right)^8 \{A_o(B_4 - B_6) + A_1(-2B_3 + 3B_5 - B_7) + A_2(-3B_4 + 3B_6)$$

$$+ A_3(2B_1 - 3B_5 + B_7) + A_4(-B_o + 3B_2 - 2B_6)$$

$$+ A_5(-3B_1 + 3B_3) + A_6(B_o - 3B_2 + 2B_4) + A_7(B_1 - B_3)\}$$

TABLE A-4 CONT'D

$$< 1S|2S >$$

$$= N_a N_b \frac{1}{2} \left(\frac{R}{2}\right)^4 \{A_0B_3 - A_1B_2 - A_2B_1 + A_3B_0\}$$

$$< 2S|2S >$$

$$= N_a N_b \frac{1}{2} \left(\frac{R}{2}\right)^5 \{A_0B_4 - 2A_2B_2 + A_4B_0\}$$

$$< 3S|2S >$$

$$= N_a N_b \frac{1}{2} \left(\frac{R}{2}\right)^6 \{A_0B_5 + A_1B_4 - 2A_2B_3 - 2A_3B_2 + A_4B_1 + A_5B_0\}$$

$$< 4S|2S >$$

$$= N_a N_b \frac{1}{2} \left(\frac{R}{2}\right)^7 \{A_0B_6 + 2A_1B_5 - A_2B_4 - 4A_3B_3 - A_4B_2 + 2A_5B_1 + A_6B_0\}$$

$$< 3S|3S >$$

$$= N_a N_b \frac{1}{2} \left(\frac{R}{2}\right)^7 \{-A_0B_6 + 3A_2B_4 - 3A_4B_2 + A_6B_0\}$$

$$< 4S|3S >$$

$$= N_a N_b \frac{1}{2} \left(\frac{R}{2}\right)^8 \{-A_0B_7 - A_1B_6 + 3A_2B_5 + 3A_3B_4 - 3A_4B_3 - 3A_2B_5 + A_6B_1 + A_7B_0\}$$

$$< 4S|4S >$$

$$= N_a N_b \frac{1}{2} \left(\frac{R}{2}\right)^9 \{A_0B_8 - 4A_2B_6 + 6A_4B_4 - 4A_6B_2 + A_8B_0\}$$

$$< 1S|2p\sigma >$$

$$= N_a N_b \frac{\sqrt{3}}{2} \left(\frac{R}{2}\right)^4 \{-A_0B_2 + A_1B_3 + A_2B_0 - A_3B_1\}$$

$$< 2S|2p\sigma >$$

$$= N_a N_b \frac{\sqrt{3}}{2} \left(\frac{R}{2}\right)^5 \{-A_0B_3 + A_1(-B_2 + B_4) + A_2(B_1 + B_3) + A_3(B_0 - B_2) - A_4B_1\}$$

TABLE A-4 CONT'D

$$\langle 3S|2p\sigma \rangle = N_a N_b \frac{\sqrt{3}}{2} \left(\frac{R}{2}\right)^6 \{-A_0B_4 + A_1(-2B_3 + B_5) + 2A_2B_4 + 2A_3B_1 + A_4(B_0 - 2B_2) - A_5B_1\}$$

$$\langle 4S|2p\sigma \rangle = N_a N_b \frac{\sqrt{3}}{2} \left(\frac{R}{2}\right)^7 \{-A_0B_5 + A_1(-3B_4 + B_6) + A_2(-2B_3 + 3B_5) + A_3(2B_2 + 2B_4) + A_4(3B_1 - 2B_3) + A_5(B_0 - 3B_2) - A_6B_1\}$$

$$\langle 2S|3p\sigma \rangle = N_a N_b \frac{\sqrt{3}}{2} \left(\frac{R}{2}\right)^6 \{A_0B_4 - A_1B_5 - 2A_2B_2 - 2A_3B_3 + A_4B_0 - A_5B_1\}$$

$$\langle 3S|3p\sigma \rangle = N_a N_b \frac{\sqrt{3}}{2} \left(\frac{R}{2}\right)^7 \{A_0B_5 + A_1(B_4 - B_6) + A_2(-2B_3 - B_5) + A_3(-2B_2 + 2B_4) + A_4(B_1 + 2B_3) + A_5(B_0 - B_2) - A_6B_1\}$$

$$\langle 4S|3p\sigma \rangle = N_a N_b \frac{\sqrt{3}}{2} \left(\frac{R}{2}\right)^8 \{A_0B_6 + A_1(2B_5 - B_7) + A_2(-B_4 - 2B_6) + A_3(-4B_3 + B_5) + A_4(-B_2 + 4B_4) + A_5(2B_1 + B_3) + A_6(B_0 - 2B_2) - A_7B_1\}$$

$$\langle 2S|4p\sigma \rangle = N_a N_b \frac{\sqrt{3}}{2} \left(\frac{R}{2}\right)^7 \{-A_0B_5 + A_1(B_4 + B_6) + A_2(2B_3 - B_5) + A_3(-2B_2 - 2B_4) + A_4(-B_1 + 2B_3) + A_5(B_0 + B_2) - A_6B_1\}$$

TABLE A-4 CONT'D

$$< 3S|4p\sigma >$$

$$= N_a N_b \frac{\sqrt{3}}{2} \left(\frac{R}{2}\right)^8 \{-A_o B_6 + A_1 B_7 + 3A_2 B_4 - 3A_3 B_5 - 3A_4 B_2 + 3A_5 B_3 + A_6 B_o - A_7 B_1\}$$

$$< 4S|4p\sigma >$$

$$= N_a N_b \frac{\sqrt{3}}{2} \left(\frac{R}{2}\right)^9 \{-A_o B_7 + A_1(-B_6 + B_8) + A_2(3B_5 + B_7) + A_3(3B_4 - 3B_6) + A_4(-3B_3 - 3B_5) + A_5(-3B_2 + 3B_4) + A_6(B_1 + 3B_3) + A_7(B_o - B_2) - A_8 B_1\}$$

$$< 2p\sigma|2p\sigma >$$

$$= N_a N_b \frac{3}{2} \left(\frac{R}{2}\right)^5 \{-A_o B_2 + A_2(B_o + B_4) - A_4 B_2\}$$

$$< 3p\sigma|2p\sigma >$$

$$= N_a N_b \frac{3}{2} \left(\frac{R}{2}\right)^6 \{-A_o B_3 - A_1 B_2 + A_2(B_1 + B_5) + A_3(B_o + B_4) - A_4 B_3 - A_5 B_2\}$$

$$< 4p\sigma|2p\sigma >$$

$$= N_a N_b \frac{3}{2} \left(\frac{R}{2}\right)^7 \{-A_o B_4 - 2A_1 B_3 + A_2 B_6 + A_3(2B_1 + 2B_5) + A_4 B_o - 2A_5 B_3 - A_6 B_2\}$$

$$< 3p\sigma|3p\sigma >$$

$$= N_a N_b \frac{3}{2} \left(\frac{R}{2}\right)^7 \{A_o B_4 + A_2(-2B_2 - B_6) + A_4(B_o + 2B_4) - A_6 B_2\}$$

TABLE A-4 CONT'D

$$< 4p\sigma | 3p\sigma >$$

$$= N_a N_b \frac{3}{2} \left(\frac{R}{2}\right)^8 \{A_o B_5 + A_1 B_4 + A_2(-2B_3 - B_7) + A_3(-2B_2 - B_6)$$

$$+ A_4(B_1 + 2B_5) + A_5(B_o + 2B_4) - A_6 B_3 - A_7 B_2\}$$

$$< 4p\sigma | 4p\sigma >$$

$$= N_a N_b \frac{3}{2} \left(\frac{R}{2}\right)^9 \{-A_o B_6 + A_2(3B_4 + B_8) + A_4(-3B_2 - 3B_6)$$

$$+ A_6(B_o + 3B_4) - A_8 B_2\}$$

$$< 2p\pi | 2p\pi >$$

$$= N_a N_b \frac{3}{4} \left(\frac{R}{2}\right)^5 \{A_o(B_2 - B_4) + A_2(-B_o + B_4) + A_4(B_o - B_2)\}$$

$$< 3p\pi | 2p\pi >$$

$$= N_a N_b \frac{3}{4} \left(\frac{R}{2}\right)^6 \{A_o(B_3 - B_5) + A_1(B_2 - B_4) + A_2(-B_1 + B_5)$$

$$+ A_3(-B_o + B_4) + A_4(B_1 - B_3) + A_5(B_o - B_2)\}$$

$$< 4p\pi | 2p\pi >$$

$$= N_a N_b \frac{3}{4} \left(\frac{R}{2}\right)^7 \{A_o(B_4 - B_6) + A_1(2B_3 - 2B_5) + A_2(-B_4 + B_6)$$

$$+ A_3(-2B_1 + 2B_5) + A_4(-B_o + B_2) + A_5(2B_1 - 2B_3) + A_6(B_o - B_2)\}$$

$$< 4p\pi | 4p\pi >$$

$$= N_a N_b \frac{3}{4} \left(\frac{R}{2}\right)^9 \{A_o(B_6 - B_8) + A_2(-3B_4 + 2B_6 + B_8) + A_4(3B_2 - 3B_6)$$

$$+ A_6(-B_o - 2B_2 + 3B_4) + A_8(B_o - B_2)\}$$

MAD Programs for Computing Overlap Integrals

Program I: This program computes the integrals $A_i(p)$ and $B_j(q)$ of Equations (A-14) and (A-15) by the recursion formulae, Equations (A-16) through (A-20), and evaluates the overlap integral between two Slater type orbitals by summing the products of A_i and B_j according to the formula Equation (A-11) (see also Table A-4). The effective nuclear charges (ZEFFA and ZEFFB), effective quantum numbers (NEFFA and NEFFB), interionic distance R and the coefficients C_{ij}'s are needed as input data. It is noted that the coefficients C_{ij}'s are either symmetric or antisymmetric with respect to the interchange of i and j, hence only "lower triangle" of the matrix (C_{ij}) is read in, and the upper triangle is developed by the machine according to the value of the variable "CSYM". CSYM = 1. if C_{ij}'s are antisymmetric, and CSYM = 2. if C_{ij}'s are symmetric. In case the succeeding calculation uses the same set of ZEFF, NEFF, and R as the previous one, we set the variable RPC (relation to the previous calculation) equals to 2, and RPC = 3 if we use the same set of C_{ij} as the previous calculation. If none of the previous data are used RPC = 1. A numerical constant coming from the angular function (e.g. $\sqrt{15}/4$ in Equation (A-11)) is called NC in the program, and also needed as input data.

The values of the integrals $A_i(p)$ and $B_j(q)$ computed by this program have been checked with the table compiled by Kotani, et al.[41] They agree with each other up to five figures or more.

The following is the MAD program. The data are for the examples of computing the following overlap integrals:

$< 3d\sigma | 2s >$ for R = 3.877 a.u. ,

$< 3d\sigma | 2p\sigma >$ for R = 3.877 a.u. ,

and $< 3d\sigma | 2p\sigma >$ for R = 3.887 a.u. .

```
$COMPILE MAD, EXECUTE
         PRINT COMMENT $1 OVERLAP INTEGRALS FOR SLATER TYPE ORBITALS$
         DIMENSION A(20),B(20),C(400, V),FACTRL(20)
         VECTOR VALUES V=2,0,0
         INTEGER I,J,IMAX,JMAX,RPC
         IMAX=15
         FACTRL (0.)=1.
         THROUGH LOOP1,FOR L=1.,1.,L.G.IMAX
LOOP1    FACTRL(L)= L*FACTRL(L-1.)
         PRINT RESULTS FACTRL(0.)...FACTRL(IMAX)
START    READ DATA
         PRINT RESULTS RPC, ZEFFA,ZEFFB,NEFFA,NEFFB,R
         WHENEVER RPC.E.2,TRANSFER TO CMTRIX
         V(1)=JMAX+2
         V(2)=JMAX+1
         MUA = ZEFFA/NEFFA
         MUB = ZEFFB/NEFFB
         NA=(2.*MUA).P.(NEFFA+0.5)/SQRT.(FACTRL(2.*NEFFA))
         NB=(2.*MUB).P.(NEFFB+0.5)/SQRT.(FACTRL(2.*NEFFB))
         P=R*(MUA+MUB)/2.
         Q=R*(MUA-MUB)/2.
         A(0)=EXP.(-P)/P
         THROUGH LOOP2, FOR I=1,1,I.G.IMAX
```

```
LOOP2    A(I)=A(0)+I*A(I-1)/P
         WHENEVER.ABS.Q.GE.0.25
         B(0)=(EXP.(Q) - EXP.(-Q))/Q
         THROUGH LOOP3, FOR J=1,1,J.G.JMAX
LOOP3    B(J)=((-1.).P.J*EXP.(Q)-EXP.(-Q)+J*B(J-1))/Q
         OTHERWISE
         THROUGH LOOP3A, FOR J=0,2,J.G.JMAX
LOOP3A   B(J)=2./(J+1.)+Q.P.2./(J+3.)
         THROUGH LOOP3B, FOR J=1,2,J.G.JMAX
LOOP3B   B(J)=-Q/(J+2.)-Q.P.3./(3.*J+12.)
         END OF CONDITIONAL
         PRINT RESULTS P,A(0)...A(IMAX),Q,B(0)...B(JMAX)
         WHENEVER RPC.E.3, TRANSFER TO CHECK
CMTRIX   EXECUTE ZERO.(C(0,0)...C(IMAX,JMAX))
         READ DATA
         THROUGH LOOP4,FOR I=1,1,I.G.IMAX
         THROUGH LOOP4,FOR J=0,1,J.E.I
LOOP4    C(J,I)=(-1.).P.CSYM*C(I,J)
CHECK    PRINT RESULTS  C(0,0)...C(IMAX,JMAX)
         SUM=0.
         THROUGH LOOP5,FOR I=0,1,I.G.IMAX
         THROUGH LOOP5,FOR J=0,1,J.G.JMAX
LOOP5    SUM=SUM+A(I)*B(J)*C(I,J)
         OVINT=NA*NB*NC*(R/2.).P.(NEFFA+NEFFB+1.)*SUM
         PRINT RESULTS  OVINT
```

```
          PRINT COMMENT $1$
          TRANSFER TO START
          END OF PROGRAM
$DATA
RPC=1,ZEFFA=4.3,ZEFFB=4.55,NEFFA=3.,NEFFB=2.,R=3.8777,IMAX=5,JMAX=5  *
CSYM=2.,NC=0.5590,C(2,1)=-3.,C(3,0)=3.,0.,-4.,C(4,1)=5.,0.,-3.,C(5,0)=-1.,3. *
RPC=2 *
CSYM=1.,NC=0.96825,C(2,0)=3.,C(3,1)=1.,C(4,0)=-1.,0.,-1.,C(5,1)=1.,0.,-3.  *
RPC= 3,  R=3.8877 *
```

Program II: Watson[25] and others have used linear combinations of Slater type orbitals for the Hartree-Fock atomic wave function. The overlap integral between two orbitals of this kind can be evaluated by simply introducing an iterative procedure in Program I, provided the effective quantum numbers of the orbitals in the combination are all the same. (If this is not the case, we can divide the combination into several parts each has the same effective quantum number). Instead of NEFF and ZEFF, we use their ratio MU(K) for k-th orbital, and FA(K), the fraction of k-th orbital in the combination A as input data. The following is the program with data which compute the overlap integral between vanadium 3dσ orbital

$$\psi_{3d\sigma} = \{0.5243\phi_3(1.83) + 0.4989\phi_3(3.61) + 0.1131\phi_3(6.80) + 0.0055\phi_3(12.43)\}\ Y_{20}(\theta,\varphi)$$

given by Watson[25], and oxygen 2s orbital obtained by Ballhausen[27] by fitting the numerical functions given by Hartree.

$$\psi_{2s} = \{0.5459\phi_2(1.80) + 0.4839\phi_2(2.80)\}\ Y_{00}(\theta,\varphi)$$

where

$$\phi_n(\mu) = N_{n\mu}\ r^{n-1}\exp(-\mu r)$$

is the normalized Slater type orbital.

```
$COMPILE MAD, EXECUTE

        PRINT COMMENT $1 OVERLAP INTEGRALS FOR WATSON TYPE ORBITALS $

        DIMENSION A(20),B(20),C(400,V),MUA(20),MUB(20),FA(20),FB(20),
              IT(400,W),FACTRL(20)
```

```
          VECTOR VALUES V=2,0,0

          VECTOR VALUES W=2,1,0

          INTEGER RPC, I,IMAX,J,JMAX,K,KMAX,N,NMAX

          IMAX=15.

          FACTRL(0.)=1.

          THROUGH LOOP1,FOR L=1.,1.,L.G.IMAX

LOOP1     FACTRL(L)=L*FACTRL(L-1.)

          PRINT RESULTS FACTRL(0.)...FACTRL(IMAX)

START     READ DATA

          PRINT RESULTS RPC, NEFFA,NEFFB,R,MUA(1)...MUA(KMAX),MUB(1)...
                MUB(NMAX)

          V(1)=JMAX+2

          V(2)=JMAX+1

          W(2)=NMAX

          WHENEVER RPC.E.3, TRANSFER TO CHECK

CMTRIX    EXECUTE ZERO.(C(0,0)...C(IMAX,JMAX))

          READ DATA

          THROUGH LOOP2, FOR I=1,1,I.G.IMAX

          THROUGH LOOP2, FOR J=0,1,J.E.I

LOOP2     C(J,I)=(-1.).P.CSYM*C(I,J)

CHECK     PRINT RESULTS C(0,0)...C(IMAX,JMAX)

          OVINT=0.

          THROUGH INTGRL, FOR K=1,1,K.G.KMAX

          NA=(2.*MUA(K)).P.(NEFFA+0.5)/SQRT.(FACTRL(2.*NEFFA))

          THROUGH INTGRL, FOR N=1,1,N.G.NMAX

          NB=(2.*MUB(N)).P.(NEFFB+0.5)/SQRT.(FACTRL(2.*NEFFB))
```

```
          P=R*(MUA(K)+MUB(N))/2.
          A(0)=EXP.(-P)/P
          THROUGH LOOP3, FOR I=1,1,I.G.IMAX
LOOP3     A(I)=A(0)+I*A(I-1)/P
          Q=R*(MUA(K)-MUB(N))/2.
          WHENEVER .ABS.Q.GE.0.25
          B(0)=(EXP.(Q)-EXP.(-Q))/Q
          THROUGH LOOP4, FOR J=1,1,J.G.JMAX
LOOP4     B(J)=((-1.).P.J*EXP.(Q)-EXP.(-Q)+J*B(J-1))/Q
          OTHERWISE
          THROUGH LOOP4A, FOR J=0,2,J.G.JMAX
LOOP4A    B(J)=2./(J+1.)+Q.P.2./(J+3.)
          THROUGH LOOP4B, FOR J=1,2,J.G.JMAX
LOOP4B    B(J)=-2.*Q/(J+2.)-Q.P.3./(3.*J+12.)
          END OF CONDITIONAL
          SUM=0.
          THROUGH LOOP5,FOR I=0,1,I.G.IMAX
          THROUGH LOOP5,FOR J=0,1,J.G.JMAX
LOOP5     SUM=SUM+A(I)*B(J)*C(I,J)
          IT(K,N)=FA(K)*FB(N)*NA*NB*NC*(R/2.).P.(NEFFA+NEFFB+1.)*SUM
          PRINT RESULTS IT(K,N)
INTGRL    OVINT=OVINT+IT(K,N)
          PRINT RESULTS OVINT
          PRINT COMMENT $1$
          TRANSFER TO START
          END OF PROGRAM
```

```
$DATA

RPC=1,NEFFA=3.,NEFFB=2.,R=3.8777,KMAX=4,NMAX=2,IMAX=5,JMAX=5,

MUA(1)=1.83,3.61,6.80,12.43,FA(1)=.5243,.4989,.1131,.0055

MUB(1)=1.80,2.80,            FB(1)=.5459,.4839      *

CSYM=2.,NC=.5590,C(2,1)=-3.,C(3,0)=3.,0.,-4.,C(4,1)=5.,0.,-3.,C(5,0)=
     -1.,0.,3.,  *

RPC = 3,      R = 3.8877  *
```

APPENDIX B

SOLUTION OF IMPROPER EIGENVALUE PROBLEM BY DIGITAL COMPUTER

The improper eigenvalue problem we met in Chapter II Equation (2.7) can be reduced into a proper eigenvalue problem by successive diagonalization and unitary transformation. This will be shown in this appendix.

The problem, stated in general, is to solve for the eigenvalues λ_i and eigenvectors X_i of the equation:

$$AX = BX\Lambda \tag{B-1}$$

where A and B are symmetric matrices and B is also positive definite. Λ is a diagonal matrix with the eigenvalues λ_i as diagonal elements. X is the matrix with the eigenvectors X_i as i-th column.

Since B is symmetric, we can find a unitary matrix U to diagonalize it,

$$U^{\dagger}BU = D \tag{B-2}$$

Since B is also positive definite, the diagonal elements of D are all positive. Take the -1/2 power of the diagonal elements and construct another diagonal matrix R, symbolically:

$$R = D^{-1/2} \tag{B-3}$$

then,

$$R^{\dagger}(U^{\dagger}BU)R = R^{\dagger}DR = D^{-1/2}DD^{-1/2} = I \text{ (Identity)} \tag{B-4}$$

Let UR = S, multiply $S^{\dagger}$ from left on both sides of Equation (B-1)

$$S^{\dagger}AX = S^{\dagger}BX\Lambda \tag{B-5}$$

or, $$S^{\dagger}AS^{-1}X = S^{\dagger}BS^{-1}X\Lambda \quad \text{(B-6)}$$

Let $$S^{\dagger}AS = A', \quad \text{(B-7)}$$

$$S^{-1}X = Y \quad \text{(B-8)}$$

then using Equation (B-4), we have

$$A'Y = Y\Lambda \quad \text{(B-9)}$$

This is in the form of a proper eigenvalue problem. Since the matrix A' is symmetric, there is a subroutine (EIGN.) available in "Michigan Executive System Subroutines" for the solution of this problem.

The eigenvalues of the original equation are the same as those of Equation (B-9), and the eigenvectors of the original equation can be obtained by a matrix multiplication:

$$X = SY \quad \text{(B-10)}$$

Since the eigenvectors are given in row form in subroutine EIGN., we actually do the multiplication

$$X^{\dagger} = Y^{\dagger}S^{\dagger} \quad \text{(B-11)}$$

For the convenience of later use we normalize the eigenvectors such that

$$\sum_{i,j} X_{ik}X_{jk}B_{ij} = 1 \quad \text{(B-12)}$$

In order to check the calculation, we calculate the error matrix E, having the elements:

$$E_{ki} = \sum_{j} (A_{ij} - \lambda_k B_{ij})X_{jk}$$

which must be zero if the solutions are perfect. In our calculations

all elements of error matrix are six orders or more smaller than

A_{ij} or $\lambda_k B_{ij}$.

The following is the MAD program which solve improper eigenvalue problems of order less than 20.

```
$COMPILE MAD, EXECUTE, PUNCH OBJECT

         PRINT COMMENT $1 SOLUTION OF THE CHARACTERISTIC VALUE PROBLEM
               (A-LB)X=0 $

         PRINT COMMENT $0 WHERE A AND B ARE SYMMETRIC MATRICES, AND B
               IS POSITIVE DEFINITE $

         DIMENSION A(400,V), B(400,V),X(400,V), APRIME(400,V),E(400,V)
               D(400,V),R(400,V),ST(400,V),UT(400,V),S(400,V),YT(400,V),
               LAMBDA(400,V)

         EQUIVALENCE (D,R,ST,E),(UT,S,YT,X),(APRIME,LAMBDA),(V(2),N)

         VECTOR VALUES V=2,1,0

         INTEGER N,I,J,K

START    READ DATA N

         PRINT COMMENT $1$

         EXECUTE ZERO.(A(1,1)...A(N,N),B(1,1)...B(N,N))

         READ DATA A(1,1)...A(N,N),B(1,1)...B(N,N)

         THROUGH  LOOP1, FOR I= 2,1,I.G.N

         THROUGH  LOOP1, FOR J= 1,1,J.E.I

         A(J,I) = A(I,J)

LOOP1    B(J,I) = B(I,J)

         PRINT RESULTS N,A(1,1)...A(N,N),B(1,1)...B(N,N)

         IND1 = 5.

         IND2 = 5.

         IND3 = 5.
```

```
          IND4 = 5.
          IND5 = 5.
          IND6 = 5.
          THROUGH LOOP1A, FOR I=1,1, I.G.N*N
LOOP1A    D(I) = B(I)
          SCFACT = 1.
          IND1=EIGN.(D(1),N,1,UT(1),SCFACT)
          WHENEVER IND1.E.3.
          CONTINUE
          OR WHENEVER IND1.E.1.
          PRINT COMMENT $0 B MATRIX NOT ACCEPTED BY SUBROUTINE $
          TRANSFER TO END
          OR WHENEVER IND1.E.2.
          PRINT COMMENT $0 CHARACTERISTIC VALUES OF B MATRIX SCALED BY$
          PRINT RESULTS SCFACT
          TRANSFER TO END
          END OF CONDITIONAL
          THROUGH LOOP2, FOR I=1,1,I.G.N
          WHENEVER D(I,I).LE.0.
          PRINT COMMENT $0 B MATRIX IS NOT POSITIVE DEFINITE $
          TRANSFER TO END
          OTHERWISE
          R(I,I)=D(I,I).P.-.5
LOOP2     END OF CONDITIONAL
```

```
          THROUGH LOOP3, FOR I=1,1,I.G.N
          THROUGH LOOP3, FOR J=1,1,J.G.N
          WHENEVER I.E.J
          CONTINUE
          OTHERWISE
          R(I,J)=0.
LOOP3     END OF CONDITIONAL
          IND2=DPMAT.(N,ST(1),UT(1))
          WHENEVER IND2.E.0., TRANSFER TO END
          THROUGH LOOP 5, FOR I=1,1,I.G.N
          THROUGH LOOP 5, FOR J=1,1,J.G.N
          S(I,J)=ST(J,I)
LOOP5     APRIME(I,J)=ST(I,J)
          IND3=DPMAT.(N,APRIME(1),A(1))
          WHENEVER IND3.E.0., TRANSFER TO END
          IND4=DPMAT.(N,APRIME(1),S(1))
          WHENEVER IND4.E.0., TRANSFER TO END
          THROUGH LOOP6, FOR I=2,1, I.G.N
          THROUGH LOOP6, FOR J=1,1, J.E.I
LOOP6     APRIME(I,J) = APRIME (J,I)
          SCFACT = 1.
          IND5=EIGN.(LAMBDA(1),N,1,YT(1),SCFACT)
          WHENEVER IND5.E.3.
          CONTINUE
          OR WHENEVER IND5.E.1.
```

```
          PRINT COMMENT $0 APRIME MATRIX NOT ACCEPTED BY SUBROUTINE $
          TRANSFER TO END
          OR WHENEVER IND5.E.2.
          PRINT COMMENT $1 CHARACTERISTIC VALUES SCALED BY $
          PRINT RESULTS SCFACT
          END OF CONDITIONAL
          IND6=DPMAT.(N,YT(1),ST(1))
          THROUGH LOOP7, FOR I=1,1,I.G.N
          XSUMSQ = 0.
          THROUGH LOOP8, FOR J=1,1, J.G.N
          THROUGH LOOP8, FOR K=1,1, K.G.N
LOOP8     XSUMSQ=XSUMSQ+X(I,J)*X(I,K)*B(J,K)
          ROOT = XSUMSQ.P..5
          THROUGH LOOP7, FOR J = 1,1, J.G.N
LOOP7     X(I,J)=X(I,J)/ROOT
          PRINT COMMENT $0 CHARACTERISTIC VALUES $
          THROUGH LOOP8A, FOR I=1,1, I.G.N
LOOP8A    PRINT FORMAT F3,LAMBDA(I,I)
          VECTOR VALUES F3=$ S20, E20.8 *$
          WHENEVER SCFACT.E.1.
          CONTINUE
          OTHERWISE
          PRINT COMMENT $0 ERROR MATRIX NOT COMPUTED $
          TRANSFER TO END
          END OF CONDITIONAL
```

```
          THROUGH LOOP9, FOR I=1,1,I.G.N
          THROUGH LOOP9, FOR J=1,1,J.G.N
          E(I,J)=0.
          THROUGH LOOP9, FOR K=1,1,K.G.N
LOOP9     E(I,J)=E(I,J)+(A(J,K)-LAMBDA(I,I)*B(J,K))*X(I,K)
          PRINT RESULTS X(1,1)...X(N,N),E(1,1)...E(N,N)
END       PRINT COMMENT $0 INDICATOR VALUES $
          PRINT RESULTS IND1, IND2, IND3, IND4, IND5, IND6
          TRANSFER TO START
          END OF PROGRAM
```

APPENDIX C

SIMPLIFIED MO CALCULATIONS OF TETRAHEDRAL COMPLEXES INCLUDING NEXT NEAREST LIGANDS

As examples of simplified MO calculations discussed in Chapter II, Section B, cadmium telluride (CdTe) and zinc sulfide (ZnS) containing Mn^{++} impurities are treated in this appendix. In the first example ($CdTe:Mn^{++}$), Slater radial functions and spectroscopic energy levels are used for the AO's. In the second example ($ZnS:Mn^{++}$), Hartree-Fock radial functions and one electron orbital energies calculated by Watson and Freeman[25] are used.

(i) $CdTe:Mn^{++}$

Radial functions used are

$$R_{3d}(Mn) = N\, r^2 \exp(-1.87\, r)$$

$$R_{5sp}(Cd) = N'r^3 \exp(-1.09\, r)$$

$$R_{5sp}(Te) = N''r^3 \exp(-1.74\, r)$$

For T_2 symmetry, the six basis functions are the AO's in D_3 of Equation (4-7), and the matrices $\{H_{ij}\}$ and $\{S_{ij}\}$ are,

$\{H_{ij}\}_{T_2}$ (in units of K cm^{-1}):

d(yz)	ϕ_{3s}	ϕ_{3z}	$\phi_{3\pi}$	χ_{3s}	χ_{3z}
-126.	-23.25	-17.94	-12.37	-8.82	-11.15
	-144.	0	0	-76.33	-65.39
		-73.	0	13.02	-3.15
			-73.	-36.84	-32.70
				-72.	0
					-42.

$\{S_{ij}\}_{T_2}$:

1.	.08633	.09355	.06447	.04632	.07661
	1.	0	0	.3748	.4204
		1.	0	-.0898	.0285
			1.	.2541	.2953
				1.	0
					1.

For E symmetry the four bases are the AO's in D_1 of Equation (4-5), and the matrices are:

$\{H_{ij}\}_E$ (in units of K cm^{-1})

d_z^2	$\phi_{1\pi}$	χ_{1s}	χ_{1z}
-126.	-21.425	-6.238	-7.881
	-73	-22.56	-12.95
		-72.	0
			-42.

$\{S_{ij}\}_E$

1.	.1117	.03275	.05417
	1.	.1556	.1169
		1.	0
			1.

Solution of secular equation gives the following eigenvalues and eigenvectors. (Table C-1 and Figure C-1)

TABLE C-1

MOLECULAR ORBITALS AND ORBITAL ENERGIES OF CdTe:Mn^{++}

T_2 Symmetry:

	Energy $K\ cm^{-1}$	Mixing Coefficients d_3	ϕ_{3s}	ϕ_{3z}	$\phi_{3\pi}$	χ_{3s}	χ_{3z}
	-152.7	.3252	.8197	.0166	.0043	.2011	.0066
*	-122.2	.9231	-.3237	.1279	.0709	-.1355	-.0395
	- 80.3	-.0033	-.2512	-.3006	.7872	.3678	-.0299
	- 70.4	-.2489	.0131	.8955	.3588	-.0434	.1531
	- 52.6	-.0018	-.0950	.3243	-.2019	.6615	-.6640
	81.5	.0394	-.8687	.0727	-.7035	.8749	1.015

E Symmetry:

	Energy $K\ cm^{-1}$	Mixing Coefficients d_1	$\phi_{1\pi}$	χ_{1s}	χ_{1z}
*	-127.1	.9727	.1320	.0433	.0084
	- 79.9	-.2244	.6178	.6864	.0377
	- 59.1	.1338	-.7431	.7258	-.2255
	- 39.2	-.0124	-.3148	.1600	.9816

*Molecular Orbitals of Unpaired Electrons.

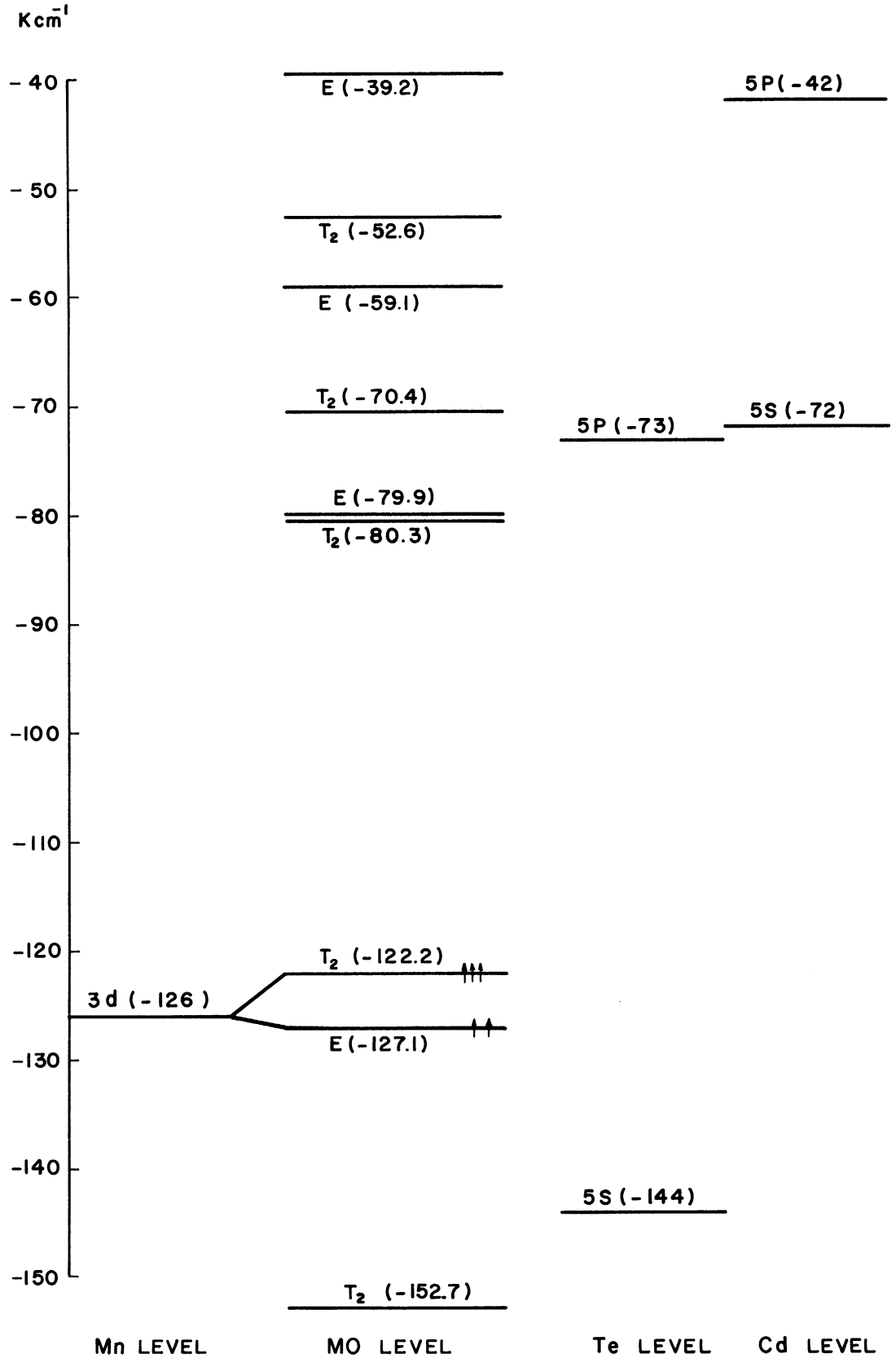

Figure C-1. MO Energy Level Diagram for CdTe:Mn^{++}.

(ii) $ZnS:Mn^{++}$

Radial functions are

$$R_{3d}(MN) = .4675\phi_3(2.0235) + .5346\phi_3(3.9754) + .1375\phi_3(7.4822) + .0053\phi_3(13.462)$$

$$R_{4sp}(Zn) = .0208\phi_1(31.455) - .0113\phi_2(28.027) + .04615\phi_2(14.673) + .0747\phi_3(13.652) - .0285\phi_3(8.3237) - .3718\phi_3(4.7860) + .1649\phi_4(5.1559) + .3653\phi_4(2.3916) + .5893\phi_4(1.4066) + .16775\phi_4(0.9130)$$

$$R_{3s}(S) = 0.0352\phi_1(17.867) + .0449\phi_1(13.924) + .0491\phi_2(13.753) - .0644\phi_2(8.9398) - .1937\phi_2(6.2464) - .1910\phi_3(5.7842) + .3003\phi_3(3.0431) + .7046\phi_3(2.0549) + .1334\phi_3(1.2872)$$

$$R_{3p}(S) = -.01305\phi_2(12.798) - .0386\phi_2(8.1734) - .2406\phi_2(5.0103) + .08715\phi_3(3.8107) + .3795\phi_3(2.1976) + .5724\phi_3(1.5528) + .09455\phi_3(0.7790).$$

Watson does not give 4p function for Zn. In this calculation it is assumed to have the same radial dependence as 4s, and its energy is estimated from spectroscopic data.

The basis functions are (as the case of $CdTe:Mn^{++}$) given by Equations (4-5) and (4-7). The matrices are:

T_2 Symmetry:

$\{H_{ij}\}_{T_2}$ (in atomic units, 1 a.u. = 2 ryd)

d_3	ϕ_{3s}	ϕ_{3z}	$\phi_{3\pi}$	χ_{3s}	χ_{3z}
-.6334	-.0850	-.0904	-.0389	-.0149	-.0173
	-.8785	0	0	-.2864	-.2337
		-.4363	0	.0637	-.0171
			-.4363	-.1803	-.1128
				-.2855	0
					-.1382

$\{S_{ij}\}_{T_2}$

1.	.057	.086	.037	.0175	.0293
	1.	0	0	.286	.335
		1.	0	-.090	.035
			1.	.255	.230
				1.	0
					1.

E Symmetry:

$\{H_{ij}\}_E$ (in atomic units, 1 a.u. = 2 ryd)

d_1	$\phi_{1\pi}$	χ_{1s}	χ_{1z}
-.6334	-.0674	-.0105	-.0122
	-.4363	-.1104	-.0409
		-.2855	0
			-.1382

$\{S_{ij}\}_E$

1.	.0641	.0124	.0207
	1.	.1564	.0834
		1.	0
			1.

TABLE C-2

MOLECULAR ORBITALS AND ORBITAL ENERGIES OF $ZnS:Mn^{++}$

T_2 Symmetry

Energy		Mixing Coefficients					
a.u.	K cm^{-1}	d_3	ϕ_{3s}	ϕ_{3z}	$\phi_{3\pi}$	χ_{3s}	χ_{3z}
-.8907	-195.4	.1360	.9931	.0087	.0145	.0510	-.0893
* -.6324	-138.7	-.9557	.1712	-.1774	-.0744	.0410	.0164
-.4563	-100.1	-.0020	.0977	.2948	-.8482	-.2662	.0046
-.4197	- 92.1	.2800	-.0271	-.9304	-.3162	-.0110	-.0306
-.1977	- 43.4	.0046	-.1180	.1739	-.2574	.7798	-.5927
.0679	14.9	.0436	-.4957	.0573	-.5304	.7349	.9379

E Symmetry

Energy		Mixing Coefficients			
a.u.	K cm^{-1}	d_1	$\phi_{1\pi}$	χ_{1s}	χ_{1z}
* -.6370	-139.7	.9827	.1310	.0114	-.0050
-.4392	- 96.4	-.1934	.9244	.2445	.0113
-.2580	- 56.6	.0345	-.3882	.9800	-.0610
-.1346	- 29.5	-.0063	-.1184	.0705	1.0018

*Molecular Orbitals of Unpaired Electrons.

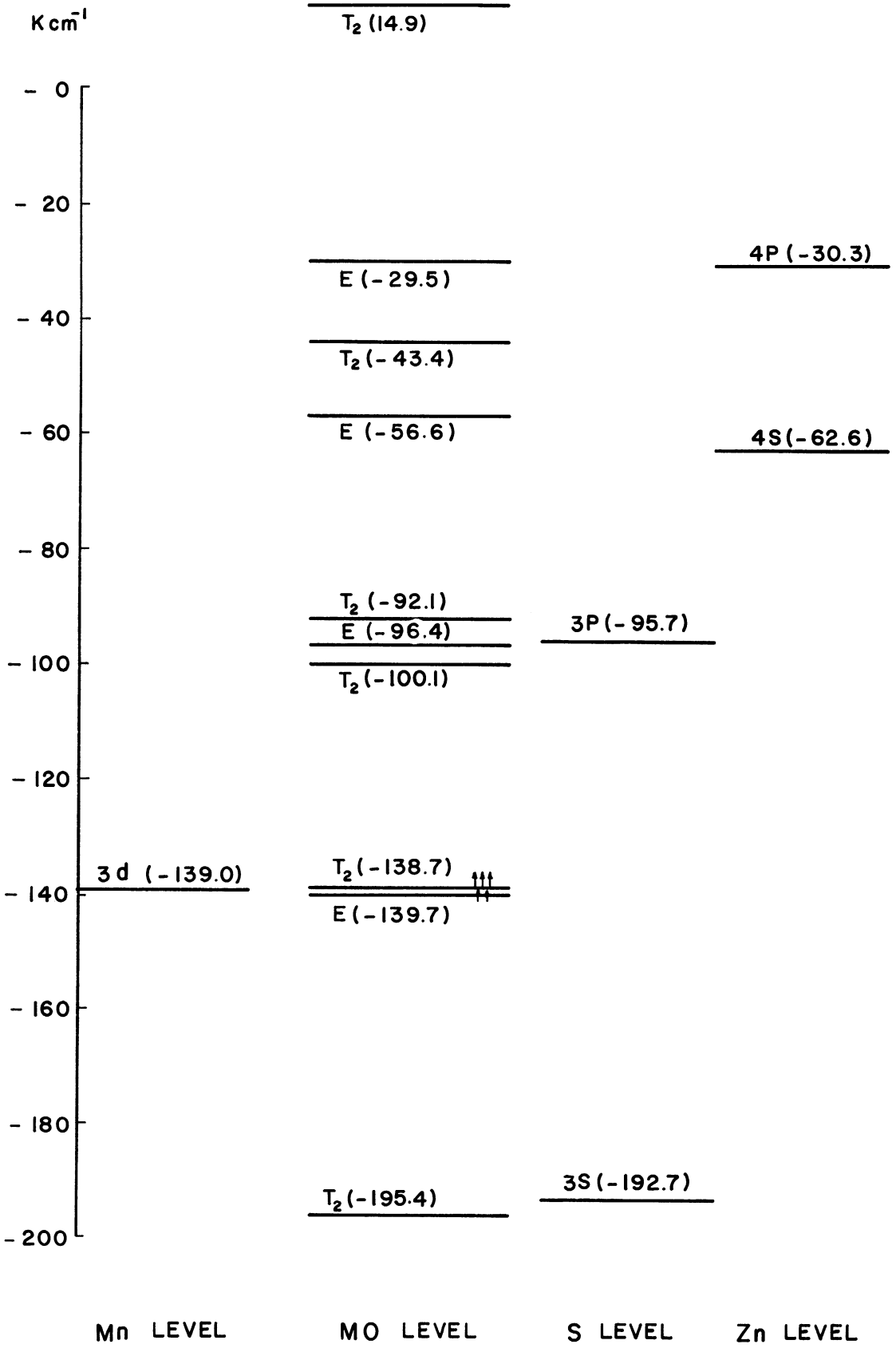

Figure C-2. MO Energy Level Diagram for ZnS:Mn^{++}.

Solutions of secular equations are given in Table C-2 and Figure C-2.

The average probabilities that one electron being found in the next nearest ligand S orbital, Equation (4-85) are for $CdTe:Mn^{++}$

$$\frac{1}{5}\left[\frac{1}{6}\gamma_{es}^2 + \frac{1}{4}\gamma_{ts}^2\right] = 0.001 = 0.1\ \%$$

for $ZnS:Mn^{++}$

$$\frac{1}{5}\left[\frac{1}{6}\gamma_{es}^2 + \frac{1}{4}\gamma_{ts}^2\right] = 0.00009 \approx 0.01\ \%$$

The result is discussed in Chapter VI.

REFERENCES

1. For review of crystal field theory, e.g., C. J. Ballhausen: Introduction to Ligand Field Theory, (1962) Chaps. 4 and 5.

   Griffith, J. S.: The Theory of Transition Metal Ions (1961), Chaps. 8 and 9.

2. Bethe, H. A.: Ann. Physik (5) 3, (1929) 133.

3. For a summary of EPR experimental results. e.g., W. Low: Electron Paramagnetic Resonance in Solids (1960) Chap. III.

4. For review of ligand field theory, e.g., C. J. Ballhausen: loc. cite, Chap. 7.

   Sugano, S.,: J. Appl. Phys. Suppl. Vol. 33, No. 1, (1962) 303.

5. Stevens, K. W. H.: Proc. Roy. Soc. (London) A219, (1953) 542.
   Owen, J.: Proc. Roy. Soc. (London) A227, (1955) 183.
   Tanabe, Y., and Sugano, S.: J. Phys. Soc. (Japan) 9, (1954) 766.

6. Griffiths, J. H. E., Owen, J., Ward, I. M.,: Proc. Roy. Soc. (London) A219, (1953) 526.

7. Tinkham, M.: Proc. Roy. Soc. (London) A236, (1956) 535, 549.

8. Shulman, R. G., and Jaccarino, V.: Phys. Rev. 108, (1957) 1219.
   Stout, J. W., and Shulman, R. G.: Phys. Rev. 118, (1960) 1136.

9. Mukherji, A., Das, T. P.: Phys. Rev. 111, (1958) 1479.

10. Keffer, F., Oguchi, T., O'Sullivan, W., and Yamashita, J.: Phys. Rev. 115, (1959) 1553.

11. Clogston, A. M., Gordon, J. P., Jaccarino, V., Peter, M., and Walker, L. R.: Phys. Rev. 117, (1960) 1222.

12. Marshall, W., and Stuart, R.: Phys. Rev. 123, (1961) 2048.

13. Alperin, H.: Phys. Rev. Letter, 6, (1961) 55.

14. Shulman, R. G., and Knox. K.: Phys. Rev. 119, (1960) 94.
    Shulman, R. G.,: Phys. Rev. 121, (1961) 125.

15. Sugano, S., and Shulman, R. G.: Phys. Rev. 130, (1963) 517.

16. Lambe, J., and Kikuchi, C.: Phys. Rev. 119, (1960) 1256.
    Hall, T.P.P., Hayes, W., and Williams, F.I.B.: Proc. Roy. Soc. (London) A78, (1961) 883.

16a. Dorain, P. B.: Phys. Rev. 112, (1958) 1058.

17. Schneider, J., Sircar, S. R., and Rauber, A.: Zeit. fur Natur. 18a (1963) 980.

18. From, W. H., Kikuchi, C., Dorain, P.: Bull. Am. Phys. Soc. 9, (1964), 37.

18a. Kasai, P. H.: Physics Letters, 7, (1963) 5.

19. Yamaka, E., and Barnes, R. G.: Ninth Annual Midwest Solid State Conference (1961), Private communication to Professor C. Kikuchi.

20. Chang, T.: Bull. Am. Phys. Soc. 8, (1963) 464.

21. Ludwig, G. W., and Lorenz, M. R.: Phys. Rev. 131, (1963) 601.

22. Lowdin, P. O.: J. Appl. Phys. Suppl. Vol. 33, No. 1 (Jan. 1962) 251.

23. Roothaan, C. C. J.: Rev. Mod. Phys. 23, (1951) 161.

24. Kotani, M.: Handbuch der Physik Bd. XXXVII/2 (1961).

25. For examples of analytical Hartree-Fock calculations:
Watson, R. E., Phys. Rev. 119, (1960) 1934.
Watson, R. E., and Freeman, A. J.: Phys. Rev. 123, (1961) 521, 124, (1961) 1117.

26. Wolfsberg, M., and Helmholz, L.: J. Chem. Phys. 20, (1952) 837.

27. Ballhausen, C. J., and Gray, H. B.: J. Inorg. Chem. 1, (1962) 111.

28. Moffitt, W.: Proc. Roy. Soc. (London) A202, (1950) 534.

29. Jørgensen, C. K.: Solid State Physics, 13, (1962) 375.

30. Gray, H. B., and Ballhausen, C. J.: J. Am. Chem. Soc. 85 (1963) 260.

31. Moore, C. E.: Atomic Energy Levels, U.S.NBS circular 467 (1949, 1952).

32. Fermi, E.: Z. Physik. 60, (1930) 320.
Fermi, E., and Segre : Z. Physik, 82, (1933) 729.
Casimir, H. B. G.: On the Interaction Between Atomic Nuclei and Electrons, (1936).

33. Blinder, S. M.,: J. Mol. Spect. 5, (1960) 17.

34. Jones, E. G.,: Proc. Phy. Soc. (London), 45, (1933) 625.

35. Chen, I., Kikuchi, C., and Watanabe, H.: Bull. Am. Phys. Soc. 9, (1964) 38.

36. Pauling, L.,: The Nature of Chemical Bonding. (1960) Chap. 5.

37. Watson, R. E., and Freeman, A. J.,: Phys. Rev. 120, (1960) 1125, 1134.

38. Shikazono, N.: J. Phys. Soc. Japan, 18, (1963) 925.

39. Mulliken, R. S., Rieke, C. A., Orloff, D., and Orloff, H.: J. Chem. Phys. 17, (1949) 1248.

40. Jaffe, H. H., and Doak, G. O.: J. Chem. Phys. 21, (1953) 196.
Jaffe, H. H.,: J. Chem. Phys., 21, (1953) 258.

41. Kotani, M., Anemiya, A., Isiguro, E., and Kimura, T.: Table of Molecular Integrals, (1955).